理學博士學位請求論文

Metabolic dynamics of nucleotide second messengers (p)ppGpp and cyclic di-GMP in bacteria

박테리아의 뉴클레오타이드 이차신호전달 물질인 (p)ppGpp와 cyclic di-GMP의 대사역학

2019년 2월

서울大學校 大學院

生物物理 및 化學生物學科

李 宰 祐

Metabolic dynamics of nucleotide second messengers (p)ppGpp and cyclic di-GMP in bacteria

by

Jaewoo Lee

Under the supervision of

Professor Yeong-Jae Seok, Ph. D

A Thesis for the Degree of **Doctor of Philosophy**

February, 2019

Department of Biophysics and Chemical Biology

Seoul National University

박테리아의 뉴클레오타이드 이차신호전달 물질인 (p)ppGpp와 cyclic di-GMP의 대사역학

指導敎授 石 暎 宰

이 論文을 理學博士 學位論文으로 提出함
2018年 12月

서울大學校 大學院
生物物理 및 化學生物學科
李 宰 祐

李宰祐의 理學博士學位論文을 認准함
2018年 12月

委 員 長 _____

副委員長 _____

委 員 _____

委 員 _____

委 員 _____

ABSTRACT

Metabolic dynamics of nucleotide second messengers (p)ppGpp and cyclic di-GMP in bacteria

Jaewoo Lee
Department of Biophysics and Chemical Biology
The Graduate School
Seoul National University

Bacterial nucleotide second messengers transduce intracellular or extracellular environmental signals to appropriate cellular responses. These signal transduction system has a wide range of effects on bacterial physiology. Thus, bacteria are equipped with a variety of enzymes that regulate its metabolism and signaling. Using these enzymes, bacteria elaborately modulate cellular concentration of second messengers in response to various cues. Since uncontrolled level of theses signal molecules causes growth inhibition, cell death and imbalanced phenotypes, its homeostatic control is very crucial for cellular physiology. While the metabolism and signaling mechanisms of cAMP have been relatively well documented to date, those of other nucleotide second messengers are not well understood.

(p)ppGpp signaling is mediated by two enzymes, (p)ppGpp synthetase RelA and the bifunctional (p)ppGpp synthetase/hydrolase SpoT proteins in *Escherichia. coli*. In response to various nutritional stresses, these two stringent factors fine-

tune the cellular (p)ppGpp concentrations, thus allowing bacterial cells to adapt to stress conditions. SpoT is the only enzyme responsible for (p)ppGpp hydrolysis in *E. coli*. Therefore, its activity needs to be tightly regulated to prevent the uncontrolled accumulation of (p)ppGpp, which causes severe growth inhibition and cell death. To date, however, little is known about how SpoT (p)ppGpp hydrolase activity is regulated in *E. coli*. The ligand fishing experiment revealed that Rsd directly interacts with SpoT and stimulates its (p)ppGpp-degrading activity. This regulation is controlled by the phosphorylation state of HPr, a general component of the PEP-dependent sugar transport system. Together, these data propose that Rsd is a carbon source-dependent regulator of the stringent response in *E. coli*.

In c-di-GMP signaling pathway, phosphodiesterases A (PDE-As) specifically degrades c-di-GMP into pGpG. However, excess amounts of pGpG inhibit phosphodiesterase A (PDE-A) activity to limit the completion of c-di-GMP signal transduction. Therefore, cells require additional phosphodiesterases B (PDE-Bs) to adjust the cellular pGpG concentrations in this signaling cascade. Orn protein has been demonstrated to mediate PDE-B activity in *Pseudomonas aeruginosa*. However, it exhibits broad substrate specificity to degrade various two to five nucleotides (nanoRNAs) including pGpG. Biochemical and structural analysis identified PggH as a new pGpG-specific phosphodiesterase and characterized its functional role as a PDE-B enzyme. These data indicate that PggH as a new PDE-B enzyme required to complete c-di-GMP signaling pathway in *Vibrio cholerae*.

Key words:
Bacterial nucleotide second messenger; (p)ppGpp; sugar signaling; protein-protein interaction; c-di-GMP; pGpG; phosphodiesterase

***Student Number*: 2013-22451**

Contents

List of Figures

List of Tables

ABBREVIATIONS

cAMP, cyclic AMP; 3',5'-cyclic adenosine monophosphate

(p)ppGpp, guanosine 3'-diphosphate-5'-di(tri)phosphate

c-di-GMP, bis-(3′-5′)-cyclic dimeric guanosine monophosphate

c-di-AMP, cyclic di-3′,5′-adenosine monophosphate

cGAMP, 3′, 3′-cyclic guanosine monophosphate-adenosine monophosphate

cGMP, 3',5'-cyclic guanosine monophosphate

PTS, phosphoenolpyruvate: carbohydrate phosphotransferase system

PEP, phosphoenolpyruvate

EI, enzyme I of the PTS

HPr, histidine-containing phosphocarrier protein

Glc, glucose

NAG, *N*-acetylglucosamine

Gal, galactose

Gly, glycerol

MALDI-TOF, matrix-associated laser desorption ionization time-of-flight

SDS, sodium dodecyl sulfate

PAGE, polyacrylamide gel electrophoresis

qRT-PCR, quantitative real-time polymerase chain reaction

DTT, dithiothreitol

X-gal, 5-bromo-4-chloro-3-indolyl-β-D-galactopyranoside

Chapter I. Literature Review

1. Overview of bacterial nucleotide second messenger

1.1. Bacterial nucleotide second messenger

In all domains of life, nucleotide-based second messengers transduce extracellular or intracellular signals into proper cellular responses. Despite the variety in the nature of these nucleotides, a common principle is applied to all nucleotide-based second messenger. The synthesis and degradation of the second messenger is catalyzed by two distinct enzymatic activities. As an allosteric regulator it can bind to an effector molecule to regulate diverse cellular processes (Pesavento and Hengge, 2009). In bacteria, cyclic adenosine monophosphate (cAMP) is the most comprehensively studied nucleotide-based second meesengers. However, other second messengers including guanosine pentaphosphate and tetraphosphate ((p)ppGpp), cyclic di-guanosine monophosphate (c-di-GMP), cyclic di-adenosine monophosphate (c-di-AMP), cyclic guanosine monophosphate–adenosine monophosphate (cGAMP) and cyclic guanosine monophosphate (cGMP) have attracted much attention due to their wide range effects on bacterial physiology.

1.2. cAMP

In bacteria, cAMP was first discovered to have a role in mediating the 'glucose response', or catabolite repression (Botsford, 1981). In prokaryotes, a variety of nucleotide second messengers are closely implicated in the regulation of bacterial physiology. Cyclic adenosine monophosphate (cAMP) is produced by a single adenylate cyclase (Cya) in response to carbon limitation and degraded by a single phosphodiesterase (CpdA) in *Escherichia coli* and most other γ-proteobacteria (Gorke and Stulke, 2008; Imamura et al., 1996). Binding of cAMP to the cAMP receptor protein (CRP) induces its conformational changes to bind to specific target DNA sequences. cAMP-CRP complex can function as a positive or negative transcriptional

regulator to induce catabolism of alternative carbon sources (Botsford and Harman, 1992). cAMP-binding to DnaA, the replication initiation protein, promote drastic reactivation of inactive ADP-bound DnaA (Hughes et al., 1988). In addition, cAMP directly and indirectly regulates various other cellular functions, such as biofilm formation, flagellum biosynthesis and virulence (Jackson et al., 2002; Liang et al., 2007).

1.3. (p)ppGpp

(p)ppGpp was first identified in a stringent strain of *E. coli* that seems to be involved in the inhibition of the synthesis of RNA (Cashel and Gallant, 1969). In response to nutrient limitation, guanosine pentaphosphate and tetraphosphate ((p)ppGpp) signaling is induced. The synthesis and hydrolysis is regulated by two protiens, homolog of the *E. coli* RelA and SpoT proteins in β-proteobacteria and γ-proteobacteria. Other bacteria contain a single RelA/SpoT homolog (RSH proteins for Rel Spo homolog), and members of the class *Firmicutes* posseses additional small fragments with synthetic activity (Potrykus and Cashel, 2008). In *E. coli*, the ribosome-associated RelA protein produces (p)ppGpp upon amino acid starvation. This response is sensed by the presence of uncharged tRNA molecules in the A site of the ribosome. The bifunctional protein SpoT and the single RSH proteins in other species hydrolyze and balance cellular (p)ppGpp concentrations in response to nutrient limitation and difference stresses (Potrykus and Cashel, 2008). (p)ppGpp directly binds to RNA polymerase as a direct effector to globally alter transcription pattern of the cell. And transcriptional regulator DksA protein potentiates (p)ppGpp-mediated effect on both stringently induced and repressed promoters (Magnusson et al., 2007). (p)ppGpp has also been shown to bind to guanine nucleotide binding proteins (Buglino et al., 2002). The increase in the intracellular (p)ppGpp concentration inhibit stable RNA synthesis, growth

and reorganization of the metabolism in the cell (Potrykus and Cashel, 2008).

1.4. c-di-GMP

It was first discovered in 1987 as an activator of the cellulose synthase from *Komagataeibacter xylinus* (formerly known as *Gluconacetobacter xylinus*) by Moshe Benziman (Ross et al., 1987). The three protein domains responsible for c-di-GMP metabolism are GGDEF, EAL and HD-GYP. These domains are named after the highly conserved amino acid motifs in their active site. Dimerization of two GGDEF domains is required for the c-di-GMP synthesis. In most cases, the formation of c-di-GMP is subjected to product inhibition, in which an inhibitory c-di-GMP binding site (I-site) is involved. Degradation of c-di-GMP is modulated by either by the EAL domain or by the less common HD-GYP domain. The hydrolysis of c-di-GMP proceeds through the linear pGpG into the final product GMP (Jenal and Malone, 2006; Ryan et al., 2006). c-di-GMP generally regulates the two different lifestyles of the most bacterial species, the motile-planktonic and the sedentary-adhesive lifestyles. As a lifestyle-switch regulator, c-di-GMP is broadly employed by various bacterial species in different physiological and ecological contexts.

c-di-GMP exhibits high diversity in its effector molecules including various protein families. Since the discovery of the first c-di-GMP effector, PilZ protein domain, the presence of transcriptional factor FleQ, putative inner membrane protein PelD from *Pseudomonas aeruginosa* and GGDEF protein PopA from *Caulobacter crescentus* were revealed (Amikam and Galperin, 2006; Duerig et al., 2009; Hickman and Harwood, 2008). Additionally, c-di-GMP has also been shown to bind to riboswitches present in the untranslated regions of different mRNAs. This interaction induces structural

changes of riboswitches to alter the expression of downstream genes (Sudarsan et al., 2008).

1.5. c-di-AMP

c-di-AMP was first identified in a research for the DNA repair mechanism in *Thermotoga maritima* (Witte et al., 2008). Many Gram-positive bacteria including the human pathogens *Staphylococcus aureus*, *Listeria monocytogenes*, and a subset of archaea produces c-di-AMP (Corrigan and Grundling, 2013). The synthesis of c-di-AMP is mediated by DisA_N domain-containing diadenylate cyclases DacA, DisA and YojJ, whereas the degradation is regulated by the phosphodiesterase enzyme GdpP (Corrigan et al., 2011; Witte et al., 2008). The intracellular levels of c-di-AMP is closely linked to a variety of different phenotypes. Increased cellular c-di-AMP concentrations influences acid resistance, antibiotic resistance and even controls essential cellular pathways (Luo and Helmann, 2012). It has been shown that the c-di-AMP interacts with the transcriptional factor DarR from *Mycobacterium smegmatis*. It also binds to potassium transporter-gating component KtrA, cation-proton antiporter CpaA and histidine kinase KdpD from *S. aureus*. In addition to these binding proteins, c-di-AMP also can bind to RNA riboswitches (Fahmi et al., 2017).

1.6. cGAMP

The presence of cGAMP was first revealed at 2012 during the study of pathogenesis of *Vibrio* seventh pandemic island-1 (VSP-1) in *Vibrio cholerae*. cGAMP is synthesized by a new class of dinucleotide cyclase DncV, which has the conserved G[G/S]$x_{9\text{-}13}$Dx[D/E] motif. DncV is required for interstinal colonization and represses *V. cholerae* chemotaxis (Davies et al., 2012). Following the discovery of DncV, cGAMP-specific PDEs with HD-GYP domains was reported in *V. cholerae*, named V-

cGAP1/2/3 (Gao and Patel, 2015). The protein effectors binding to cGAMP are still unknown. However, recent study revealed that cGAMP binds to phospholipase CapV and directly activates its hydrolase activity in *V. choleare*. This discovery sheds light on the functions and basic principles of cGAMP signaling (Severin et al., 2018). The cGAMP riboswitches were identified in the Gram-negative bacterium *Geobacter sulfurreducens* and *Deltaproteobacteria* (Kellenberger et al., 2015).

1.7. cGMP

The regulation of cGMP in bacteria has only recently been appreciated since it has been viewed as a nonfunctional by-product of adenylate cyclases. However, recent studies demonstrated the role of cGMP in adaption to the UV stress in cyanobacteria and in formation of cysts (dormant cells) in *alphaproteobacteria*. Thus, it is recognized as a genuine bacterial second messenger (Gomelsky and Galperin, 2013). Several cGMP effector proteins have been suggested in bacteria. The newly characterized fusion protein from *Xanthomonas campestris* contains a cyclic mononucleotide-binding (cNMP) domain and a GGDEF diguanylate cyclase domain to produce c-di-GMP under the control of cGMP.

2. (p)ppGpp metabolism and signaling

2.1. RSH enzyme

The enzymes that synthesize and hydrolyze (p)ppGpp are broadly conserved in bacteria except for the phyla Planctomycetes, Verrucomicrobia and Chlamydiae as well as obligate intracellular endosymbionts such as *Buchnera aphidicola*, and pathogen with decreased genome size such as *Treponema pallidumi* (Atkinson et al., 2011). Historically, stringent response was initially studied in the gammaproteobacterium *E. coli*. In this organism, two multidomain RelA-SpoT homologue (RSH) enzymes orchestrate the stringent response. These two enzymes are originated from a genome duplication event in the evolutionary lineage of the classes Betaproteobacteria and Gammaproteobacteria. These enzymes share a common six-domain structures, a (p)ppGpp hydrolysis domain (HD); a (p)ppGpp synthesis domain (SD); a threonyl-tRNA synthetase (ThrRS), GTPase and SpoT domain (TGS); a helical domain; a conserved cysteines containing domain (CC); and an aspartokinase, chorismate mutase and TyrA domain (ACT). The carboxy-terminal domain containing TGS, helical, CC and ACT domain has been suggested to regulate the enzymatic activities of the amino-terminal domain containing HD, SD domain (Mechold et al., 2002).

2.1.1. RelA

RelA is a ribosome-associated protein only capable of (p)ppGpp synthesis, and this (p)ppGpp synthetic activity is induced by amino acid starvation and heat shock (Gallant et al., 1977; Haseltine et al., 1972). During normal growth, amino acids in the form of amino-acylated tRNA are delivered to the ribosome acceptor site (A-stie). However, during amino acid starvation, the accumulated deacylated tRNAs occupy the A-site, thus dramatically inductin the (p)ppGpp synthesis activity of RelA protein (Haseltine and

Block, 1973). Free 3'-OH group of the terminal adenosine of the tRNA is indispensable for the RelA activity. This indicats that RelA directly inspects the aminoacylation state of tRNA to monitor translational capacity of the cell (Sprinzl and Richter, 1976). Recent single-molecule *in vivo* analysis suggests that RelA maintains its active state even after disassociation from the ribosome, implying the presence of a molecular memory in the regulation of RelA activity (English et al., 2011). Furthermore, ppGpp itself activates the RelA activity, resulting in a positive feedback loop, and fully activated together with the ribosome and deacylated tRNA (Shyp et al., 2012). Recent low-resolution cryoelectron microscopy (cryp-EM) broaden the knowledge of structural aspects of RelA enzymatic activity. Upon binding to the ribosome A-stie, RelA interacts with the sarcin-ricin loop (SRL) and 50S L11 to stabilize an unusual distorted form of the tRNA (Agirrezabala et al., 2013).

2.1.2. SpoT

SpoT has both weak (p)ppGpp synthetic activity and strong (p)ppGpp hydrolase activity. In response to various stress signals such as fatty acid (Seyfzadeh et al., 1993), iron (Vinella et al., 2005) and carbon source (Xiao et al., 1991) starvation, SpoT functions as a hub protein to modulate cellular (p)ppGpp concentrations. Interestingly, SpoT synthetic activity is gradually being losted based on the patterns of its sequence conservation in the Moraxellaceae family of gammaproteobacteria, suggesting that the functional partitioning for RelA and SpoT proteins is ongoing in this lineage (Atkinson et al., 2011). SpoT hydrolytic activity is essential for balancing cellular (p)ppGpp levels, thus disruption of *spoT* gene is lethal in the presence of RelA in *E. coli* (Xiao et al., 1991). Despite its importance in (p)ppGpp metabolism, the molecular details are still unknown due to its instability and insolubility. These difficulties have limited biochemical

studies and structural analysis. The GTPase Obg has been shown to interact with and repress its (p)ppGpp synthetase activity under nutrient-rich conditions (Raskin et al., 2007). During fatty acid starvation, acyl carrier protein (ACP) binds to and activates SpoT activity (Battesti and Bouveret, 2006). However, further studies are needed to verify its various regulatory mechanisms given that the SpoT protein is crucial component in stringent response under diverse stress conditions as a hub protein.

2.1.3. Rel

Except for the Gammaproteobacteria and Betaproteobacteria, the majority of bacteria regulates the (p)ppGpp concentrations using a single RSH protein, Rel. This enzyme has both (p)ppGpp synthetic and hydrolytic activities like SpoT protein. In *mycobacterium tuberculosis*, the accumulated deacylated tRNA in the A-site of ribosomes dramatically induces Rel (p)ppGpp synthetic activity like RelA protein (Avarbock et al., 2000). Amino acid starvation is sufficient to trigger (p)ppGpp synthesis by Rel in *Enterococcus faecalis*, *Myxococcus xanthus* and *Streptomyces coelicolor* A3(2). However, additional starvation signals are required to induce Rel-mediated (p)ppGpp synthesis in *Caulobacter crescentus* (Hauryliuk et al., 2015), reflecting that the stringent response is distinct depending on the different lifestyles of each species. Although the X-ray ctystal structure of a truncated Rel from *Streptococcus dysgalactiae* subsp. *equisimilis* is solved, but that of its regulatory domains are unresolved yet.

2.2. Physiological roles of (p)ppGpp

2.2.1. Transcription regulation by (p)ppGpp

During starvation conditions, (p)ppGpp regulates expression of various genes through altering RNAP activity. In *E. coli*, (p)ppGpp binds to RNAP to destabilize the short-lived open complexes, thus directly inhibiting

transcription initiation (Barker et al., 2001). During amino acid starvation, (p)ppGpp represses transcription from the promoters of rRNA and ribosomal protein genes, whereas it activates transcription from the promoters of amino acid biosynthesis and transport genes (Paul et al., 2005). Unlike *E. coli*, in other bacteria such as *Bacilus subtilis*, (p)ppGpp represses transcription without directly interacting with RNAP. It inhibits the enzymes responsible for GTP synthesis to decrease the GTP/ATP ratio. These initiating nucleotides govern the expression of genes sensitive to its concentration, thus transcription for genes beginning with a guanosine is repressed but transcription for genes beginning with adenosine is activated (Krasny and Gourse, 2004). A crystal structure of RNAP in complex with ppGpp revealed that ppGpp interacts with the surface of a double-psi β-barrel (DPBB) domain in the β'-subunit and with the N terminus of the ω-subunit. pppGpp also binds to the same site on RNAP but with lower potency (Mechold et al., 2013; Zuo et al., 2013). Together with the (p)ppGpp, transcriptional regulator DksA also has a crucial role in the stringent response. It manifests the effect of (p)ppGpp on the transcriptional regulation. Recently, it has been demonstrated that ppGpp binds to two distinct sites (Site 1 and Site 2) on *E. coli* RNAP, and also it binds to the interface of RNAP and the DksA at Site 2. These results accounts for the ppGpp enhancement of DksA's effect on RNAP (Ross et al., 2016).

2.2.2. Toxin-antitoxin systems and persistence

Given the recent global problems with antibiotic resistance, there has been growing interests in bacterial persisters, which are tolerant to multiple antibiotics. It has been suggested that slow growth of bacteria cells is associated with recalcitrance to killing by antibiotics and the drug tolerance phenotype (Levin et al., 2014). Since (p)ppGpp directly regulate bacterial growth rate and metabolism, this raised the possibility that persistence could

be regulated by the stringent response. A decade ago, an exponentially growing *hipA* mutant of *E. coli* was demonstrated to generate presisters stochastically and exhibit high survival rate when treated with ampicillin (Balaban et al., 2004). Since *hipA* encodes the toxin component of a toxin-antitoxin module (TA module), HipAB, the connection between TA module, (p)ppGpp and persistence was suggested (Korch et al., 2003). This rather enigmatic connection became obvious with the observations that HipA triggers (p)ppGpp synthesis in a RelA-dependent manner to induce the formation of persister cells (Germain et al., 2015). A more general implication of TA modules in persistence came from the discovery that the transcription of TA operons encoding mRNA endonucleases (mRNases) was more increased in persisters than in non-persister cells in the same population (Shah et al., 2006). While TA-encoded mRNases are inhibitors of bacterial cell growth, their corresponding antitoxins are readily degraded by Lon protease (Gerdes and Maisonneuve, 2012). That is, the activity of Lon regulates the activities of the toxins by modulating the levels of antitoxins. TA-encoded toxins were shown to cause a marked increase in persistence as an inducers of persistence. The progressive deletion of ten type II TA operons in *E. coli* leads to a progressive reduction in persistence. These data suggested that TA modules encode cell growth inhibitors, which is crucial to bacterial persistence. Several studies further demonstrated that the connection between (p)ppGpp, TA modules and persistence. These studies showed that (p)ppGpp functions as a master regulator of persistence and the TA modules encode persistence effectors. Increased cellular (p)ppGpp levels inhibits exopolyphosphatase activity (Kuroda et al., 1997) to increase the amount of polyphosphate. This in turn binds to and activates Lon protease, which causes activation of the toxins by degrading their cognate antitoxin (Maisonneuve et al., 2018).

2.2.3. Persistence and virulence

Given that the alarmone (p)ppGpp is present in the majority of bacterial species and bacteria encounter hostile and stress-inducing environments during infection, (p)ppGpp has been suggested to control persistence during infection. During infection, *Salmonella enterica* subsp. reside in acidic and nutrient poor *Salmonela*-containing vacuole inside macrophage. The impairment in stringent response, in fact, induces fewer persistence formation in macrophage (Helaine et al., 2014). Furthermore, persistence formation in macrophage depends on Lon protease and TA-encoding genes. This supports a smilar mechanism present between *E. coli* and *Salmonella* spp. persistence formation. Another study showed that slow growing *S.* typhimurium exhibits more increased survival rate following antibiotic treatment than fast growing cells in host tissues (Claudi et al., 2014). (p)ppGpp also influences the persistence formation of *Pseudomonas aeruginosa* during amino acid stravtion, in biofilms and under oxidative stress (Khakimova et al., 2013; Nguyen et al., 2011).

3. c-di-GMP metabolism and signaling

3.1. Diguanylate cyclases (DGCs)

Cellular c-di-GMP concentrations are regulated by two antagonistic enzyme families in response to internal and external cues. Diguanylate cyclases (DGCs) and c-di-GMP-specific phosphodiesterases (PDEs) are responsible for the synthesis and degradation of c-di-GMP, respectively. These enzymes are identified in all major bacterial phyla as a representative signaling proteins in the bacterial kingdom (Romling et al., 2013). Structural studies on DGC enzymes suggested the modes of substrate binding, catalytic mechanism, enzyme activation and product inhibition for this class of enzymes (Paul et al., 2004; Wassmann et al., 2007). DGCs catalyze the synthesis of c-di-GMP via the cooperative action of their two catalytic GGDEF domains, which arrange in an antiparallel manner. Two GTP molecules positioned in an antiparallel manner at GGDEF domains are finally condensed into c-di-GMP. This mechanism also requires an accessory domain to control the activity of DGC enzymes. In the case of PleD or the WspR from *Pseudomonas aeruginosa*, an amino-terminal reveiver domain that forms homodimers facilitates this c-di-GMP synthesis process (De et al., 2008; Paul et al., 2007). The antiparallel arrangement of GGDEF domains also implicated in the feedback inhibition of c-di-GMP synthesis. Interestingly, various DGC enzymes are subject to non-competitive product inhibition through the c-di-GMP binding to the allosteric I site on the GGDEF domain. Product inhibition of DGCs may establish precise cellular threshold concentrations of c-di-GMP and increase stability of c-di-GMP signalling networks by maintaining c-di-GMP levels in defined concentration windows (Christen et al., 2006).

3.2. c-di-GMP-specific phosphodiesterases (PDEs)

c-di-GMP-specific PDEs possess EAL domain or an HD-GYP domain to specifically degrade c-di-GMP. EAL domain-containing proteins actively hydrolyze c-di-GMP to yield pGpG as dimers (Sundriyal et al., 2014). Structural analysis revealed that there is a hinge joint to connect EAL conformation to catalytic activity, thus locating metal ions in the active site. This region undergoes rearrangements during the clam-like opening and closing movements of the EAL dimer (Sundriyal et al., 2014). Another c-di-GMP-specific phosphodiesterases possess conserved HD-GYP domains. It hydrolyzes c-di-GMP into two molecules of GMP in a one-step reaction. Recent crystal structure of an active HD-GYP-containing PDE indicates that a trinuclear iron-binding site is implicated in its catalytic activity and HD-GYP family splits into two distinct subgroups involving bi- and trinuclear metal centres (Bellini et al., 2014). Despite the knowledge on the function and structure of c-di-GMP-metabolizing enzymes (DGCs and PDEs), only a few input signals including oxygen, light, nitric oxide, metals, nutrients or surface contact have been revealed (Jenal et al., 2017). This is due to the limited physiological conditions that are tested in the laboratory. Furthermoer, DGCs and PDEs are involved in downstream signalling cascades by direct interactions with their effector molecules. The EAL domain protein YciR, DGC YdaM and transcription factor MlrA from *E.* coli make the complex formation. In this regulatory process, YciR functions as regulatory triggers, thereby coupling c-di-GMP concentrations to transcriptional control (Lindenberg et al., 2013).

3.3. Physiological roles of c-di-GMP

3.3.1. Development and morphogenesis

Bacteria adopt c-di-GMP to control morphogenesis and developmental transitions. *C. crescentus*, which has an inherently asymmetric life cycle,

generates a motile swarmer cell and a sessile stalked cell during division cycle. In this process, *C. crescentus* cells are highly polarized, with a stalk cell exposed at one cell pole and a flagellum, pili and chemotaxis apparatus assembled at the opposite pole. Recent study suggested c-di-GMP as a major dirver of pole morphogenesis and cell cycle control in *C. crescentus*. In fact, all polar appendages and cell morphology were severely abberrated in mutants that were unable to produce c-di-GMP (Abel et al., 2013). Cellular c-di-GMP concentrations oscillate during the cycle of *C. crescentus*. During the swarmer-to-stalked cell transition, DGC PleD protein is activated by phosphotylation to increase the levels of c-di-GMP. PleC keeps the levels of phosphorylated PleD low as a phosphatase in swarmer cells, DivJ drives the phosphorylation of PleD as a kinase in stalked cells (Paul et al., 2008). In addition, c-di-GMP regulates complex multicellular behavior. Germinating spores of streptomycetes develop into vegetative hyphae. However, following nutrient depletion, aerial hyphae are formed, which eventually differentiate into long chains of spores (Bush et al., 2015). Recently, it has been revealed that c-di-GMP has a key role in the transition from vegetative mycelial growth to the formation of a reproductive aerial mycelium. The deletion of genes that encode proteins that are implicated in the metabolism of c-di-GMP had a significant effect on colony morphology and development. Increasing internal levels of c-di-GMP blocked development, whereas decreasing levels of c-di-GMP caused premature spore production (Tschowri et al., 2014).

3.3.2. Motile-sessile transition

General feature of c-di-GMP is to modulate the motile-sessile transition of bacteria. Increased levels of c-di-GMP induce surface attachment, thereby promoting the formation of biofilms, whereas low levels of c-di-GMP increase the motility of individual cells. But, more complex regulatory steps

are implicated in this process to influence surface colonization (Valentini and Filloux, 2016). In *E. coli* and *Salmonella enterica* subsp. *enterica* serovar Typhimurium, high concentrations of c-di-GMP bind to the c-di-GMP effector protein YcgR to inhibit motor function. To decrease the activity of YcgR and increase swimming motility, these bacteria co-express the PDE PdeH and flagellar genes (Paul et al., 2010). Once bacteria contact with a surface, it protects developing microcolonies by rapidly exposing adhesins, activating surface organelles and producing an extracellular matrix. This process is coordinated by c-di-GMP at the transcriptional (Park et al., 2015), translational (Kariisa et al., 2016) and post-translational levels (Steiner et al., 2013). In fact, c-di-GMP regulates the prototypical surface adherence and motility organelles, type IV pili (T4P) and the production of the biofilm matrix components such as curli fibres and cellulose (Jenal et al., 2017; Serra et al., 2013).

3.3.3. Bacterial virulence

c-di-GMP has been shown to modulate the virulence of animal and plant pathogens (Romling et al., 2013). It regulates multiple cellular processes including host cell adherence, the secretion of virulence factors, cytotoxicity, invasion, resistance to oxidative stress and the modulation of the immune response of the host (Jenal et al., 2017). Furthermore, it was recently revealed that the most prominent secretion systems for virulence factors involving T2SSs, T3SSs and T6SSs are linked to c-di-GMP (Moscoso et al., 2011; Roelofs et al., 2015; Trampari et al., 2015). The role of c-di-GMP in virulence was apparently manifested by the outbreak of *E. coli* O104:H4. The genome of this causative strain prevalently encodes a highly expressed DGC to produce high levels of c-di-GMP, thereby promoting the formation of biofilms in the host (Richter et al., 2014).

3.4. c-di-GMP effectors

Considering the global role of c-di-GMP on bacterial cell physiology, it is reasonable to assume that various c-di-GMP effectors and its cellular targets exist. Several effector proteins and RNAs have been structurally and functionally characterized (Chou and Galperin, 2016). These involve PilZ domains-containing proteins, transcriptional regulators and mRNA riboswitches. c-di-GMP binds to the carboxy-terminal PilZ domain of BcsA to activates the membrane-bound BcsA-BcsB cellulose synthase comple (Morgan et al., 2014). Interestingly, the activity of bacterial enhancer-binding protein (bEBP) FleQ from *P. aeruginosa* is regulated by its direct interaction with c-di-GMP (Baraquet and Harwood, 2013). Structural anaylsis revealed that the binding of c-di-GMP inhibits the ATPase activity of FleQ to alter its quaternary structure, thereby changing its transcriptional activity (Matsuyama et al., 2016). The function of c-di-GMP riboswitches is well known in *Clostridium difficile*. During the infection, *C. difficile* undergoes a c-di-GMP-mediated transition from a motile to sessile state, and this switch is regulated by 16 c-di-GMP-responsive riboswitches (Soutourina et al., 2013). These regulatory elements control the expression of flagella, adhesion factors and main virulence factors, toxins TcdA and TcdB (McKee et al., 2013).

4. The aims of this study

Bacterial nucleotide second messengers transduce intracellular or extracellular environmental signals to proper cellular responses. Bacteria are equipped with diverse enzymes that regulate its metabolism and signaling. Using these enzymes, bacteria fine-tune the concentration of second messengers in response to a variety of environmental cues. Since these signal transduction system has a wide range of effects on bacterial physiology, its homeostatic control is very crucial for cellular physiology. While the metabolism and signaling mechanisms of cAMP have been relatively well known to date, those of other nucleotide second messengers are not well documented.

(p)ppGpp signaling is mediated by two enzymes, RelA and SpoT proteins in *E. coli*. In response to various stress signals, these two stringent factors fine-tune the cellular (p)ppGpp concentrations, thus bacterial cells can adapt to stress conditions. While the structural and functional mechanism of RelA is relatively well known, those of SpoT is not. In this study, I revealed that Rsd as a stimulator of the (p)ppGpp-degrading activity of SpoT during carbon source downshift, and this regulation is controlled by the phosphorylation state of HPr, a general component of the PEP-dependent sugar transport system. These provide a direct link between sugar signaling and the bacterial stringent response.

In c-di-GMP signaling pathway, excess amounts of pGpG inhibit PDE-A activity to limit the completion of c-di-GMP signal transduction. Therefore, adjusting the cellular pGpG concentrations is important for this signaling cascade. I identified PggH as a new pGpG-specific phosphodiesterase with its structural analysis, and characterized its functional role as a PDE-B enzyme in *V. cholerae*.

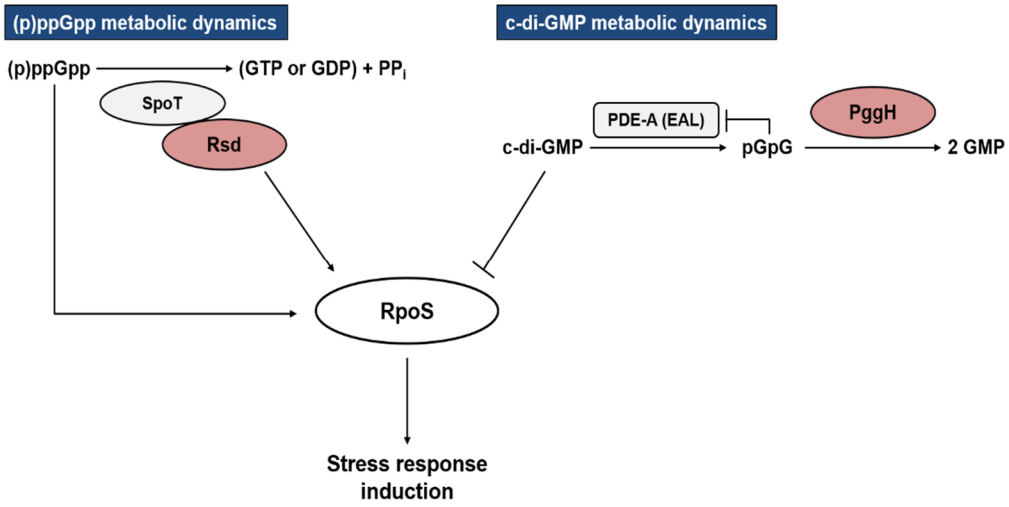

Figure I-1. Model for the metabolic dynamics of nucleotide second messengers (p)ppGpp and cyclic di-GMP in bacteria.

During a carbon source downshift, the (p)ppGpp level abruptly increases upon depletion of glucose in *relA*$^{+}$ strains. Under this stress condition, Rsd binds and activates the (p)ppGpp hydrolase activity of SpoT to balance the (p)ppGpp metabolic dynamics, which contributes to the growth resumption of *Escherichia coli* cell. This homeostatic control of cellular (p)ppGpp concentrations may regulate the expression of *rpoS*, since ppGpp positively regulates the synthesis of RpoS (Chapter II).

Excess amounts of pGpG inhibits PDE-A activity to elevate c-di-GMP concentrations, thus cells require PggH, a second phosphodiesterase (PDE-B), to degrade pGpG and complete c-di-GMP metabolic dynamics in *Vibrio cholerae.* The pGpG-specific hydrolase activity of PggH is required for regulating the expression level of *rpoS*, which allows *V. cholerae* cells to respond to oxidative stress conditions (Chapter III).

5. References

Abel, S., T. Bucher, M. Nicollier, I. Hug, V. Kaever, P. Abel Zur Wiesch, and U. Jenal. 2013. Bi-modal distribution of the second messenger c-di-GMP controls cell fate and asymmetry during the *caulobacter* cell cycle. *PLoS Genet*. 9:e1003744.

Agirrezabala, X., I.S. Fernandez, A.C. Kelley, D.G. Carton, V. Ramakrishnan, and M. Valle. 2013. The ribosome triggers the stringent response by RelA via a highly distorted tRNA. *EMBO Rep*. 14:811-816.

Amikam, D., and M.Y. Galperin. 2006. PilZ domain is part of the bacterial c-di-GMP binding protein. *Bioinformatics*. 22:3-6.

Atkinson, G.C., T. Tenson, and V. Hauryliuk. 2011. The RelA/SpoT homolog (RSH) superfamily: distribution and functional evolution of ppGpp synthetases and hydrolases across the tree of life. *PLoS One*. 6:e23479.

Avarbock, D., A. Avarbock, and H. Rubin. 2000. Differential regulation of opposing Rel_{Mtb} activities by the aminoacylation state of a tRNA.ribosome.mRNA.Rel_{Mtb} complex. *Biochemistry*. 39:11640-11648.

Balaban, N.Q., J. Merrin, R. Chait, L. Kowalik, and S. Leibler. 2004. Bacterial persistence as a phenotypic switch. *Science*. 305:1622-1625.

Baraquet, C., and C.S. Harwood. 2013. Cyclic diguanosine monophosphate represses bacterial flagella synthesis by interacting with the Walker A motif of the enhancer-binding protein FleQ. *Proc Natl Acad Sci U S A*. 110:18478-18483.

Barker, M.M., T. Gaal, C.A. Josaitis, and R.L. Gourse. 2001. Mechanism of regulation of transcription initiation by ppGpp. I. Effects of ppGpp on transcription initiation *in vivo* and *in vitro*. *J Mol Biol*. 305:673-

688.

Battesti, A., and E. Bouveret. 2006. Acyl carrier protein/SpoT interaction, the switch linking SpoT-dependent stress response to fatty acid metabolism. *Mol Microbiol*. 62:1048-1063.

Bellini, D., D.L. Caly, Y. McCarthy, M. Bumann, S.Q. An, J.M. Dow, R.P. Ryan, and M.A. Walsh. 2014. Crystal structure of an HD-GYP domain cyclic-di-GMP phosphodiesterase reveals an enzyme with a novel trinuclear catalytic iron centre. *Mol Microbiol*. 91:26-38.

Botsford, J.L. 1981. Cyclic nucleotides in procaryotes. *Microbiol Rev*. 45:620-642.

Botsford, J.L., and J.G. Harman. 1992. Cyclic AMP in prokaryotes. *Microbiol Rev*. 56:100-122.

Buglino, J., V. Shen, P. Hakimian, and C.D. Lima. 2002. Structural and biochemical analysis of the Obg GTP binding protein. *Structure*. 10:1581-1592.

Bush, M.J., N. Tschowri, S. Schlimpert, K. Flardh, and M.J. Buttner. 2015. c-di-GMP signalling and the regulation of developmental transitions in streptomycetes. *Nat Rev Microbiol*. 13:749-760.

Cashel, M., and J. Gallant. 1969. Two compounds implicated in the function of the RC gene of *Escherichia coli*. *Nature*. 221:838-841.

Chou, S.H., and M.Y. Galperin. 2016. Diversity of Cyclic Di-GMP-Binding Proteins and Mechanisms. *J Bacteriol*. 198:32-46.

Christen, B., M. Christen, R. Paul, F. Schmid, M. Folcher, P. Jenoe, M. Meuwly, and U. Jenal. 2006. Allosteric control of cyclic di-GMP signaling. *J Biol Chem*. 281:32015-32024.

Claudi, B., P. Sprote, A. Chirkova, N. Personnic, J. Zankl, N. Schurmann, A. Schmidt, and D. Bumann. 2014. Phenotypic variation of *Salmonella* in host tissues delays eradication by antimicrobial chemotherapy. *Cell*. 158:722-733.

Corrigan, R.M., J.C. Abbott, H. Burhenne, V. Kaever, and A. Grundling. 2011. c-di-AMP is a new second messenger in *Staphylococcus aureus* with a role in controlling cell size and envelope stress. *PLoS Pathog*. 7:e1002217.

Corrigan, R.M., and A. Grundling. 2013. Cyclic di-AMP: another second messenger enters the fray. *Nat Rev Microbiol*. 11:513-524.

Davies, B.W., R.W. Bogard, T.S. Young, and J.J. Mekalanos. 2012. Coordinated regulation of accessory genetic elements produces cyclic di-nucleotides for *V. cholerae* virulence. *Cell*. 149:358-370.

De, N., M. Pirruccello, P.V. Krasteva, N. Bae, R.V. Raghavan, and H. Sondermann. 2008. Phosphorylation-independent regulation of the diguanylate cyclase WspR. *PLoS Biol*. 6:e67.

Duerig, A., S. Abel, M. Folcher, M. Nicollier, T. Schwede, N. Amiot, B. Giese, and U. Jenal. 2009. Second messenger-mediated spatiotemporal control of protein degradation regulates bacterial cell cycle progression. *Genes Dev*. 23:93-104.

English, B.P., V. Hauryliuk, A. Sanamrad, S. Tankov, N.H. Dekker, and J. Elf. 2011. Single-molecule investigations of the stringent response machinery in living bacterial cells. *Proc Natl Acad Sci U S A*. 108:E365-373.

Fahmi, T., G.C. Port, and K.H. Cho. 2017. c-di-AMP: An Essential Molecule in the Signaling Pathways that Regulate the Viability and Virulence of Gram-Positive Bacteria. *Genes (Basel)*. 8.

Gallant, J., L. Palmer, and C.C. Pao. 1977. Anomalous synthesis of ppGpp in growing cells. *Cell*. 11:181-185.

Gao, P., and D.J. Patel. 2015. V-cGAPs: attenuators of 3'3'-cGAMP signaling. *Cell Res*. 25:529-530.

Gerdes, K., and E. Maisonneuve. 2012. Bacterial persistence and toxin-antitoxin loci. *Annu Rev Microbiol*. 66:103-123.

Germain, E., M. Roghanian, K. Gerdes, and E. Maisonneuve. 2015. Stochastic induction of persister cells by HipA through (p)ppGpp-mediated activation of mRNA endonucleases. *Proc Natl Acad Sci U S A*. 112:5171-5176.

Gomelsky, M., and M.Y. Galperin. 2013. Bacterial second messengers, cGMP and c-di-GMP, in a quest for regulatory dominance. *EMBO J*. 32:2421-2423.

Gorke, B., and J. Stulke. 2008. Carbon catabolite repression in bacteria: many ways to make the most out of nutrients. *Nat Rev Microbiol*. 6:613-624.

Haseltine, W.A., and R. Block. 1973. Synthesis of guanosine tetra- and pentaphosphate requires the presence of a codon-specific, uncharged transfer ribonucleic acid in the acceptor site of ribosomes. *Proc Natl Acad Sci U S A*. 70:1564-1568.

Haseltine, W.A., R. Block, W. Gilbert, and K. Weber. 1972. MSI and MSII made on ribosome in idling step of protein synthesis. *Nature*. 238:381-384.

Hauryliuk, V., G.C. Atkinson, K.S. Murakami, T. Tenson, and K. Gerdes. 2015. Recent functional insights into the role of (p)ppGpp in bacterial physiology. *Nat Rev Microbiol*. 13:298-309.

Helaine, S., A.M. Cheverton, K.G. Watson, L.M. Faure, S.A. Matthews, and D.W. Holden. 2014. Internalization of *Salmonella* by macrophages induces formation of nonreplicating persisters. *Science*. 343:204-208.

Hickman, J.W., and C.S. Harwood. 2008. Identification of FleQ from *Pseudomonas aeruginosa* as a c-di-GMP-responsive transcription factor. *Mol Microbiol*. 69:376-389.

Hughes, P., A. Landoulsi, and M. Kohiyama. 1988. A novel role for cAMP in the control of the activity of the *E. coli* chromosome replication initiator protein, DnaA. *Cell*. 55:343-350.

Imamura, R., K. Yamanaka, T. Ogura, S. Hiraga, N. Fujita, A. Ishihama, and H. Niki. 1996. Identification of the *cpdA* gene encoding cyclic 3',5'-adenosine monophosphate phosphodiesterase in *Escherichia coli*. *J Biol Chem*. 271:25423-25429.

Jackson, D.W., J.W. Simecka, and T. Romeo. 2002. Catabolite repression of *Escherichia coli* biofilm formation. *J Bacteriol*. 184:3406-3410.

Jenal, U., and J. Malone. 2006. Mechanisms of cyclic-di-GMP signaling in bacteria. *Annu Rev Genet*. 40:385-407.

Jenal, U., A. Reinders, and C. Lori. 2017. Cyclic di-GMP: second messenger extraordinaire. *Nat Rev Microbiol*. 15:271-284.

Kariisa, A.T., K. Weeks, and R. Tamayo. 2016. The RNA Domain Vc1 Regulates Downstream Gene Expression in Response to Cyclic Diguanylate in *Vibrio cholerae*. *PLoS One*. 11:e0148478.

Kellenberger, C.A., S.C. Wilson, S.F. Hickey, T.L. Gonzalez, Y. Su, Z.F. Hallberg, T.F. Brewer, A.T. Iavarone, H.K. Carlson, Y.F. Hsieh, and M.C. Hammond. 2015. GEMM-I riboswitches from *Geobacter* sense the bacterial second messenger cyclic AMP-GMP. *Proc Natl Acad Sci U S A*. 112:5383-5388.

Khakimova, M., H.G. Ahlgren, J.J. Harrison, A.M. English, and D. Nguyen. 2013. The stringent response controls catalases in *Pseudomonas aeruginosa* and is required for hydrogen peroxide and antibiotic tolerance. *J Bacteriol*. 195:2011-2020.

Korch, S.B., T.A. Henderson, and T.M. Hill. 2003. Characterization of the *hipA7* allele of *Escherichia coli* and evidence that high persistence is governed by (p)ppGpp synthesis. *Mol Microbiol*. 50:1199-1213.

Krasny, L., and R.L. Gourse. 2004. An alternative strategy for bacterial ribosome synthesis: *Bacillus subtilis* rRNA transcription regulation. *EMBO J*. 23:4473-4483.

Kuroda, A., H. Murphy, M. Cashel, and A. Kornberg. 1997. Guanosine

tetra- and pentaphosphate promote accumulation of inorganic polyphosphate in *Escherichia coli*. *J Biol Chem*. 272:21240-21243.

Levin, B.R., J. Concepcion-Acevedo, and K.I. Udekwu. 2014. Persistence: a copacetic and parsimonious hypothesis for the existence of non-inherited resistance to antibiotics. *Curr Opin Microbiol*. 21:18-21.

Liang, W., A. Pascual-Montano, A.J. Silva, and J.A. Benitez. 2007. The cyclic AMP receptor protein modulates quorum sensing, motility and multiple genes that affect intestinal colonization in *Vibrio cholerae*. *Microbiology*. 153:2964-2975.

Lindenberg, S., G. Klauck, C. Pesavento, E. Klauck, and R. Hengge. 2013. The EAL domain protein YciR acts as a trigger enzyme in a c-di-GMP signalling cascade in *E. coli* biofilm control. *EMBO J*. 32:2001-2014.

Luo, Y., and J.D. Helmann. 2012. Analysis of the role of *Bacillus subtilis* sigma(M) in beta-lactam resistance reveals an essential role for c-di-AMP in peptidoglycan homeostasis. *Mol Microbiol*. 83:623-639.

Magnusson, L.U., B. Gummesson, P. Joksimovic, A. Farewell, and T. Nystrom. 2007. Identical, independent, and opposing roles of ppGpp and DksA in *Escherichia coli*. *J Bacteriol*. 189:5193-5202.

Maisonneuve, E., M. Castro-Camargo, and K. Gerdes. 2018. (p)ppGpp Controls Bacterial Persistence by Stochastic Induction of Toxin-Antitoxin Activity. *Cell*. 172:1135.

Matsuyama, B.Y., P.V. Krasteva, C. Baraquet, C.S. Harwood, H. Sondermann, and M.V. Navarro. 2016. Mechanistic insights into c-di-GMP-dependent control of the biofilm regulator FleQ from *Pseudomonas aeruginosa*. *Proc Natl Acad Sci U S A*. 113:E209-218.

McKee, R.W., M.R. Mangalea, E.B. Purcell, E.K. Borchardt, and R. Tamayo. 2013. The second messenger cyclic Di-GMP regulates *Clostridium difficile* toxin production by controlling expression of *sigD*. *J*

Bacteriol. 195:5174-5185.

Mechold, U., H. Murphy, L. Brown, and M. Cashel. 2002. Intramolecular regulation of the opposing (p)ppGpp catalytic activities of $Rel_{(Seq)}$, the Rel/Spo enzyme from *Streptococcus equisimilis*. *J Bacteriol*. 184:2878-2888.

Mechold, U., K. Potrykus, H. Murphy, K.S. Murakami, and M. Cashel. 2013. Differential regulation by ppGpp versus pppGpp in *Escherichia coli*. *Nucleic Acids Res*. 41:6175-6189.

Morgan, J.L., J.T. McNamara, and J. Zimmer. 2014. Mechanism of activation of bacterial cellulose synthase by cyclic di-GMP. *Nat Struct Mol Biol*. 21:489-496.

Moscoso, J.A., H. Mikkelsen, S. Heeb, P. Williams, and A. Filloux. 2011. The *Pseudomonas aeruginosa* sensor RetS switches type III and type VI secretion via c-di-GMP signalling. *Environ Microbiol*. 13:3128-3138.

Nguyen, D., A. Joshi-Datar, F. Lepine, E. Bauerle, O. Olakanmi, K. Beer, G. McKay, R. Siehnel, J. Schafhauser, Y. Wang, B.E. Britigan, and P.K. Singh. 2011. Active starvation responses mediate antibiotic tolerance in biofilms and nutrient-limited bacteria. *Science*. 334:982-986.

Park, J.H., Y. Jo, S.Y. Jang, H. Kwon, Y. Irie, M.R. Parsek, M.H. Kim, and S.H. Choi. 2015. The *cabABC* Operon Essential for Biofilm and Rugose Colony Development in *Vibrio vulnificus*. *PLoS Pathog*. 11:e1005192.

Paul, B.J., M.B. Berkmen, and R.L. Gourse. 2005. DksA potentiates direct activation of amino acid promoters by ppGpp. *Proc Natl Acad Sci U S A*. 102:7823-7828.

Paul, K., V. Nieto, W.C. Carlquist, D.F. Blair, and R.M. Harshey. 2010. The c-di-GMP binding protein YcgR controls flagellar motor direction and speed to affect chemotaxis by a "backstop brake" mechanism.

Mol Cell. 38:128-139.

Paul, R., S. Abel, P. Wassmann, A. Beck, H. Heerklotz, and U. Jenal. 2007. Activation of the diguanylate cyclase PleD by phosphorylation-mediated dimerization. *J Biol Chem*. 282:29170-29177.

Paul, R., T. Jaeger, S. Abel, I. Wiederkehr, M. Folcher, E.G. Biondi, M.T. Laub, and U. Jenal. 2008. Allosteric regulation of histidine kinases by their cognate response regulator determines cell fate. *Cell*. 133:452-461.

Paul, R., S. Weiser, N.C. Amiot, C. Chan, T. Schirmer, B. Giese, and U. Jenal. 2004. Cell cycle-dependent dynamic localization of a bacterial response regulator with a novel di-guanylate cyclase output domain. *Genes Dev*. 18:715-727.

Pesavento, C., and R. Hengge. 2009. Bacterial nucleotide-based second messengers. *Curr Opin Microbiol*. 12:170-176.

Potrykus, K., and M. Cashel. 2008. (p)ppGpp: still magical? *Annu Rev Microbiol*. 62:35-51.

Raskin, D.M., N. Judson, and J.J. Mekalanos. 2007. Regulation of the stringent response is the essential function of the conserved bacterial G protein CgtA in *Vibrio cholerae*. *Proc Natl Acad Sci U S A*. 104:4636-4641.

Richter, A.M., T.L. Povolotsky, L.H. Wieler, and R. Hengge. 2014. Cyclic-di-GMP signalling and biofilm-related properties of the Shiga toxin-producing 2011 German outbreak *Escherichia coli* O104:H4. *EMBO Mol Med*. 6:1622-1637.

Roelofs, K.G., C.J. Jones, S.R. Helman, X. Shang, M.W. Orr, J.R. Goodson, M.Y. Galperin, F.H. Yildiz, and V.T. Lee. 2015. Systematic Identification of Cyclic-di-GMP Binding Proteins in *Vibrio cholerae* Reveals a Novel Class of Cyclic-di-GMP-Binding ATPases Associated with Type II Secretion Systems. *PLoS Pathog*.

11:e1005232.

Romling, U., M.Y. Galperin, and M. Gomelsky. 2013. Cyclic di-GMP: the first 25 years of a universal bacterial second messenger. *Microbiol Mol Biol Rev*. 77:1-52.

Ross, P., H. Weinhouse, Y. Aloni, D. Michaeli, P. Weinberger-Ohana, R. Mayer, S. Braun, E. de Vroom, G.A. van der Marel, J.H. van Boom, and M. Benziman. 1987. Regulation of cellulose synthesis in *Acetobacter xylinum* by cyclic diguanylic acid. *Nature*. 325:279-281.

Ross, W., P. Sanchez-Vazquez, A.Y. Chen, J.H. Lee, H.L. Burgos, and R.L. Gourse. 2016. ppGpp Binding to a Site at the RNAP-DksA Interface Accounts for Its Dramatic Effects on Transcription Initiation during the Stringent Response. *Mol Cell*. 62:811-823.

Ryan, R.P., Y. Fouhy, J.F. Lucey, and J.M. Dow. 2006. Cyclic di-GMP signaling in bacteria: recent advances and new puzzles. *J Bacteriol*. 188:8327-8334.

Serra, D.O., A.M. Richter, G. Klauck, F. Mika, and R. Hengge. 2013. Microanatomy at cellular resolution and spatial order of physiological differentiation in a bacterial biofilm. *MBio*. 4:e00103-00113.

Severin, G.B., M.S. Ramliden, L.A. Hawver, K. Wang, M.E. Pell, A.K. Kieninger, A. Khataokar, B.J. O'Hara, L.V. Behrmann, M.B. Neiditch, C. Benning, C.M. Waters, and W.L. Ng. 2018. Direct activation of a phospholipase by cyclic GMP-AMP in El Tor *Vibrio cholerae*. *Proc Natl Acad Sci U S A*. 115:E6048-E6055.

Seyfzadeh, M., J. Keener, and M. Nomura. 1993. *spoT*-dependent accumulation of guanosine tetraphosphate in response to fatty acid starvation in *Escherichia coli*. *Proc Natl Acad Sci U S A*. 90:11004-11008.

Shah, D., Z. Zhang, A. Khodursky, N. Kaldalu, K. Kurg, and K. Lewis. 2006.

Persisters: a distinct physiological state of *E. coli*. *BMC Microbiol*. 6:53.

Shyp, V., S. Tankov, A. Ermakov, P. Kudrin, B.P. English, M. Ehrenberg, T. Tenson, J. Elf, and V. Hauryliuk. 2012. Positive allosteric feedback regulation of the stringent response enzyme RelA by its product. *EMBO Rep*. 13:835-839.

Soutourina, O.A., M. Monot, P. Boudry, L. Saujet, C. Pichon, O. Sismeiro, E. Semenova, K. Severinov, C. Le Bouguenec, J.Y. Coppee, B. Dupuy, and I. Martin-Verstraete. 2013. Genome-wide identification of regulatory RNAs in the human pathogen *Clostridium difficile*. *PLoS Genet*. 9:e1003493.

Sprinzl, M., and D. Richter. 1976. Free 3'-OH group of the terminal adenosine of the tRNA molecule is essential for the synthesis *in vitro* of guanosine tetraphosphate and pentaphosphate in a ribosomal system from *Escherichia coli*. *Eur J Biochem*. 71:171-176.

Steiner, S., C. Lori, A. Boehm, and U. Jenal. 2013. Allosteric activation of exopolysaccharide synthesis through cyclic di-GMP-stimulated protein-protein interaction. *EMBO J*. 32:354-368.

Sudarsan, N., E.R. Lee, Z. Weinberg, R.H. Moy, J.N. Kim, K.H. Link, and R.R. Breaker. 2008. Riboswitches in eubacteria sense the second messenger cyclic di-GMP. *Science*. 321:411-413.

Sundriyal, A., C. Massa, D. Samoray, F. Zehender, T. Sharpe, U. Jenal, and T. Schirmer. 2014. Inherent regulation of EAL domain-catalyzed hydrolysis of second messenger cyclic di-GMP. *J Biol Chem*. 289:6978-6990.

Trampari, E., C.E. Stevenson, R.H. Little, T. Wilhelm, D.M. Lawson, and J.G. Malone. 2015. Bacterial rotary export ATPases are allosterically regulated by the nucleotide second messenger cyclic-di-GMP. *J Biol Chem*. 290:24470-24483.

Tschowri, N., M.A. Schumacher, S. Schlimpert, N.B. Chinnam, K.C. Findlay, R.G. Brennan, and M.J. Buttner. 2014. Tetrameric c-di-GMP mediates effective transcription factor dimerization to control *Streptomyces* development. *Cell*. 158:1136-1147.

Valentini, M., and A. Filloux. 2016. Biofilms and Cyclic di-GMP (c-di-GMP) Signaling: Lessons from *Pseudomonas aeruginosa* and Other Bacteria. *J Biol Chem*. 291:12547-12555.

Vinella, D., C. Albrecht, M. Cashel, and R. D'Ari. 2005. Iron limitation induces SpoT-dependent accumulation of ppGpp in *Escherichia coli*. *Mol Microbiol*. 56:958-970.

Wassmann, P., C. Chan, R. Paul, A. Beck, H. Heerklotz, U. Jenal, and T. Schirmer. 2007. Structure of BeF3- -modified response regulator PleD: implications for diguanylate cyclase activation, catalysis, and feedback inhibition. *Structure*. 15:915-927.

Witte, G., S. Hartung, K. Buttner, and K.P. Hopfner. 2008. Structural biochemistry of a bacterial checkpoint protein reveals diadenylate cyclase activity regulated by DNA recombination intermediates. *Mol Cell*. 30:167-178.

Xiao, H., M. Kalman, K. Ikehara, S. Zemel, G. Glaser, and M. Cashel. 1991. Residual guanosine 3',5'-bispyrophosphate synthetic activity of *relA* null mutants can be eliminated by *spoT* null mutations. *J Biol Chem*. 266:5980-5990.

Zuo, Y., Y. Wang, and T.A. Steitz. 2013. The mechanism of *E. coli* RNA polymerase regulation by ppGpp is suggested by the structure of their complex. *Mol Cell*. 50:430-436.

Chapter II.

Rsd balances (p)ppGpp level by stimulating the hydrolase activity of SpoT during carbon source downshift in *Escherichia coli*

1. Abstract

Bacteria respond to nutritional stresses by changing the cellular concentration of the alarmone (p)ppGpp. This control mechanism, called the stringent response, depends on two enzymes, the (p)ppGpp synthetase RelA and the bifunctional (p)ppGpp synthetase/hydrolase SpoT in *Escherichia coli* and related bacteria. Since SpoT is the only enzyme responsible for (p)ppGpp hydrolysis in these bacteria, SpoT activity needs to be tightly regulated to prevent the uncontrolled accumulation of (p)ppGpp, which is lethal. To date, however, no such regulation of SpoT (p)ppGpp hydrolase activity has been documented in *E. coli*. In this study, we show that Rsd directly interacts with SpoT and stimulates its (p)ppGpp hydrolase activity. Dephosphorylated HPr, but not phosphorylated HPr, of the phosphoenolpyruvate-dependent sugar phosphotransferase system could antagonize the stimulatory effect of Rsd on SpoT (p)ppGpp hydrolase activity. Thus, we suggest that Rsd is a carbon source-dependent regulator of the stringent response in *E. coli*.

2. Introduction

Bacteria possess several molecular mechanisms that allow them to respond and adapt to various environmental stresses. The stringent response is a stress response of bacteria (and plant chloroplasts) which orchestrates pleiotropic adaptations to nutritional starvation and some other stress conditions by fine-tuning the cellular levels of the 'alarmones' ppGpp and pppGpp (collectively named (p)ppGpp) (Cashel and Gallant, 1969; Potrykus and Cashel, 2008). As the effector molecule of the stringent response, (p)ppGpp regulates a variety of biological processes such as growth, adaptation, secondary metabolism, survival, persistence, cell division, motility, biofilms, development, competence, and virulence (Potrykus and Cashel, 2008). In Escherichia coli, the intracellular level of (p)ppGpp is regulated by two enzymes, RelA and SpoT. RelA catalyzes the pyrophosphorylation of GDP (or GTP) using ATP to synthesize (p)ppGpp in a ribosome-dependent manner (Haseltine and Block, 1973). The bifunctional enzyme SpoT has a strong (p)ppGpp hydrolase activity, converting (p)ppGpp into GDP (or GTP) and pyrophosphate (PPi), and a weak (p)ppGpp synthetase activity (An et al., 1979; Murray and Bremer, 1996). During amino acid starvation, ribosomes containing uncharged tRNAs accumulate, thereby activating the (p)ppGpp synthetase activity of RelA (Brown et al., 2016). SpoT responds to various nutrient stresses such as carbon (Xiao et al., 1991), iron (Vinella et al., 2005), phosphate (Bougdour and Gottesman, 2007), and fatty acid starvation (Seyfzadeh et al., 1993) with its (p)ppGpp synthetic and hydrolytic activities to balance cellular (p)ppGpp concentrations.

(p)ppGpp coordinates the transcriptome and metabolism in response to many sources of nutrient stress to facilitate bacterial adaptation (Potrykus and Cashel, 2008). Regulation of transcription by (p)ppGpp has been demonstrated in a genome-wide scale in many bacterial species. (p)ppGpp,

in conjunction with DksA, directly binds to RNA polymerase (RNAP) to inhibit transcription from rRNA and tRNA promoters (Haugen et al., 2008), whereas they activate transcription from amino acid biosynthesis promoters and some other σ^{70} promoters in *E. coli* (Paul et al., 2005). (p)ppGpp also directly binds and inhibits translational GTPases (IF2, EF-G, and EF-Tu), DNA primase (DnaG), polyphosphate kinase (PPK), and lysine decarboxylase LdcI, whereas its direct binding to RelA activates (p)ppGpp synthesis (Hauryliuk et al., 2015). In Gram-positive bacteria, (p)ppGpp binds and inhibits enzymes required for the GTP synthesis pathway and negatively impacts transcription and ribosome assembly rather than by directly binding to RNAP (Corrigan et al., 2016; Kriel et al., 2012).

Maintaining proper intracellular (p)ppGpp levels is important in cell physiology. To adjust appropriate intracellular (p)ppGpp levels in response to nutrient starvation, the (p)ppGpp hydrolase activity of SpoT plays a pivotal role since it is the only enzyme capable of hydrolyzing (p)ppGpp in *E. coli*. Therefore, the spoT null mutant exhibits uncontrolled accumulation of (p)ppGpp, which leads to the severe inhibition of cell growth (Xiao et al., 1991). However, little is known about how the (p)ppGpp hydrolase activity of SpoT is regulated except its inhibition by accumulated uncharged tRNA (Murray and Bremer, 1996). Thus, we assumed the existence of a molecular mechanism stimulating the reaction of SpoT-catalyzed (p)ppGpp hydrolysis.

In a recent study, it was found that dephosphorylated HPr of the bacterial phosphoenolpyruvate: sugar phosphotransferase system (PTS) interacts with and antagonizes the anti-sigma activity of Rsd (Park et al., 2013), which was named for its regulatory effect on the sigma factor RpoD (σ^{70}) (Jishage and Ishihama, 1998). The PTS catalyzes the phosphorylation-coupled transport of various sugars. This system consists of two general components, enzyme I (EI) and the histidine-containing phosphocarrier protein HPr, which are common to most PTS sugars, and several sugar-specific enzyme IIs (EIIs)

(Barabote and Saier, 2005; Postma et al., 1993). Each EII complex generally consists of one integral membrane domain forming the sugar translocation channel (EIIC) and two cytosolic domains (EIIA and EIIB). EI transfers a phosphoryl group from PEP to HPr. HPr then transfers the phosphoryl group to EIIA, which phosphorylates EIIB. In the presence of a PTS sugar, the phosphoryl group of EIIB is transferred to the sugar that is transported through the EIIC channel across the membrane. Thus, the phosphorylation states of the PTS components change depending on the availability of PTS sugar substrates (Deutscher et al., 2006). In this way, the PTS monitors nutritional changes in the environment and plays multiple regulatory roles in various metabolic processes, in addition to sugar transport (Park et al., 2013; Park et al., 2015).

In this study, we show that Rsd interacts with SpoT and activates its (p)ppGpp hydrolase activity in *E. coli*. Only the dephosphorylated form of HPr inhibits the formation of the Rsd-SpoT complex and thus antagonizes the effect of Rsd on the (p)ppGpp hydrolase activity of SpoT. We propose that Rsd functions as a regulator for the intracellular concentration of (p)ppGpp through direct interaction with SpoT, and this interaction is involved in the stringent response to a nutrient downshift from a preferred carbon source to a less preferred one.

3. Materials and Methods

3.1. Bacterial strains, plasmids, and culture conditions.

The bacterial strains, plasmids and oligonucleotides used in this study are listed in Tables II-1 and II-2. Bacterial cells were grown at 37°C in LB medium or MOPS minimal medium (pH 7.2) supplemented with the indicated carbon sources. All plasmids were constructed using standard polymerase chain reaction (PCR)-based cloning procedures and verified by sequencing. In-frame deletion mutants used in this study were constructed using the pKD46 plasmid as previously described (Datsenko and Wanner, 2000). The *relA* gene was replaced by the kanamycin-resistance gene and the *spoT* gene was replaced by the chloramphenicol-resistance (*cat*) gene or streptomycin-resistance gene.

To construct pJK1113-HPr(H15A), the *bla* gene in pJK1113 was replaced with the *cat* gene as described previously (Park et al., 2016). The *cat* gene PCR product and the linearized PCR product of pJK1113 were combined using the EZ-Fusion^{TM} Cloning kit (Enzynomics). Then, the *ptsH* promoter and ORF (His15 to Ala) amplified by PCR from pACYC-HPr(H15A) (Choe et al., 2017) using the primers RS963 and RS964 (Table II-2) was digested with SalI and inserted into the corresponding site of pJK1113.

3.2. Purification of overexpressed proteins.

Purification of EI and HPr was accomplished using MonoQ^{TM} 10/100 GL and HiLoad 16/60 Superdex 75 prepgrade columns (GE Healthcare Life Sciences) as recently reported (Choe et al., 2017; Kim et al., 2015; Park et al., 2013), and Rsd was purified in a similar manner. His-tagged protein (His-Rsd) was purified using TALON metal affinity resin according to the manufacturer's instructions (Takara Bio). The protein was eluted with the binding buffer (20 mM HEPES-NaOH, pH 7.6, 100 mM NaCl, 5 mM β-mercaptoethanol, and 5% glycerol) containing 150 mM imidazole. The

fractions containing His-Rsd were concentrated using Amicon Ultracel-3K centrifugal filters (Merck Millipore). To obtain homogeneous His-tagged protein (>98% pure) and to remove imidazole, the concentrated pool was chromatographed on a HiLoad 16/60 Superdex 75 prepgrade column equilibrated with the binding buffer. The purified protein was stored at -80°C until use. GST-tagged protein (GST-SpoT) was purified using Glutathione-S-agarose beads (Sigma Aldrich) according to the manufacturer's instructions. The protein was eluted with the binding buffer containing 10 mM reduced glutathione (GSH). The fractions containing GST-SpoT was concentrated using Amicon Ultracel-3K centrifugal filters. To remove GSH and to purify the protein to homogeneity (<95% purity), the concentrated pool was dialyzed against a large volume of GSH-free buffer (50 mM Tris-HCl, pH 8, 270 mM potassium acetate, 5% glycerol, and 10 mM DTT).

3.3. Ligand fishing experiments using metal affinity chromatography.

E. coli MG1655 cells grown overnight in LB medium were harvested and resuspended in the binding buffer. Cells were disrupted by two passages through a French pressure cell at 10,000 psi. After centrifugation at 100,000 × *g* for 25 min at 4°C, the supernatant was divided into aliquots and mixed either with a His-tagged protein as bait or with binding buffer as a control. Each mixture was then incubated with 50 μl TALON metal affinity resin in a 1.5 ml tube at 4°C for 20 min. After three brief washes with the binding buffer containing 10 mM imidazole, proteins bound to the resin were eluted with the binding buffer containing 150 mM imidazole. Aliquots of the eluted protein sample (10 μl each) were analyzed by SDS-PAGE and stained with Coomassie brilliant blue. Protein bands specifically bound to the His-tagged bait protein were excised from the gel, and in-gel digestion and peptide mapping of the tryptic digests were performed as described previously (Lee

et al., 2007; Park et al., 2013).

3.4. Bacterial two-hybrid (BACTH) assays.

Protein-protein interactions in live *E. coli* cells were assayed using the BACTH system based on the reconstitution of adenylate cyclase activity as described previously (Karimova et al., 1998). Briefly, the *cya*-deficient *E. coli* K-12 strain, BTH101, was co-transformed with derivatives of pUT18C and pKT25 encoding T18 and K25 fragments of *B. pertussis* adenylate cyclase, respectively. The co-transformants were spotted on LB plates containing 100 μg/ml streptomycin, 100 μg/ml ampicillin, and 50 μg/ml kanamycin with 40 μg/ml 5-bromo-4-chloro-3-indolyl-β-D-galactopyranoside (X-gal) as the color indicator for β-galactosidase activity and then incubated at 30°C overnight. To quantify the strength of the interaction, the co-transformants were grown in LB medium at 30°C to stationary growth phase, and the β-galactosidase activity was measured as described by Miller (Miller, 1972).

3.5. *In vitro* assay for ppGpp hydrolase activity of SpoT.

The *in vitro* ppGpp hydrolase activity of SpoT was assayed in a 30 μl reaction mixture containing 50 mM Tris-HCl (pH 8.0), 4 mM $MnCl_2$, 15 mM Mg-acetate, 10 mM DTT, 90 mM sodium formate, 25 mM ammonium acetate, and indicated concentrations of ppGpp and GST-SpoT protein in the presence of Rsd, HPr or both. After incubation at 37°C for the indicated time, the reaction was terminated by the addition of 1 μl 88% formic acid, and then trifluoroacetic acid was added to a final concentration of 10%. The reaction product generated from ppGpp was then analyzed by high performance liquid chromatography (HPLC) using a Varian dual pump system connected to an ultraviolet-visible detector. A 20 μl reaction mixture

was applied to a Supelcosil LC-18-T reverse phase chromatography column (Sigma Aldrich) equilibrated with 100 mM KH_2PO_4 and 8 mM tetrabutyl ammonium hydrogen sulfate (pH 2.6) in water and then chromatographed using a linear gradient of 0–30% methanol containing 100 mM KH_2PO_4 and 8 mM tetrabutyl ammonium hydrogen sulfate (pH 2.6) at a flow rate of 1 ml/min for 30 min. The eluted nucleotides were detected at 254 nm.

3.6. Detection of intracellular (p)ppGpp levels.

Overnight grown *E. coli* culture was inoculated into fresh low-phosphate (0.2 mM) MOPS minimal medium (Mechold et al., 2013) containing 0.2% galactose and 0.02% arabinose and 100 μCi/ml $^{32}PO_4^{3-}$ to an OD_{600} of 0.05 and incubated with shaking at 37°C. When OD_{600} reached ~0.2, serine hydroxamate (1 mg/ml) was added to trigger the stringent response. At the indicated times, 20 μl samples were mixed with an equal volume of 17 M formic acid (Mechold et al., 2002). After four freeze-thaw cycles in liquid nitrogen, the samples were centrifuged at 16,000 × *g* for at least 1 min to remove cell debris. Then 5 μl of supernatants was spotted onto a polyethyleneimine plate (Merck Millipore) and developed in 1.5 M KH_2PO_4 (pH 3.4) as mobile phase at room temperature. The plate was autoradiographed using Bio-imaging Analyzer (FujiFilm) and (p)ppGpp signals were measured using myImageAnalysis™ Software (Thermo Fisher Scientific).

3.7. Determination of the *in vivo* phosphorylation state of HPr.

The phosphorylation state of HPr was determined as previously described with some modifications (Choe et al., 2017). N^1-Phosphohistidine residues are known to be very unstable at neutral and acidic pH, thus exposure of samples to pH <9.0 was minimized. *E. coli* MG1655/pACYC-HPr was

cultivated in LB medium containing the indicated sugars. Cell cultures (0.2 ml at OD_{600} = 0.3) were quenched, the phosphorylation states of HPr were fixed, and the cells were disrupted at the same time by mixing with 15 μl of 5 M NaOH, followed by vortexing for 20 s. After the addition of 45 μl of 3 M sodium acetate (pH 5.2) and 0.65 ml of ethanol, the samples were centrifuged at 16,000 × *g* at 4°C for 10 min. The pellet was suspended in 20 μl of native PAGE sample buffer containing 1 M urea, and immediately analyzed by 16% native PAGE. Proteins were then electrotransferred onto Immobilon-P (Merck Millipore) following the manufacturer's protocol and HPr was detected by immunoblotting using antiserum against HPr raised in rabbits. The protein bands were visualized using Immobilon Western chemiluminescent HRP substrate (Merck Millipore) following the manufacturer's instructions.

3.8. RNA isolation and qRT-PCR.

E. coli cells were grown to late logarithmic phase in LB medium containing appropriate antibiotics and 0.02% arabinose. Cells were harvested and total RNA was prepared using MiniBEST Universal RNA Extraction Kit (Takara Bio). Genomic DNA was removed using RNase-free DNase I (Promega). The same amount of RNA (2000 ng) from each culture was converted into cDNA using cDNA EcoDry^{TM} Premix (Takara Bio). cDNAs were diluted 40-fold and subjected to qRT-PCR analyses using gene-specific primers and SYBR Premix Ex Taq II (Takara Bio). Amplification and detection of specific products were performed using the CFX96 Real-Time System (Bio-Rad). For normalization of the transcript level, the *rrsG* gene was used as a reference. The relative expression level was calculated as the difference between the threshold cycle (Ct) of the target gene and the Ct of the reference gene for each template.

Table II-1. Bacterial strains and plasmids used in this study

Strain or plasmid	Genotype or phenotype	Source
Strains		
MG1655	WT *E. coli* K-12	(Blattner et al., 1997)
ER2566	F⁻ λ⁻ f*huA2* [*lon*] *ompT lacZ::T7 gene 1 gal sulA11* Δ(*mcrC-mrr*)*114::IS10 R*(*mcr-73::miniTn10-TetS*)*2 R*(*zgb-210::Tn10*)(*TetS*) *endA1* [*dcm*]	New England Biolabs
BTH101	F⁻, *cya-99*, *araD139*, *galE15*, *galK16*, *rpsL1* (Str^R), *hsdR2*, *mcrA1*, *mcrB1*	(Karimova et al., 2000)
MG1655Δ*rsd*	MG1655 *rsd*::Tet^R	(Park et al., 2013)
MG1655Δ*relA*Δ*spoT*	MG1655 *relA*::Km^R, *spoT*::Cm^R	This study
MG1655Δ*relA*	MG1655 *relA*::Km^R	This study
MG1655Δ*relA*Δ*rsd*	MG1655 *relA*::Km^R, *rsd*::tet^R	This study
GI698	F⁻ λ⁻ *lacI*^{q} *lacPL8 ampC*::P_{trp} cI	(LaVallie et al., 1993)
Plasmids		
pETDuet-1	Cloning vector; Amp^R	Novagen
pET-HisRsd	pETDuet-1–derived expression vector for His-Rsd	(Park et al., 2013)
pET-Rsd	pETDuet-1–derived expression vector for Rsd	(Park et al., 2013)
pET-SpoTC1	pETDuet-1–derived expression vector for truncated version of SpoT (384-702)	This study
pET-SpoTN2	pETDuet-1–derived expression vector for truncated version of SpoT (1-447)	This study
pUT18C	ColEI-ori, P_{lac}::*cyaA* 225–399, encoding *B. pertussis* CyaA T18 fragment, Amp^R	(Karimova et al., 1998)
pUT18C-zip	ColEI-ori, P_{lac}::*cyaA* 225–399φGCN4-zip, Amp^R	(Karimova et al., 2001)
pUT18C-Rsd	Contains *E. coli* Rsd fused to *B. pertussis* CyaA T18 fragment, Amp^R	This study
pUT18C-Rsd(D63A)	Asp63 was mutated to Ala in pUT18C-Rsd	This study
pUT18C-SpoT	Contains *E. coli* SpoT fused to *B. pertussis* CyaA T18 fragment, Amp^R	This study
pKT25	ori p15A, P_{lac}::*cyaA* 1–224, encoding *B. pertussis* CyaA T25 fragment, Km^R	(Karimova et al., 1998)
pKT25-zip	ori p15A, P_{lac}::*cyaA* 1–224φGCN4-zip, Km^R	(Karimova et al., 2005)
pKT25-Rsd	Contains *E. coli* Rsd fused to *B. pertussis* CyaA T25 fragment, Km^R	This study
pKT25-SpoT	Contains *E. coli* SpoT fused to *B. pertussis* CyaA T25 fragment, Km^R	This study
pKT25-SpoTN1	Contains *E. coli* SpoT (1-347) fused to *B. pertussis* CyaA T25 fragment, Km^R	This study
pKT25-SpoTC1	Contains *E. coli* SpoT (384-702) fused to *B. pertussis*	This study

	CyaA T25 fragment, Km^R	
pKT25-SpoTN2	Contains *E. coli* SpoT (1-447) fused to *B. pertussis* CyaA T25 fragment, Km^R	This study
pKT25-SpoTC2	Contains *E. coli* SpoT (448-702) fused to *B. pertussis* CyaA T25 fragment, Km^R	This study
pKT25-RelA	Contains *E. coli* RelA fused to *B. pertussis* CyaA T25 fragment, Km^R	This study
pKT25-$EIIA^{Ntr}$	Contains *E. coli* $EIIA^{Ntr}$ fused to *B. pertussis* CyaA T25 fragment, Km^R	Gift from CR Lee
pKT25-$EIIA^{Ntr}$(H73A)	His73 was mutated to Ala in pKT25-$EIIA^{Ntr}$	Gift from CR Lee
pKT25-$EIIA^{Ntr}$(H73E)	His73 was mutated to Glu in pKT25-$EIIA^{Ntr}$	Gift from CR Lee
pGEX-4T-1	Cloning vector; Amp^R	GE Healthcare
pGEX-SpoT	pGEX-4T-1–derived expression vector for GST-SpoT	This study
pJK1113	pBAD24 with *oriT* of RP4 and *nptI*, P_{BAD}; Km^R, Amp^R	(Park et al., 2016)
pJK1113-Rsd	pJK1113-derived expression vector for Rsd, Km^R, Amp^R	This study
pJK1113-HPr(H15A)	pJK1113-derived expression vector for HPr (His15 to Ala), Km^R, Cm^R	This study
pKD46	Red recombinase expression plasmid under the control of arabinose inducible promoter	(Datsenko and Wanner, 2000)
pRE1	Expression vector under control of λP_L promoter, Amp^R	(Reddy et al., 1989)
pRE-$HisEIIA^{Ntr}$	pRE1-based expression vector for His-$EIIA^{Ntr}$	(Lee et al., 2005)
pRE-HIcrr	pRE1-based expression vector for HPr, EI and $EIIA^{Glc}$	(Choe et al., 2017)
pACYC184	A low copy number cloning vector; Cm^R Tet^R	(Chang and Cohen, 1978)
pACYC-HPr	*E. coli ptsH* promoter and its ORF cloned between SphI and SalI sites of pACYC184	(Choe et al., 2017)
pACYC-Rsd	*E. coli rsd* promoter and its ORF cloned between BamHI and SphI sites of pACYC184	(Park et al., 2013)
pACYC-Rsd(D63A)	Asp63 was mutated to Ala in pACYC-Rsd	This study

Table II-2. Oligonucleotides used in this study

Name	Oligonucleotide sequence (5'-3')	Use(s)
RS925	AGTTCGCATATGGAATTTATCGAGAGCGTTAAATC (NdeI)	Construction of
RS926	GTTCATAAACTCGAGATTTCGGTTTCGGGTGAC (XhoI)	pET-SpoTC1
RS927	AGCGGGCCATGGCCTTGTATCTGTTTGAAAGCCTG (NcoI)	Construction of
RS928	CGACAAAGAATTCTTACCAAGCGGCATTCGGGCGA (EcoRI)	pET-SpoTN2
RS929	ACAAACTTGCGGAGGATCCCATGCTTAACC (BamHI)	Construction of
RS930	CTGCGCTGTTAAGAATTCATTTACATTCAA (EcoRI)	pUT18C-Rsd
RS931	TTGTCAGAGCCTGGTCGCTTACTTGTCTGCCGGAC	Construction of
RS932	GTCCGGCAGACAAGTAAGCGACCAGGCTCTGACAA	pUT18C-Rsd(D63A)
RS933	CAAAGCGGGGATCCCTTGTATCTGTTTGAAAGCCT (BamHI)	Construction of
RS934	CCCAACACGTTATGCACGCATGAATTCAATGCTCG (EcoRI)	pUT18C-SpoT
RS935	ACAAACTTGCGGAGGATCCCATGCTTAACC (BamHI)	Construction of
RS936	CTGCGCTGTTAAGAATTCATTTACATTCAA (EcoRI)	pKT25-Rsd
RS937	CAAAGCGGGGATCCCTTGTATCTGTTTGAAAGCCT (BamHI)	Construction of
RS938	CCCAACACGTTATGCACGCATGAATTCAATGCTCG (EcoRI)	pKT25-SpoT
RS939	AGCGGGGGATCCATTGTATCTGTTTGAAAGCCTG (BamHI)	Construction of
RS940	ATTTGTGAATTCGTACTTTAGGTTTCGCCGTGCTC (EcoRI)	pKT25-SpoTN1
RS941	GATCTCGGATCCATTCCCGGATGAGATTTACG (BamHI)	Construction of
RS942	GTTCATGAATTCTTAATTTCGGTTTCGGGTGAC (EcoRI)	pKT25-SpoTC1
RS943	AGCGGGGGATCCATTGTATCTGTTTGAAAGCCTG (BamHI)	Construction of
RS944	AGCGCCGAATTCTTAGGTAATGATTTCAACGGTT (EcoRI)	pKT25-SpoTN2
RS945	GAAATCGGATCCAGCTCCGGGCGCTCGCCCGAATG (BamHI)	Construction of
RS946	GTTCATGAATTCTTAATTTCGGTTTCGGGTGAC (EcoRI)	pKT25-SpoTC2
RS947	AAGGAGGGATCCAATGGTTGCGGTAAGAAGTGCAC (BamHI)	Construction of
RS948	GCAAATGAATTCCTAACTCCCGTGCAACCGACGCG (EcoRI)	pKT25-RelA
RS949	AGCGGGGGATCCTTGTATCTGTTTGAAAGCCTG (BamHI)	Construction of
RS950	GTTCATCTCGAGTTAATTTCGGTTTCGGG (XhoI)	pGEX-SpoT
RS951	GCGGAGGAATTCATGCTTAACCAGCTCG (EcoRI)	Construction of
RS952	ACAGCGGTCGACTCAAGCAGGATGTTTGACGC (SalI)	pJK1113-Rsd
RS953	AATACAGTCGACATGTTCCAGCAAGAAGTTACC (SalI)	Construction of
RS954	GGGAAAGTCGACTTACTCGAGTTCCGCCATC (SalI)	pJK1113-HPr(H15A)
RS955	TTGTCAGAGCCTGGTCGCTTACTTGTCTGCCGGAC	Construction of
RS956	GTCCGGCAGACAAGTAAGCGACCAGGCTCTGACAA	pACYC-Rsd(D63A)
SpoT-F	GCCACCTACCAGGATATGGA	qRT-PCR
SpoT-R	GTACGGTCGGCAAGTTTGAT	
RelA-F	GAAGATGTGCTGCGTGAGAG	
RelA-R	GTACACGTTCATCTTCCGGC	

4. Results

4.1. (p)ppGpp hydrolase SpoT interacts with Rsd.

4.1.1. Identify a factor that interacts with His-tagged Rsd in *E. coli* extract.

Several reasons led us to explore the possibility that Rsd might have a specific role other than as an antagonist of the house-keeping sigma factor σ^{70} in *E. coli*. First, cellular levels of Rsd have been measured to be lower than that of σ^{70} (Jishage and Ishihama, 1998; Piper et al., 2009; Schmidt et al., 2016), indicating that Rsd may reduce but not fully antagonize σ^{70} activity. Second, although Rsd was identified as an antagonist of σ^{70} in *E. coli* 20 years ago (Jishage and Ishihama, 1998), no obvious phenotype has been observed in *rsd* deletion or overexpression strains to date. Therefore, the importance of Rsd as a σ^{70} antagonist *in vivo* has still remained elusive. For this reason, we set up a study to explore an *in vivo* role for Rsd other than what its name implies, and thereby establish a characteristic phenotype associated with the deletion or overexpression of Rsd.

In order to find a new physiological function of Rsd, we conducted ligand fishing experiment (Choe et al., 2017; Lee et al., 2007; Lee et al., 2014; Park et al., 2013) using an N-terminally hexahistidine-tagged Rsd (His-Rsd) as bait. A crude extract of *E. coli* MG1655 grown to stationary phase was mixed with TALON metal affinity resin (Takara Bio) in the absence or presence of His-Rsd. After brief washes, proteins bound to the resin were eluted with 150 mM imidazole and analyzed by SDS-PAGE and staining with Coomassie brilliant blue. The elution of a protein band for HPr, previously identified as the binding partner of Rsd (Park et al., 2013), appearing only in the fraction containing His-Rsd, supports the reliability of

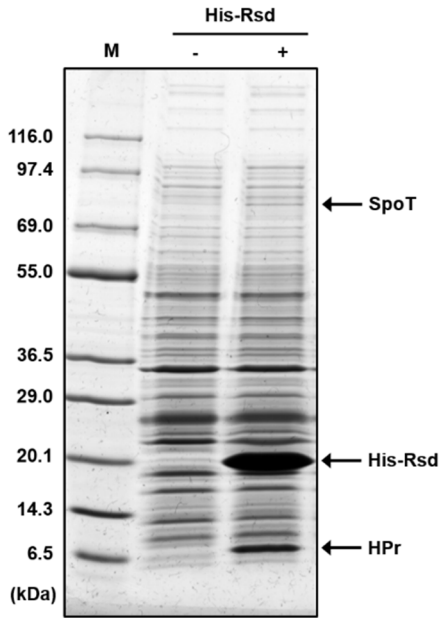

Figure II-1. Interaction of Rsd with SpoT.

Ligand fishing experiment was carried out to search for protein(s) specifically interacting with Rsd. Crude extract prepared from *E. coli* strain MG1655 was mixed with (lane +) or without (lane -) 150 μg of purified His-Rsd. Each mixture was incubated with 50 μl TALON resin for metal affinity chromatography. Proteins bound to each column were analyzed by SDS-PAGE using 4-20% gradient gel (KOMA Biotech). Protein bands bound specifically to His-Rsd are indicated by arrows. Lane M refers to the molecular mass markers (KOMA Biotech).

this ligand fishing experiment. Noteworthily, another protein band (migrating at apparent molecular mass of ~80 kDa) was also significantly enriched in the fraction containing His-Rsd (Figure II-1). Peptide mapping of the in-gel tryptic digests revealed that the digested band corresponded to SpoT, the bifunctional (p)ppGpp synthase/hydrolase (Hernandez and Bremer, 1991).

4.1.2. Confirmation of interaction between Rsd and SpoT.

To confirm the specific interaction between SpoT and Rsd, glutathione S-transferase (GST) was fused to the N-terminus of SpoT because the native form of SpoT was barely soluble when expressed from a plasmid. The crude extract containing the overexpressed GST-SpoT fusion protein was mixed with various amounts of purified Rsd and each mixture was incubated with TALON resin. After brief washes, proteins bound to the resin were eluted with 150 mM imidazole and analyzed by SDS-PAGE and Coomassie brilliant blue staining. As shown in Figure II-2A, a concentration-dependent interaction of Rsd with the GST-SpoT fusion protein was observed, indicating a specific interaction between the two proteins *in vitro*.

To test whether the interaction between SpoT and Rsd occurs *in vivo*, we performed bacterial two-hybrid (BACTH) assays (Karimova et al., 1998), which use the reconstitution of the activity of split *Bordetella pertussis* adenylate cyclase CyaA in the *cya*-deficient *E. coli* strain BTH101. While the BTH101 strain co-expressing T18-SpoT and T25-Rsd hybrid proteins produced measurable β-galactosidase activity, those co-expressing T18 and T25, T18-SpoT and T25, and T18 and T25-Rsd did not develop blue color on X-gal plates (Figure II-2B). These data indicate that Rsd interacts with SpoT both *in vitro* and *in vivo*.

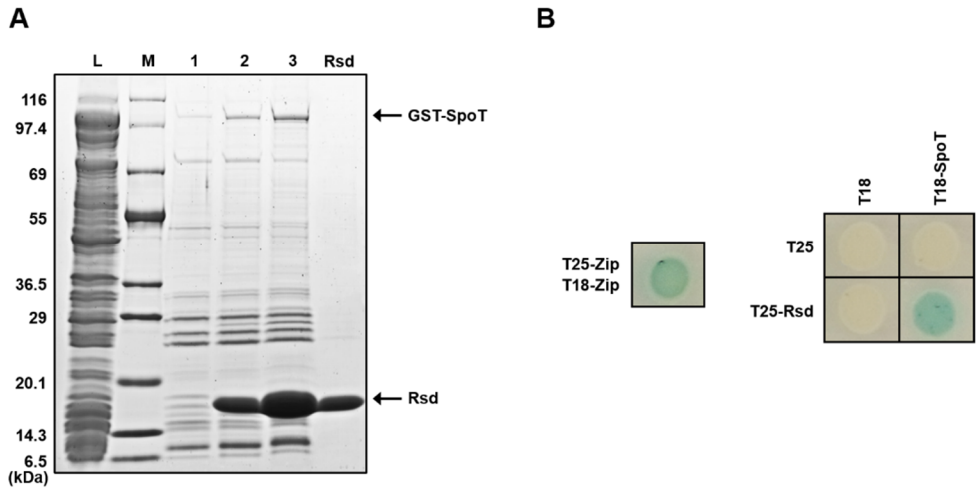

Figure II-2. *In vitro* and *in vivo* interaction of Rsd with SpoT.

(A) *E. coli* cell extract expressing GST-SpoT was mixed with various amounts of purified Rsd (0, 120, and 360 μg in lanes 1-3, respectively), and each mixture was incubated with 50 μl of TALON resin for metal affinity chromatography. Proteins bound to the resin were eluted with 2x SDS loading buffer (70 μl) and analyzed by SDS-PAGE and stained with Coomassie brilliant blue. Lane L, the *E. coli* cell lysate expressing GST-SpoT; lane M, the molecular mass markers (KOMA Biotech). (B) The bacterial two-hybrid (BACTH) assays to analyze the specific interaction of Rsd with SpoT *in vivo*. *E. coli* strain BTH101 coexpressing the indicated proteins was spotted on LB agar plates supplemented with 40 μg/ml X-gal as the color indicator for β-galactosidase activity and incubated at 30°C overnight. Zip, the leucine zipper of *Saccharomyces cerevisiae* GCN4, served as a positive control. The transformant coexpressing the unfused T25- and T18-fragments themselves served as a negative control.

4.1.3. Interaction of Rsd with the TGS domain of SpoT.

SpoT consists of an N-terminal enzymatic domain (NTD) and a C-terminal domain (CTD) (Figure II-3A). The enzymatic domain is composed of a (p)ppGpp hydrolase domain (HD) and a (p)ppGpp synthetase domain (SD) and it has been suggested that these enzyme activities are controlled by a C-terminal regulatory domain (Gentry and Cashel, 1996; Mechold et al., 2002). However, the regulation mechanism of SpoT activity in response to diverse starvation stresses remains largely unknown. It has been suggested that the CTD is involved in the regulation of SpoT activities, probably by ligand binding, by modification of the protein folding, or by both (Battesti and Bouveret, 2006). The TGS region of the CTD consists of ~50 amino acid residues and is predicted to predominantly carry a beta-sheet structure, which has been named after three protein families containing it (threonyl-tRNA synthetase, Obg family of GTPases and SpoT) (Atkinson et al., 2011; Sankaranarayanan et al., 1999; Wolf et al., 1999). Acyl carrier protein (ACP) was shown to stimulate the (p)ppGpp synthetase activity of SpoT by directly interacting with the TGS domain (Battesti and Bouveret, 2006).

To determine the domain(s) of SpoT required for the interaction with Rsd, we constructed several truncated fragments of SpoT fused to the T25 domain of *B. pertussis* adenylate cyclase (Figure II-3B). Each SpoT fragment fused to the T25 domain was co-expressed with Rsd fused to the T18 domain (T18-Rsd) in the *cya*-deficient *E. coli* strain BTH101 and their interactions were assessed by measuring β-galactosidase activity (Figure 3B). While Rsd interacted with the CTD of SpoT (SpoTC1), little interaction was detected with the NTD (SpoTN1). To pinpoint the domain in the CTD of SpoT that interacts with Rsd, we examined the interaction of Rsd with two more nonoverlapping fragments of SpoT: one consisting of the NTD and the TGS domain (construct SpoTN2; amino acid 1 to 447) and the other corresponding to the CTD lacking the TGS domain (construct SpoTC2;

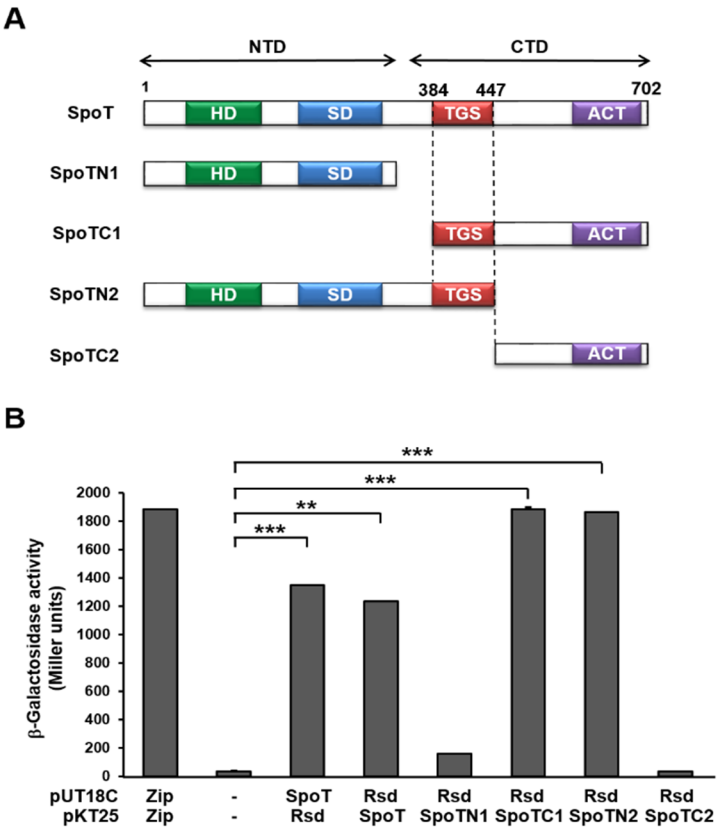

Figure II-3. Interaction of Rsd with the TGS domain of SpoT.

(A) A schematic diagram of SpoT and its truncated forms. HD domain indicates ppGpp hydrolase domain; SD domain, ppGpp synthetase domain; TGS domain named for three protein families containing it (threonyl-tRNA synthetase, Obg family of GTPases and SpoT); ACT domain, named after aspartokinase, chorismate mutase and TyrA. (B) Quantitative BACTH assays to assess the *in vivo* interaction of Rsd with SpoT. β-Galactosidase activity was measured with permeabilized cells co-transformed with derivatives of pUT18C and pKT25 as indicated by direct enzyme assay (Miller units). Zip, the leucine zipper domain of *S. cerevisiae* GCN4, served as a positive control. The mean and standard deviation (SD) of three independent measurements are shown. Statistical significance was determined using Student's t-test (**, $P < 0.005$, and ***, $P < 0.001$).

amino acid 448 to 702), both fused to the T25 domain. While Rsd interacted with SpoTN2, no interaction was detected with SpoTC2. These data suggest that the TGS domain of SpoT is necessary for the interaction with Rsd.

The TGS domain-dependent interaction between Rsd and SpoT was further confirmed using metal affinity pull-down assays with His-Rsd and crude extracts of *E. coli* cells overexpressing the truncated constructs SpoTN2 and SpoTC1 (Figure II-4). As the amount of His-Rsd increased, the amounts of pulled down SpoTN2 and SpoTC1 proteins also increased. Together, these data confirmed that Rsd interacts with the TGS domain of SpoT. We could not test the direct interaction of Rsd with the TGS domain alone, because we could not express the TGS domain itself even after repeated trials.

4.1.4. Specific interaction of Rsd with SpoT.

RelA and SpoT share a similar domain organization and significant amino acid sequence identity (~31% throughout the entire protein) in *E. coli*. While both of them possess (p)ppGpp synthetase activity, the most conserved region between the two proteins corresponds to the TGS domain, with ~52% amino acid sequence identity with each other, rather than with the SD domain (~50% identity). To examine whether RelA can also interact with Rsd through its TGS domain, RelA was fused to the T25 domain (T25-RelA) and the resulting hybrid protein was tested in two-hybrid assays with T18-Rsd (Figure II-5A). While the BTH101 strain co-expressing T18-Rsd and T25-SpoT showed a significantly higher β-galactosidase activity than the negative control co-expressing T18 and T25, the strain co-expressing T18-Rsd and T25-RelA did not produce β-galactosidase. This

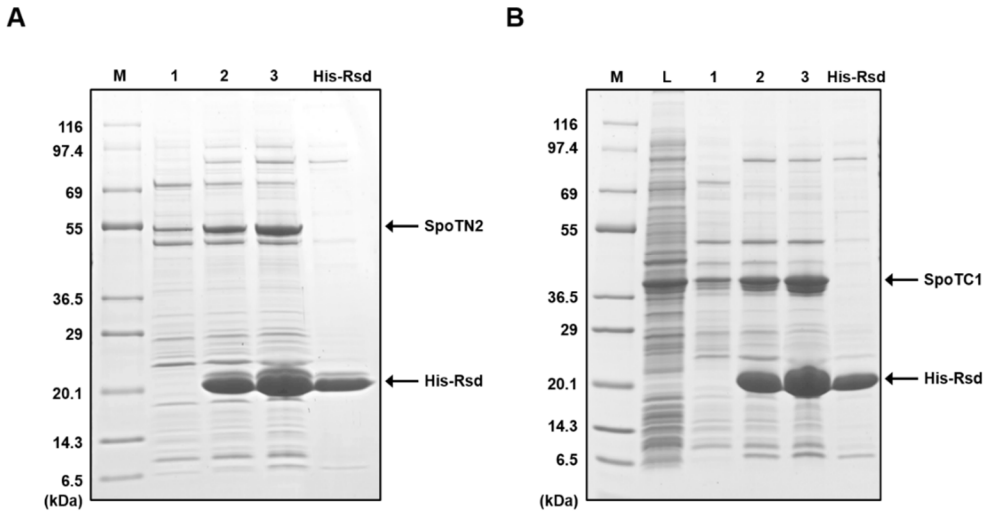

Figure II-4. Direct interaction of Rsd with the TGS domain of SpoT.

Two truncated forms of SpoT containing the TGS domain, SpoTN2 (A) and SpoTC1 (B), were expressed in *E. coli*, and crude extracts were mixed with various amounts of purified His-Rsd (0, 120, and 360 μg in lanes 1-3, respectively). Each mixture was incubated with 50 μl TALON resin for metal affinity chromatography. Bound proteins were eluted with 70 μl of 2x SDS sample buffer and analyzed by SDS-PAGE and Coomassie blue staining. Purified His-Rsd was run as a control. Lane M, the molecular mass markers (KOMA Biotech); lane L in panel *B*, the crude cell lysate loaded on the TALON resin.

result suggests that Rsd specifically interacts with SpoT. It is interesting to note that ACP also interacts with SpoT but not with RelA in *E. coli* (Battesti and Bouveret, 2006).

Enzyme IIA^{Ntr} of the nitrogen PTS was previously shown to interact with SpoT in *Ralstonia eutropha*, the orthologue of *E. coli* SpoT protein (Karstens et al., 2014) and a single RelA/SpoT homologue protein of *Caulobacter crescentus* (Ronneau et al., 2016). Rsd has a similar molecular mass and pI (18.24 kDa and 5.65, respectively) to $EIIA^{Ntr}$ (17.96 kDa and 5.57, respectively) in *E. coli*. Therefore, we wanted to test whether the interaction of $EIIA^{Ntr}$ with SpoT also occurs in *E. coli*. Since SpoTC1 showed a relatively higher solubility than other SpoT constructs, we used SpoTC1 to study its interaction with $EIIA^{Ntr}$. The crude extract overexpressing the truncated constructs SpoTC1 was mixed with various amounts of purified Rsd or $EIIA^{Ntr}$ and incubated with TALON resin. To the mixture containing $EIIA^{Ntr}$, pyruvate was added to dephosphorylate or PEP to phosphorylate $EIIA^{Ntr}$. After brief washes, proteins bound to the resin were eluted with 150 mM imidazole and analyzed by SDS-PAGE and Coomassie brilliant blue staining. As shown in Figure II-5B, SpoTC1 interacted with Rsd but not with $EIIA^{Ntr}$, regardless of its phosphorylation state. The interaction between $EIIA^{Ntr}$ and full-length SpoT was also tested *in vivo* by BACTH assays (Figure II-5A). Neither of wild-type $EIIA^{Ntr}$, its phosphomimetic (H73E) and dephosphomimetic mutant (H73A) could interact with SpoT, indicating that the SpoT-Rsd interaction is specific in *E. coli*. Our data also suggest that stress signals and regulatory mechanisms for the stringent response could be diverse among microorganisms, consistent with the previous report (Karstens et al., 2014).

Figure II-5. Specific interaction of Rsd with SpoT.

(A) *E. coli* strain BTH101 coexpressing the indicated fusion proteins was spotted on LB agar plates supplemented with 40 μg/ml X-gal as the color indicator for β-galactosidase activity and incubated at 30°C overnight. β-Galactosidase activity was measured in strains coexpressing indicated proteins by direct enzyme assay (Miller units). Zip, the leucine zipper domain of *S. cerevisiae* GCN4, served as a positive control. The transformant coexpressing the unfused T25- and T18-fragments served as a negative control. The mean and standard deviation (SD) of three independent measurements are shown. Statistical significance was determined using Student's t-test (***, $P < 0.001$). (B) An *E. coli* extract expressing SpoTC1 was mixed with binding buffer (lane 1), 300 μg of purified His-EIIA^{Ntr} in the presence of 1 mM pyruvate (lane 2) or 1 mM PEP (lane 3), and 300 μg of purified His-Rsd (lane 4). Each mixture was incubated with 50 μl of TALON resin for metal affinity chromatography. Proteins bound to the resin were eluted with 2x SDS loading buffer (70 μl) and analyzed by SDS-PAGE and stained with Coomassie brilliant blue. Lane L, the *E. coli* extract expressing SpoTC1; lane M, the molecular mass markers (Thermo Fisher Scientific).

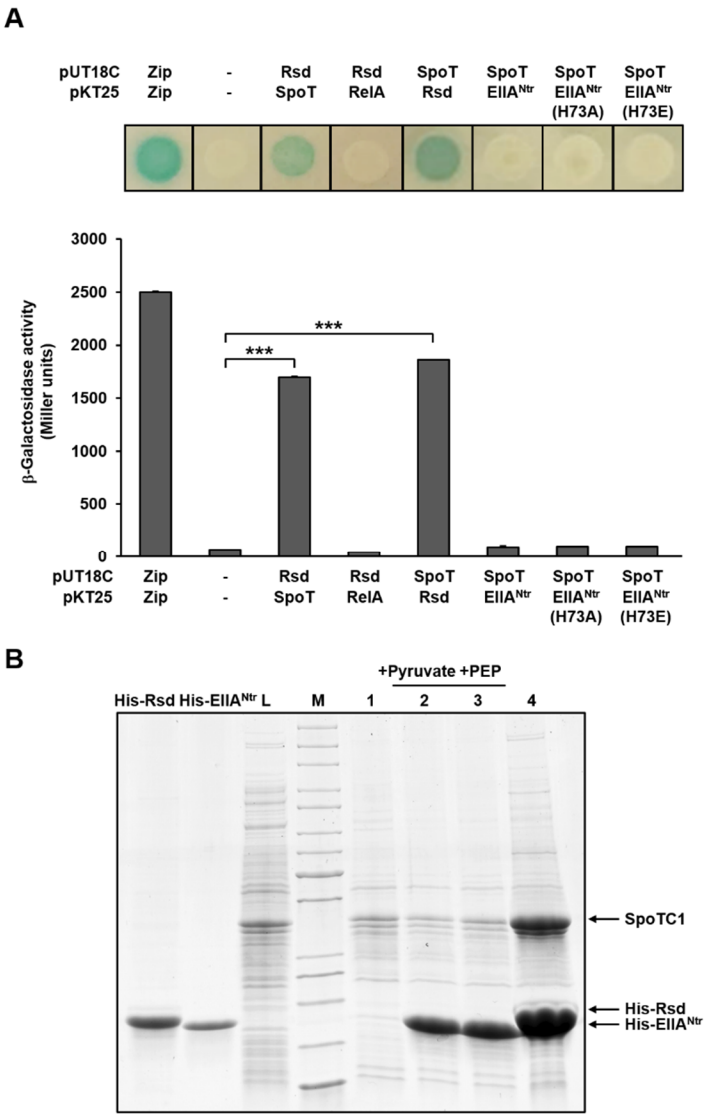
A
pUT18C Zip - Rsd Rsd SpoT SpoT SpoT SpoT
pKT25 Zip - SpoT RelA Rsd EIIA^Ntr EIIA^Ntr (H73A) EIIA^Ntr (H73E)
β-Galactosidase activity (Miller units)
3000
2500
2000
1500
1000
500
0
***
***
B
+Pyruvate +PEP
His-Rsd His-EIIA^Ntr L M 1 2 3 4
SpoTC1
His-Rsd
His-EIIA^Ntr

4.2. Activation of the (p)ppGpp hydrolase activity of SpoT by Rsd.

4.2.1. The stimulatory effect of Rsd on the (p)ppGpp hydrolase activity of SpoT *in vitro*.

Since Rsd specifically interacts with SpoT through the TGS domain, we predicted that Rsd could regulate the catalytic activity of SpoT. The (p)ppGpp hydrolysis function of SpoT is critical for balancing cellular (p)ppGpp concentrations in the stringent (*relA*$^+$) strains, and therefore disruption of the *spoT* gene is lethal in *E. coli relA*$^+$ strains (Xiao et al., 1991). Thus, we first tested the effect of Rsd on the ppGpp hydrolase activity of SpoT by measuring the amounts of hydrolyzed ppGpp and produced GDP using HPLC. As shown in Figure II-6, GST-SpoT hydrolyzed ppGpp to GDP *in vitro*, with the Km and k_{cat} values of SpoT for ppGpp being 24.48 μM and 3.38 min^{-1}, respectively. The Km value is well within the physiological ppGpp concentrations given that the cellular level of ppGpp corresponds to 1 mM during the stringent response (Kuroda et al., 1997). Interestingly, the ppGpp hydrolase activity of SpoT increased with the addition of Rsd but not by the same amount of bovine serum albumin (BSA), a known carrier protein (Figure II-7). Rsd alone did not show ppGpp hydrolase activity, indicating no contamination with SpoT during purification of Rsd. Therefore, these data suggest that Rsd activates the ppGpp hydrolase activity of SpoT by direct interaction *in vitro*.

As shown in Figure II-8, the stimulatory effect of Rsd on the SpoT ppGpp hydrolase activity appeared to be concentration-dependent and saturable. The concentration of Rsd required for half-maximum stimulation of the ppGpp hydrolase activity ($K_{0.5}$) was approximately 3.65 μM. This $K_{0.5}$ value corresponds to approximately 2,200 molecules per cell when calculated assuming an *E. coli* cell volume of 1 x 10^{-15} L (Piper et al., 2009). Rsd levels were reported to increase by approximately twofold during

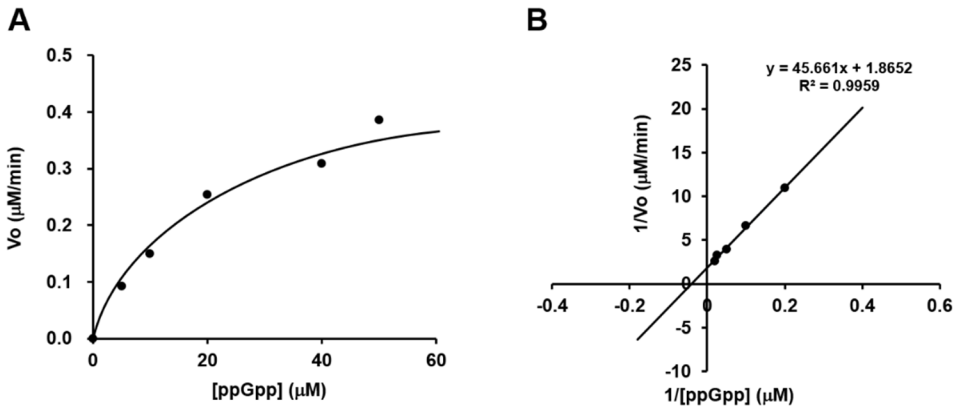

Figure II-6. Kinetic characterization of SpoT ppGpp hydrolase activity.
(A) The ppGpp hydrolase activity of purified GST-SpoT (0.4 μM) was assayed in reaction mixtures containing various amounts of ppGpp. After incubation at 37°C for 7 min, reactions were stopped by the addition of formic acid to ~ 3%, then trifluoroacetic acid was added to a final concentration of 10%. The reaction products were analyzed by HPLC as described in Materials and Methods. The initial velocity of ppGpp hydrolysis (or GDP production) was plotted as a function of ppGpp concentration. Representative data from two independent experiments are shown. The data were fitted to Michaelis-Menten kinetics. (B) A Lineweaver-Burk plot of the data in panel A.

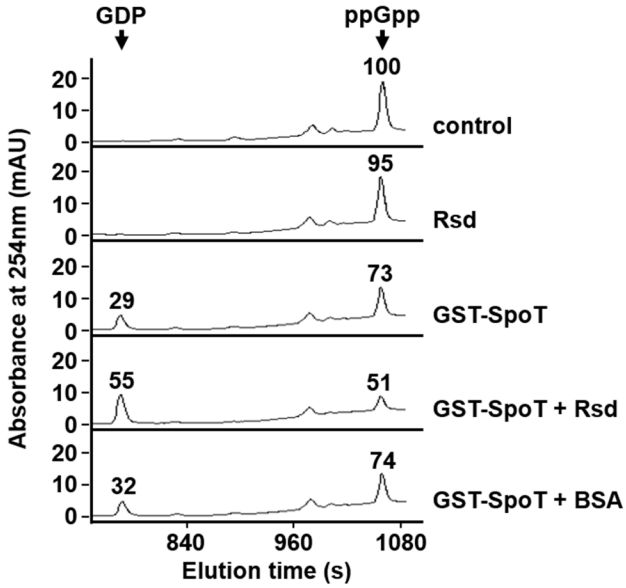

Figure II-7. Activation of the (p)ppGpp hydrolase activity of SpoT by Rsd.

The stimulatory effect of Rsd on the ppGpp hydrolase activity of SpoT was measured *in vitro*. The ppGpp hydrolase activity of purified GST-SpoT (3 μg) was assayed in a reaction mixture containing 23.33 μM ppGpp in the presence of purified Rsd or BSA (19 μg each). After incubation at 37°C for 5 min, the reaction mixtures were applied to a Supelcosil LC-18-T HPLC column (Sigma Aldrich), and ppGpp and GDP were monitored by measuring the absorbance at 254 nm (A_{254}). Relative peak areas are shown above each peak, considering the peak area of ppGpp in the control sample as 100. Representative data from three independent experiments are shown.

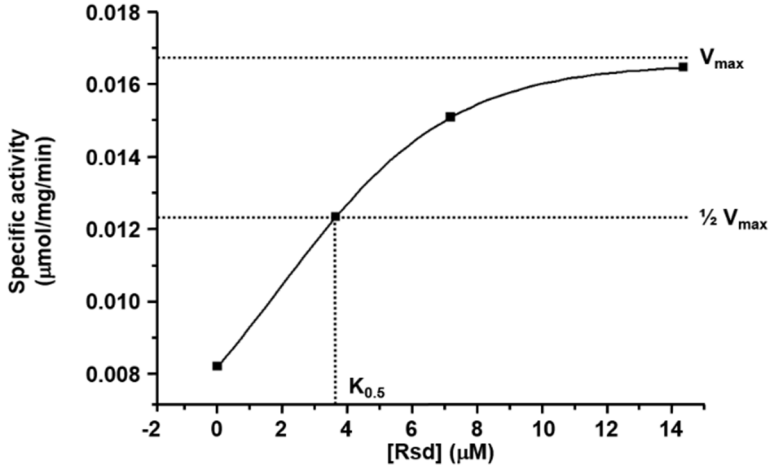

Figure II-8. Concentration-dependent stimulation of the ppGpp hydrolase activity of SpoT by Rsd.

The ppGpp hydrolase activity of purified GST-SpoT (0.4 μM) was assayed in reaction mixtures containing 30 μM ppGpp and various amounts of purified Rsd (0, 3.7, 7.3, and 14.6 μM). Non-linear regression fits of experimental data were performed using Origin software. The concentration of Rsd required for half-maximum stimulation of the ppGpp hydrolase activity ($K_{0.5}$) was 3.65 μM. Representative data from two independent experiments are shown.

stationary phase, with ~6,200 molecules in an *E. coli* cell, compared with the levels in exponentially growing cells (~3,300 molecules per cell) (Piper et al., 2009). The cellular levels of SpoT are approximately one tenth of that for Rsd (Schmidt et al., 2016). Thus, it is reasonable to assume that regulation of the SpoT ppGpp hydrolase activity by Rsd can occur *in vivo*, especially in the stationary phase or under stress conditions.

4.2.2. Rsd stimulates (p)ppGpp hydrolase activity of SpoT *in vivo*.

Because (p)ppGpp plays a crucial role in the stringent response to amino acid starvation, strains lacking (p)ppGpp are unable to grow on minimal medium without amino acids (Xiao et al., 1991). Therefore, we assumed that, if Rsd stimulates the (p)ppGpp hydrolysis function of SpoT *in vivo*, increased expression of Rsd might deplete intracellular (p)ppGpp pools, resulting in a growth defect under amino acid starvation conditions. To test this assumption, we compared the growth of *E. coli relA* mutant strains with different levels of Rsd expression in the absence and presence of serine hydroxamate (SHX), an inhibitor of seryl-tRNA synthetase as a serine homolog (Figure II-9). It is known that the addition of SHX induces serine starvation and thereby the stringent response (Dalebroux and Swanson, 2012). As expected, an *E. coli relA spoT* double mutant lacking (p)ppGpp ((p)ppGpp^0 strain) could not grow in MOPS minimal medium with galactose as a sole carbon source in the absence of amino acids, whereas the *relA rsd* double mutant carrying the control plasmid pACYC184 showed normal growth regardless of the presence of SHX, indicating that the weak (p)ppGpp synthetic activity of SpoT alone is enough to cope with serine starvation. However, the *relA* mutant carrying pACYC184 and the *relA rsd* double mutant carrying pACYC184-Rsd expressing Rsd from its own promoter (Park et al., 2013) had a severe growth defect similar to the (p)ppGpp^0 strain as the SHX concentration increased, while they exhibited a

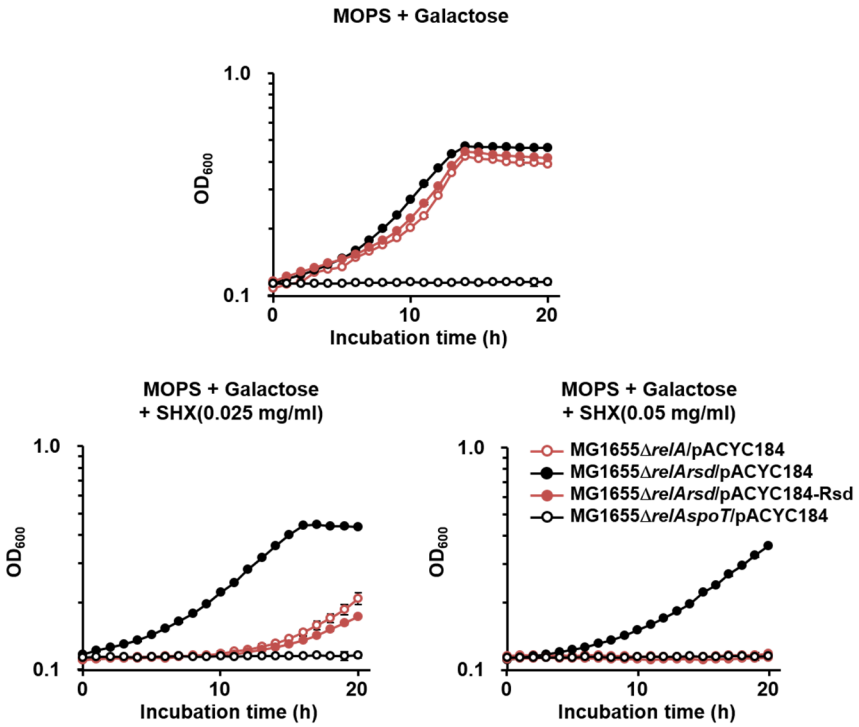

Figure II-9. Activation of the (p)ppGpp hydrolase activity of SpoT by Rsd *in vivo*.

Growth curves of *E. coli* strains in MOPS minimal medium (pH 7.2) supplemented with 0.2% galactose in the absence and presence of SHX. After inoculation, 100-µl aliquots of each strain were transferred into a 96-well plate and growth was monitored at 600 nm using a multimode microplate reader (TECAN). The mean and standard deviation (SD) of three measurements are shown

similar growth rate to the *relA rsd* double mutant carrying pACYC184 in the absence of SHX. These data indicate that Rsd stimulates SpoT-mediated (p)ppGpp hydrolysis *in vivo*.

To confirm that the effect of Rsd was due to an increase in the (p)ppGpp hydrolase activity of SpoT, we measured the intracellular (p)ppGpp levels (Figure II-10). A robust induction of (p)ppGpp synthesis was observed in both *rsd* deletion and overexpression strains 30 min after the addition of SHX, indicating that induction of the stringent response by SHX is little affected by the expression level of Rsd. However, the cellular levels of (p)ppGpp decreased much more rapidly in the *rsd* mutant strain carrying pJK1113-Rsd than in the same strain carrying pJK1113, indicating that Rsd stimulates the hydrolysis of (p)ppGpp *in vivo*. This observation explains that the growth defect of *rsd*$^{+}$ strains under SHX-induced serine starvation (Figure II-9) is due to the increased degradation of (p)ppGpp.

4.2.3. Stimulatory effect of Rsd on the (p)ppGpp hydrolase activity of SpoT is dependent on the TGS domain.

Since the TGS domain of SpoT is required for the Rsd-SpoT interaction (Figures II-3 and II-4), it was expected that the regulation of the SpoT hydrolase activity by Rsd would depend on the presence of the TGS domain. To test this assumption, the *relA spoT* double mutant was complemented with plasmids expressing the truncated forms of SpoT and the growth of each strain was examined (Figure II-11A). The expression of the truncated forms of SpoT (SpoTN1 and SpoTN2) was confirmed by quantitative RT-PCR (qRT-PCR) (Figure II-11B). While the *relA spoT* double mutant expressing SpoTN1 devoid of the TGS domain grew well in MOPS medium containing galactose and SHX, severe growth defect was observed for the same strain expressing SpoT or SpoTN2 carrying the TGS domain (Figure II-11C). Interestingly, however, this growth inhibition due to the expression

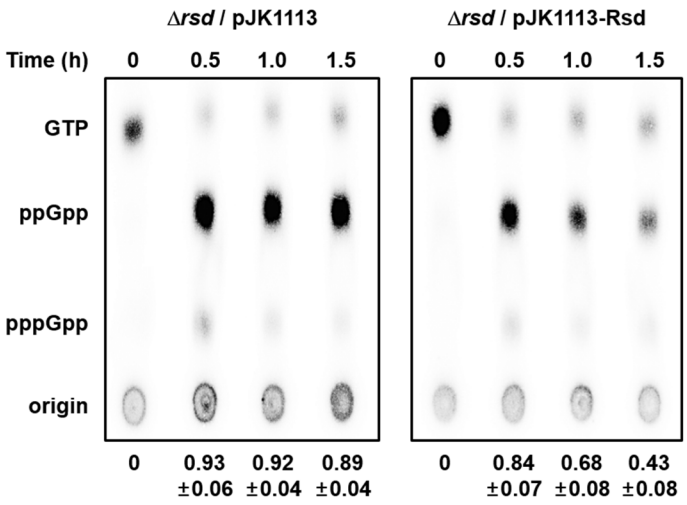

Figure II-10. Activation of the (p)ppGpp hydrolysis by Rsd *in vivo*.

The MG1655Δ*rsd* strain carrying pJK1113 or pJK1113-Rsd was incubated in low-phosphate MOPS minimal medium containing 0.2% galactose, 0.02% arabinose and 100 μCi/ml $^{32}PO_4^{3-}$. Exponentially growing cells were treated with SHX (1 mg/ml) and intracellular (p)ppGpp concentrations were analyzed by TLC at the indicated times. Relative amounts of (p)ppGpp were calculated as the intensity of (p)ppGpp divided by that of (p)ppGpp plus GTP. The mean and standard deviation (SD) of three independent measurements are shown below each lane.

Figure II-11. Stimulatory effect of Rsd on the (p)ppGpp hydrolase activity of SpoT is dependent on the TGS domain.

(A) A schematic diagram of SpoT and its truncated forms used in this experiment. (B) The relative transcript levels of *spoT* were determined by qRT-PCR in the *relA* mutant harboring pJK1113 and the *relA spoT* double mutant harboring pJK1113, pJK1113-SpoT, pJK1113-SpoTN1, or pJK1113-SpoTN2, as described in the Materials and Methods. The mean and standard deviation (SD) of three independent measurements are shown. (C) Growth curves of the *relA spoT* double mutant or the *relA spoT rsd* triple mutant harboring pJK1113 (blue lines), pJK1113-SpoT (red lines), pJK1113-SpoTN1 (green lines), or pJK1113-SpoTN2 (black lines) in MOPS minimal medium (pH 7.2) supplemented with 0.2% galactose and 0.02% arabinose. SHX (0.05 mg/ml) was added to induce the stringent response. Three 100-μl aliquots of each culture were transferred into a 96-well plate and the growth rate was monitored at 37°C by measuring the OD_{600} in multimode microplate reader (TECAN). The mean and standard deviation (SD) of three measurements are shown.

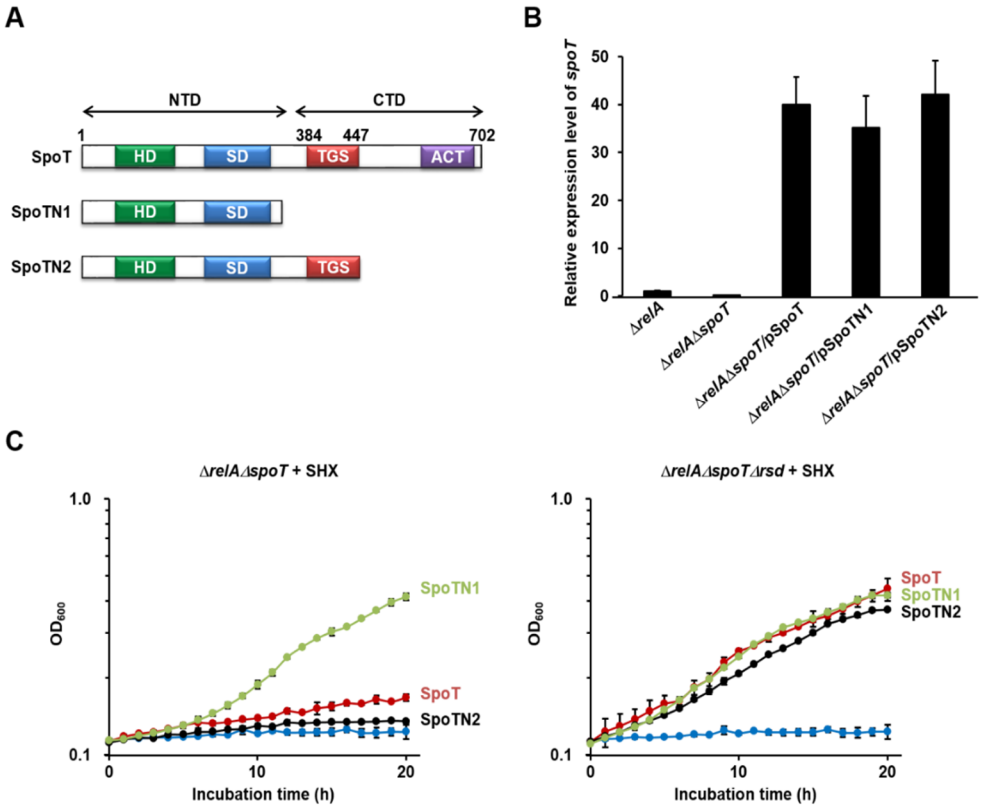
A
NTD
CTD
1
384
447
702
SpoT
HD
SD
TGS
ACT
SpoTN1
HD
SD
SpoTN2
HD
SD
TGS
B
Relative expression level of spoT
50
40
30
20
10
0
ΔrelA
ΔrelAΔspoT
ΔrelAΔspoT/pSpoT
ΔrelAΔspoT/pSpoTN1
ΔrelAΔspoT/pSpoTN2
C
ΔrelAΔspoT + SHX
ΔrelAΔspoTΔrsd + SHX
OD600
1.0
0.1
0
10
20
Incubation time (h)
SpoTN1
SpoT
SpoTN2
SpoT
SpoTN1
SpoTN2

of SpoT or SpoTN2 was almost completely reversed in a *relA spoT rsd* triple mutant. These data suggest that the TGS domain of SpoT receives the regulatory signal through its interaction with Rsd and that this interaction stimulates the SpoT-mediated (p)ppGpp hydrolysis.

4.2.4. Activation of SpoT (p)ppGpp hydrolase activity is indepdendent of σ^{70} activity of Rsd.

While the Rsd(D63A) mutant (substitution of Asp 63 to Ala) was shown unable to interact with and therefore to antagonize the activity of σ^{70} in a previous study (Mitchell et al., 2007), this mutant protein could still interact, as tightly as wild-type Rsd, with SpoT (Figure II-12) and overexpression of Rsd(D63A) resulted in the same phenotype as overexpression of the wild-type Rsd (Figure II-13). Moreover, no obvious difference in the transcriptional levels of *relA* and *spoT* was detected in *rsd* deletion and overexpression strains (Figure II-14). Thus, we verified that the growth defect of *rsd*$^+$ strains in the *relA* mutant background under amino acid starvation conditions is not due to the anti-σ^{70} activity of Rsd.

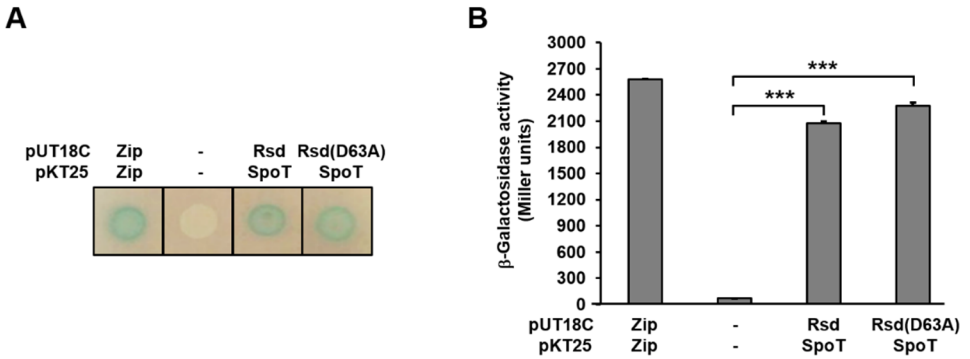

Figure II-12. Complex formation with SpoT is independent of the anti-σ^{70} activity of Rsd.

(A and B) The bacterial two-hybrid assays to analyze the specific interaction of Rsd and Rsd(D63A) with SpoT *in vivo*. *E. coli* BTH101 coexpressing T25-SpoT and T18-Rsd or T18-Rsd(D63A) was spotted on LB plates supplemented with 40 μg/ml X-gal (A) and β-galactosidase activity was monitored by direct enzyme assay (Miller units) (B). Zip served as a positive control. The transformant coexpressing the unfused T25- and T18-fragments served as a negative control. The mean and standard deviation (SD) of three independent measurements are shown. Statistical significance was determined using Student's t-test (***, $P < 0.001$).

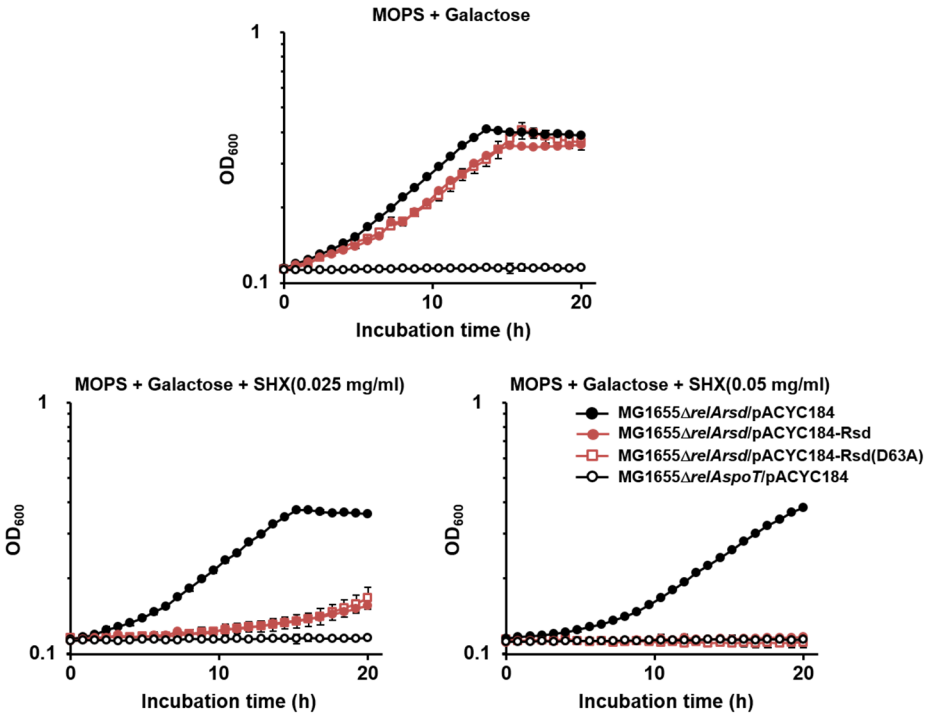

Figure II-13. Activation of the (p)ppGpp hydrolase activity of SpoT is independent of the anti-σ^{70} activity of Rsd.

Growth curves of *E. coli* strains in MOPS minimal medium (pH 7.2) supplemented with 0.2% galactose with or without SHX. After inoculation, 100-µl aliquots of each strain were transferred into a 96-well plate and growth was monitored at 600 nm using a multimode microplate reader (TECAN). The mean and standard deviation (SD) of three measurements are shown.

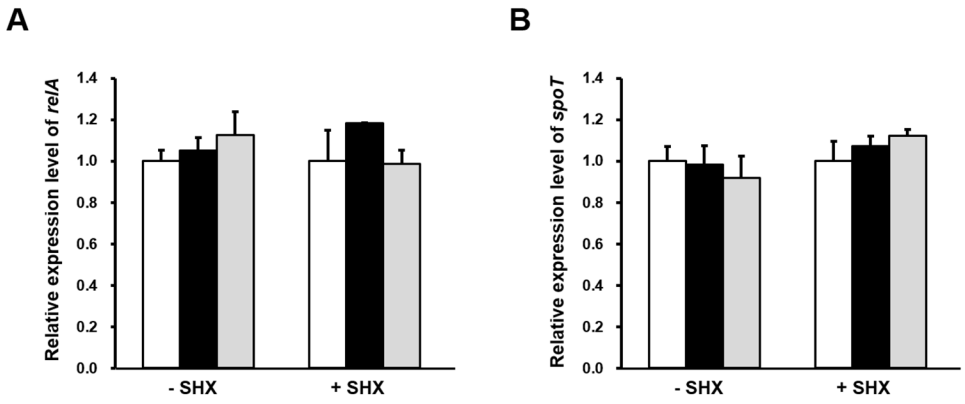

Figure II-14. The effect of Rsd on the transcription of *relA* and *spoT*.

(A and B) *E. coli* cells were grown in LB medium containing appropriate antibiotics and 0.02% arabinose. At OD_{600} ~0.6, each culture was divided into two parts and SHX (0.5 mg/ml) was added to one of them. After 30-min incubation, the relative transcript levels of *relA* (A) and *spoT* (B) were determined by quantitative reverse transcriptase PCR (qRT-PCR), as described in the Materials and Methods. The mean and standard deviation (SD) of three independent measurements are shown. MG1655/pJK1113, white; MG1655Δ*rsd*/pJK1113, black; MG1655Δ*rsd*/pJK1113-Rsd, gray.

4.3. (p)ppGpp hydrolase activity of SpoT is regulated by different carbon sources.

4.3.1. Dephosphorylated HPr blocks the stimulatory effect of Rsd on the (p)ppGpp hydrolase activity of SpoT.

In a previous study, we showed that HPr, a general component of the sugar PTS, is predominantly dephosphorylated during glucose transport and only dephosphorylated HPr interacts with Rsd to antagonize its activity (Neira et al., 2018; Park et al., 2013; Park et al., 2015). We therefore expected that the Rsd-SpoT interaction could be affected by the phosphorylation state of HPr, resulting in changes in the intracellular level of (p)ppGpp. To verify this assumption, we first examined the effect of the phosphorylation state of HPr on formation of the Rsd-SpoT complex by pull-down assays under various conditions (Figure II-15). After the *E. coli* cell lysate containing overexpressed SpoTC1 was mixed with purified His-Rsd alone or together with HPr and enzyme I (EI), this mixture was incubated either with glucose to dephosphorylate or with PEP to phosphorylate HPr. Then each mixture was incubated with TALON resin for metal affinity chromatography. After brief washes, proteins bound to the resin were eluted and analyzed by SDS-PAGE (Figure II-15). The amount of eluted SpoTC1 significantly increased in the presence of His-Rsd, supporting the specific interaction of SpoTC1 with Rsd (compare lanes 1 and 2). When the mixture of the SpoTC1 lysate and His-Rsd was incubated with HPr and glucose (thus HPr dephosphorylated), the amount of SpoTC1 bound to Rsd significantly decreased with a concomitant increase in the amount of HPr bound to His-Rsd (compare lanes 2 and 3). However, when the same mixture was incubated with HPr and PEP (and thus HPr phosphorylated), formation of the Rsd-SpoTC1 complex was little affected by HPr (lane 4). These data indicate that only the

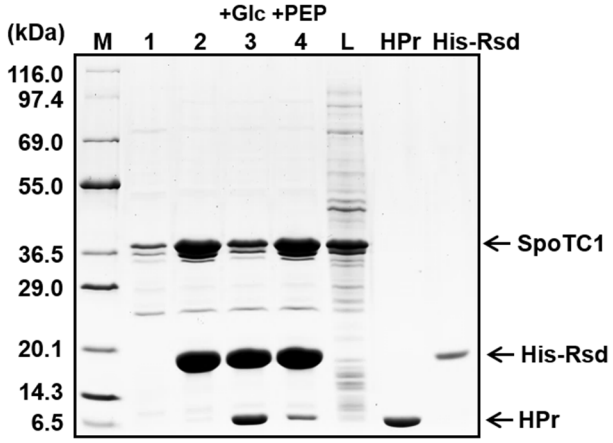

Figure II-15. The stimulatory effect of Rsd on the SpoT ppGpp hydrolase activity is abolished by dephosphorylated HPr.

Interference of the Rsd-SpoT complex formation by a dephosphorylated form of HPr. To test the effect of the phosphorylation state of HPr on the formation of the Rsd-SpoT complex, an *E. coli* cell extract expressing SpoTC1 was mixed with binding buffer (lane 1), 170 μg His-Rsd (lane 2) or a mixture of 170 μg His-Rsd, 240 μg HPr and 2 μg EI (lanes 3 and 4), and HPr was dephosphorylated by adding 2 mM glucose (lane 3) or phosphorylated by adding 2 mM PEP (lane 4). Each mixture was incubated with 50 μl TALON resin for metal affinity chromatography. After elution with imidazole, proteins bound to each TALON resin were analyzed by SDS-PAGE and Coomassie blue staining. Lane M, molecular mass markers; lane L, *E. coli* cell lysate expressing SpoTC1 before metal affinity chromatography. Purified HPr and His-Rsd were also run as a control.

dephosphorylated form of HPr can interact with Rsd and sequesters it from SpoTC1. We then tested the effect of HPr on the stimulation of the SpoT ppGpp hydrolase activity by Rsd *in vitro* using HPLC (Figure II-16). Interestingly, whereas dephosphorylated HPr apparently inhibited the stimulatory effect of Rsd on the ppGpp hydrolysis by SpoT, phosphorylated HPr did not.

We also determined the effect of dephosphorylated HPr on the cellular level of (p)ppGpp *in vivo* (Figure II-17). Consistent with the data in Figure II-10, the level of (p)ppGpp decreased more rapidly in the Rsd-overexpressing strain than in the *rsd*-deficient strain. However, the (p)ppGpp hydrolysis rate was significantly lower in the strain co-expressing Rsd and unphosphorylatable HPr(H15A), compared with that in the strain overexpressing Rsd alone. These results suggest that HPr of the sugar PTS can influence the formation of the Rsd-SpoT complex and thereby regulate the cellular level of (p)ppGpp depending on its phosphorylation state *in vivo*.

4.3.2. Regulation of (p)ppGpp hydrolase activity of SpoT by Rsd is dependent on carbon sources.

We have previously shown that the phosphorylation state of HPr is determined by sugars supplemented to the medium (Choe et al., 2017; Park et al., 2013). As shown in Figure II-18, HPr was mostly dephosphorylated in the presence of glucose or *N*-acetylglucosamine, whereas it was predominantly phosphorylated in the presence of galactose or glycerol. Therefore, we assumed that the (p)ppGpp level would be less, since the concentration of free Rsd should be higher, thus cells might be more sensitive to the SHX-induced serine starvation in the presence of galactose or glycerol than in the presence of glucose or *N*-acetylglucosamine. To verify this assumption, we constructed a *relA rsd* double mutant, and

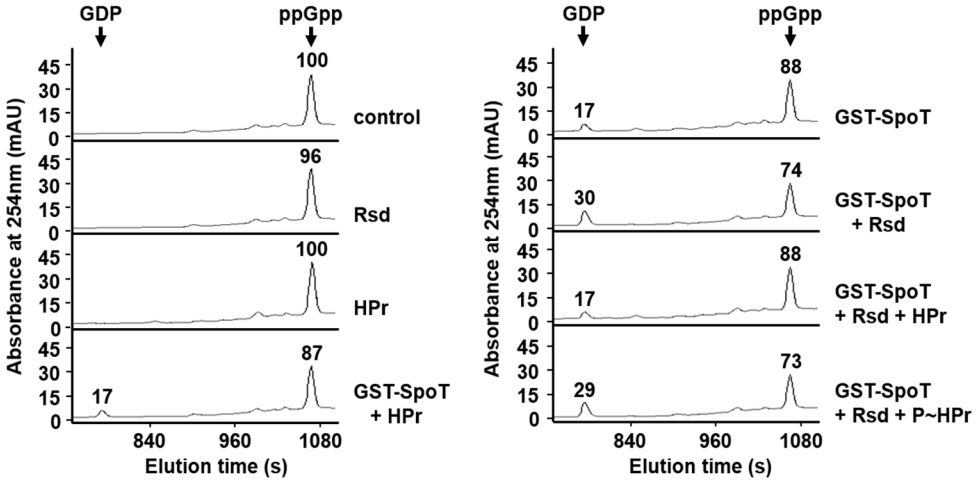

Figure II-16. Stimulation of the SpoT ppGpp hydrolase activity by Rsd is blocked by the dephosphorylated form of HPr.

The ppGpp hydrolase activity of purified GST-SpoT (2.5 μg) was assayed in a reaction mixture containing 38.49 μM ppGpp in the presence of different combinations of Rsd (15.6 μg) and HPr (28 μg), as indicated. HPr was phosphorylated by adding EI and 2 mM PEP (P~HPr). After incubation at 37°C for 5 min, the reaction mixture was applied to a Supelcosil LC-18-T HPLC column, and ppGpp and GDP were monitored by measuring the A_{254}. Relative peak areas are shown above each peak, considering the peak area of ppGpp in the control sample as 100. Representative data from three independent experiments are shown.

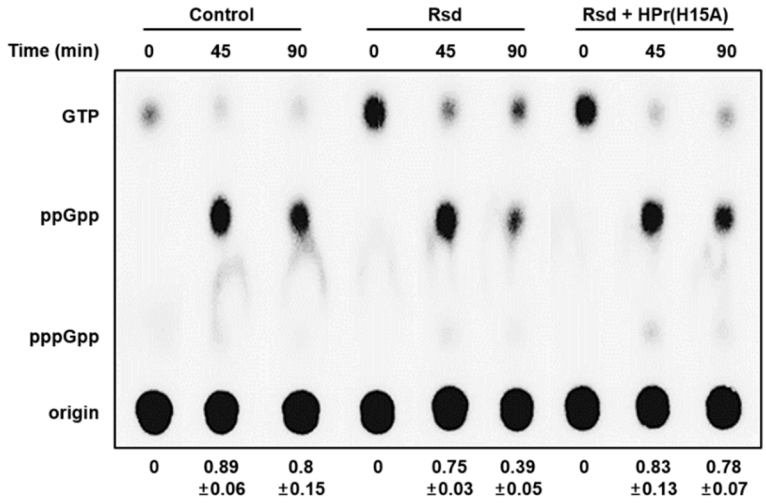

Figure II-17. Dephosphorylated form of HPr abolishes the stimulatory effect of Rsd on the (p)ppGpp hydrolase activity of SpoT.

The MG1655Δ*rsd* strain carrying pJK1113 (Control), pJK1113-Rsd (Rsd), or both pJK1113-Rsd and pJK1113-H15A (Rsd + HPr(H15A)) was incubated in low-phosphate MOPS minimal medium containing 0.2% galactose and 0.02% arabinose and 100 μCi/ml $^{32}PO_4^{3-}$. Exponentially growing cells were treated with SHX (1 mg/ml) and intracellular (p)ppGpp concentrations were analyzed by TLC at three time points (indicated above each lane). Relative amounts of (p)ppGpp were calculated as the intensity of (p)ppGpp divided by that of (p)ppGpp plus GTP. The mean and standard deviation (SD) of three independent measurements are shown below each lane.

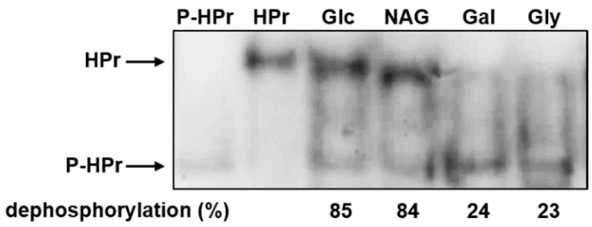

Figure II-18. Determination of the *in vivo* phosphorylation state of HPr.
The phosphorylation state of HPr was determined in the *E. coli* strain MG1655/pACYC-HPr grown in LB medium containing the indicated sugars as described in Materials and Methods. Purified HPr (3.5 ng) was used as a positive control. Band intensities were analyzed using ImageJ software. The percentages of dephosphorylated HPr over total HPr are shown below the gel. Glc, glucose; NAG, *N*-acetylglucosamine; Gal, galactose; Gly, glycerol

transformed this mutant with the low-copy-number plasmid pACYC184 (as a control) or the plasmid pACYC-Rsd expressing Rsd from its own promoter, in an attempt to examine only the direct effects of Rsd on the SpoT-triggered stringent response depending on carbon sources. Thus the growth patterns of these strains were compared in the presence of various carbon sources with or without SHX (Figures II-19 and II-20). While the *relA spoT* double mutant ((p)ppGpp^0) strain carrying pACYC184 showed a severe growth defect in MOPS medium containing glucose, *N*-acetylglucosamine, galactose, or glycerol as the sole carbon source regardless of the presence of SHX, the *relA rsd* double mutant carrying pACYC184 exhibited normal growth regardless of the supplemented carbon source, although the addition of SHX caused some growth retardation (compare Figures II-19 and II-20). Expression of Rsd from its own promoter on pACYC-Rsd caused a slight but not significant growth retardation of the *relA rsd* double mutant compared with the same strain carrying pACYC184 regardless of the supplemented carbon sources in MOPS medium in the absence of SHX (Figure II-19). Interestingly, however, growth of the *relA rsd* double mutant expressing Rsd was significantly inhibited by SHX in the presence of galactose or glycerol as the sole carbon source, to a similar level to that of the (p)ppGpp^0 strain carrying pACYC184 (Figures II-20 C and D), whereas the same strain showed only moderate growth retardation as compared with the *relA rsd* double mutant carrying pACYC184 when glucose or *N*-acetylglucosamine was supplemented as the sole carbon source (Figures II-20 A and B). These data suggest that the carbon source can influence the stringent response by regulating the stimulatory effect of Rsd on the SpoT (p)ppGpp hydrolase activity through altering the phosphorylation state of HPr *in vivo*.

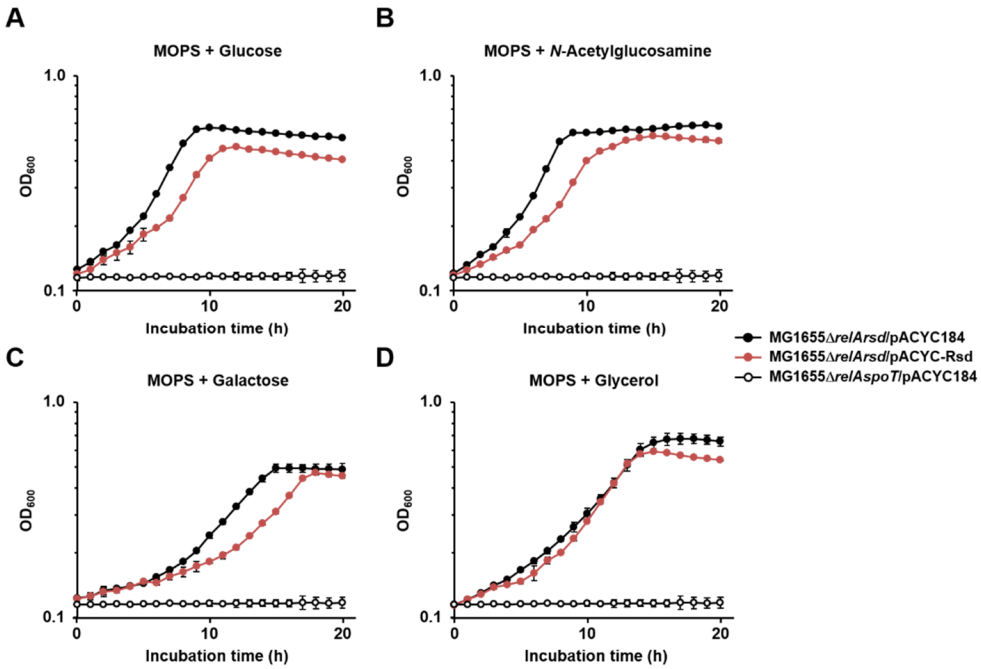

Figure II-19. Growth curves of *E. coli* strains in MOPS minimal medium containing different carbon sources.

Each strain was inoculated in MOPS minimal medium (pH 7.2) supplemented with 0.2% glucose (A), *N*-acetylglucosamine (B), galactose (C), or glycerol (D). After inoculation, 100-µl aliquots of each strain were transferred into a 96-well plate and growth was monitored at 37°C by measuring the OD_{600} in multimode microplate reader (TECAN). The mean and standard deviation (SD) of three measurements are shown.

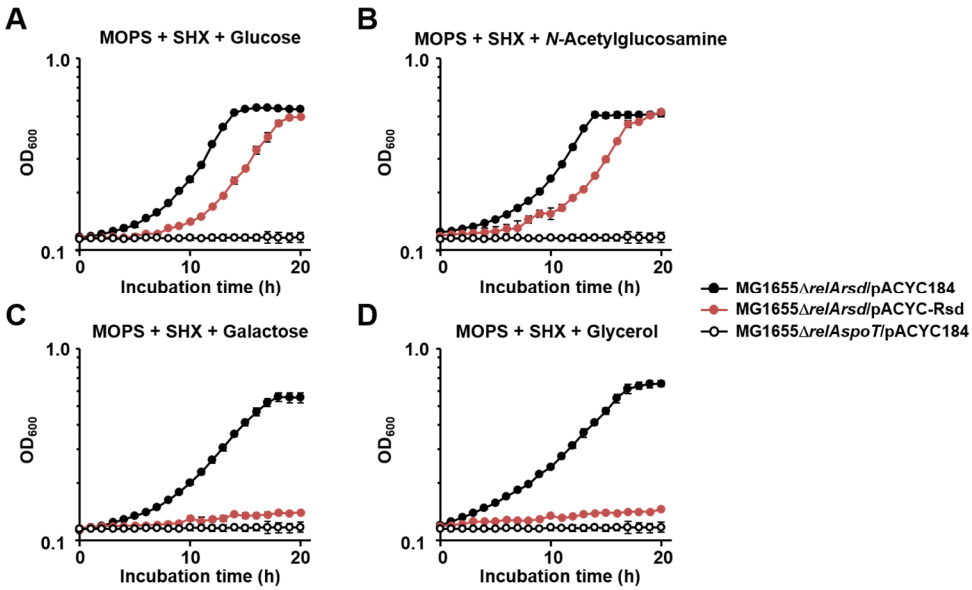

Figure II-20. Regulation of (p)ppGpp hydrolase activity of SpoT by Rsd is dependent on carbon sources.

Growth curves of *E. coli* strains treated with SHX (0.025 mg/ml) in MOPS minimal medium (pH 7.2) supplemented with 0.2% glucose (B), *N*-acetylglucosamine (C), galactose (D), or glycerol (E). After inoculation, 100-µl aliquots of each strain were transferred into a 96-well plate and growth was monitored at 600 nm using a multimode microplate reader (TECAN). The mean and standard deviation (SD) of three measurements are shown.

4.4. Implication of Rsd during a carbon source downshift.

4.4.1. Rsd regulates the stringent response during carbon source downshift.

Microorganisms face the constant challenge of fluctuating conditions in their natural environments such as nutrient shifts. On exposure to nutrient downshifts, the cellular concentration of (p)ppGpp displays an abrupt increase followed by a gradual decrease (Lazzarini et al., 1971). This mechanism of balancing the (p)ppGpp level by stimulating the hydrolase activity of SpoT appears to be important since the uncontrolled accumulation of (p)ppGpp is lethal (Sun et al., 2010). Because the stimulatory effect of Rsd on SpoT (p)ppGpp hydrolase activity is mediated by the type and availability of carbon sources, we assumed that Rsd may function in response to a carbon source downshift from a preferred carbon source to a less preferred one. When *E. coli* is cultured on a mixture of various carbon sources, glucose is preferentially utilized by inhibiting the consumption of other carbon sources (Deutscher et al., 2014). Once glucose is depleted, growth is transiently arrested and (p)ppGpp accumulates rapidly in the cell (Harshman and Yamazaki, 1971). As a result, the accumulated (p)ppGpp controls regulatory networks that coordinate resumption of growth (Traxler et al., 2006). Considering that the phosphorylation state of HPr is determined by the availability of preferred PTS sugars, such as glucose (Choe et al., 2017; Park et al., 2013) (Figure II-18), it seems reasonable to assume that (p)ppGpp levels need to be reduced before growth can resume during a carbon source downshift, and this explains the requirement of Rsd for the stimulation of SpoT-catalyzed (p)ppGpp hydrolysis.

To verify this assumption, we examined the effect of Rsd on the diauxic shift of *E. coli* cells during growth in the medium supplemented with 0.02% glucose and 0.1% casamino acids (Figure II-21). To rule out the effect of

amino acid starvation during the diauxic shift and to assess only the effect of the carbon downshift, casamino acids were added at a much higher concentration than glucose. All strains showed similar growth curves during the glucose consumption period, and then transient growth arrest after glucose was exhausted. As shown in Figure II-21, the *rsd* mutant carrying pACYC184 (red triangles), had a longer diauxic lag and showed less efficient growth on casamino acids than the wild-type strain carrying pACYC184 (black circles). The lag time and growth of the *rsd* mutant was restored by complementation with pACYC-Rsd (grey squares) or pACYC-Rsd(D63A) (white diamonds). Likewise, prolonged lag time and inefficient growth of the *rsd* mutant was completely reversed in a single-copy Rsd(D63A) mutant (Figure II-22), indicating that the phenotype of the *rsd* mutant is not due to loss of the anti-σ^{70} activity.

The effect of the *rsd* mutation on the growth of *E. coli* was also examined during the carbon source downshift from glucose to succinate (Figure II-23). An *rsd*-deficient mutant exhibited a longer diauxic lag and showed less efficient growth on succinate than the wild-type strain. These results suggest that Rsd functions as a direct link between the PTS-dependent diauxic shift and the SpoT-mediated stringent response.

4.4.2. Rsd counterbalances RelA-mediated (p)ppGpp accumulation during a carbon source downshift.

Since the (p)ppGpp level was previously shown to increase in a RelA-dependent manner during a nutrient downshift in *E. coli* (Braedt and Gallant, 1977; Lazzarini et al., 1971), we examined whether Rsd is required to balance the RelA-mediated (p)ppGpp accumulation. While the *rsd*-deficient mutant showed a longer diauxie lag than the wild-type strain, the *relA* mutant strain exhibited a remarkably decreased lag time (Figure II-24). In addition, the effect of *rsd* deletion disappeared in the *relA* mutant

background, indicating that Rsd counterbalances the RelA-dependent accumulation of (p)ppGpp by stimulating the (p)ppGpp hydrolase activity of SpoT during a carbon downshift.

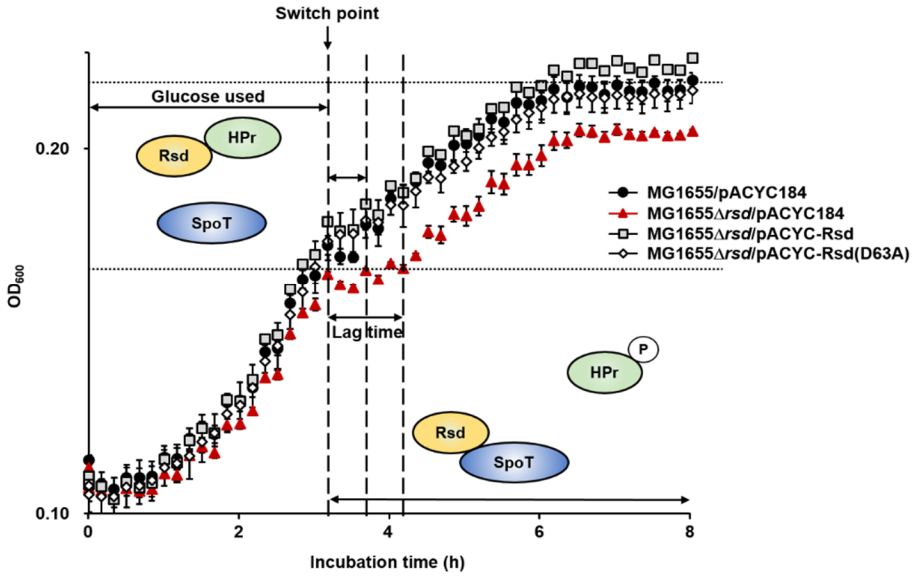

Figure II-21. Implication of Rsd during a carbon source downshift.

Growth curves were measured during a carbon downshift from glucose to casamino acids. Cells grown overnight in LB medium were harvested, washed, suspended in MOPS minimal medium containing 0.1% casamino acids and 0.02% glucose. Then 100-μl aliquots of each strain were transferred into a 96-well plate and growth was monitored at 600 nm using a multimode microplate reader (TECAN). The mean and standard deviation (SD) of three measurements are shown. In the presence of glucose, HPr is predominantly dephosphorylated and then sequesters Rsd from SpoT to maintain the (p)ppGpp hydrolytic activity at basal levels. On depletion of glucose, however, the ppGpp level abruptly increases in *relA*$^+$ strains. Therefore, the (p)ppGpp hydrolase activity of SpoT needs to be stimulated to counterbalance the RelA-dependent large accumulation of (p)ppGpp. This appears to be achieved by phosphorylation of HPr. Because phospho-HPr cannot interact with Rsd, Rsd can bind and activate the (p)ppGpp hydrolase activity of SpoT to balance the intracellular (p)ppGpp concentrations, which contributes to the growth resumption of *E. coli* cell during a carbon downshift.

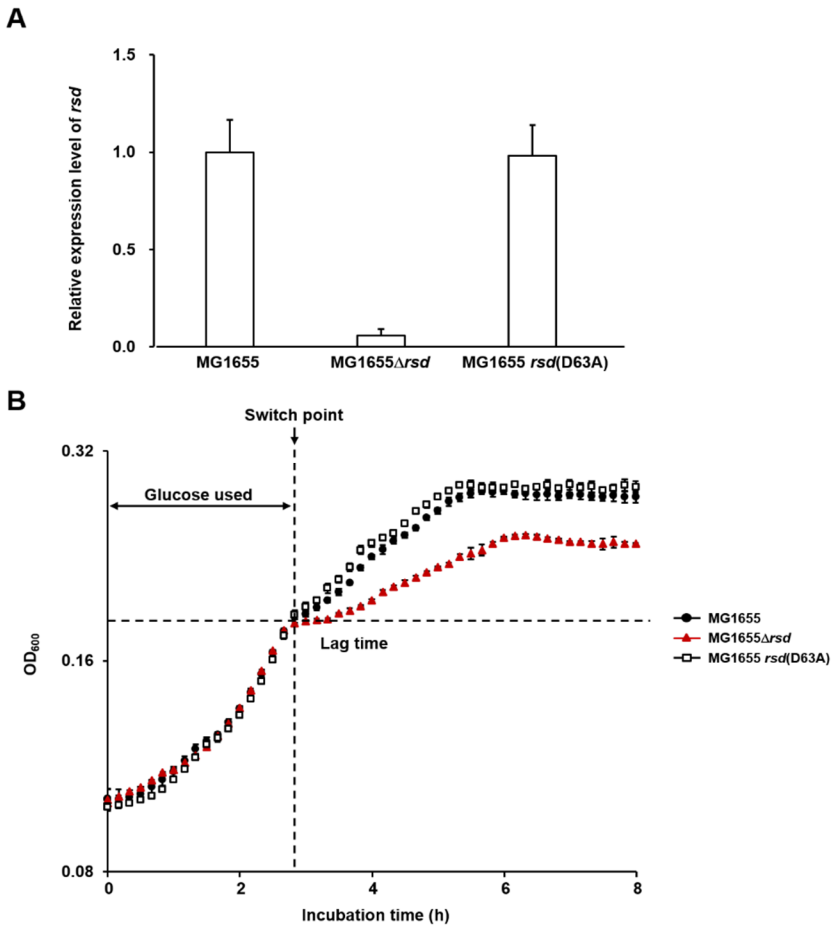

Figure II-22. Implication of Rsd during a carbon source downshift is independent of the anti-σ^{70} activity of Rsd.

(A) The relative transcript levels of *rsd* were determined by qRT-PCR, as described in the Materials and Methods. The mean and standard deviation (SD) of three independent measurements are shown. (B) *E. coli* strains grown overnight in LB medium were harvested, washed, and then suspended in MOPS minimal medium containing 0.1% casamino acids and 0.02% glucose. After inoculation, 100-μl aliquots of each strain were transferred into a 96-well plate and growth was monitored at 600 nm using a multimode microplate reader (TECAN). The mean and standard deviation (SD) of three measurements are shown.

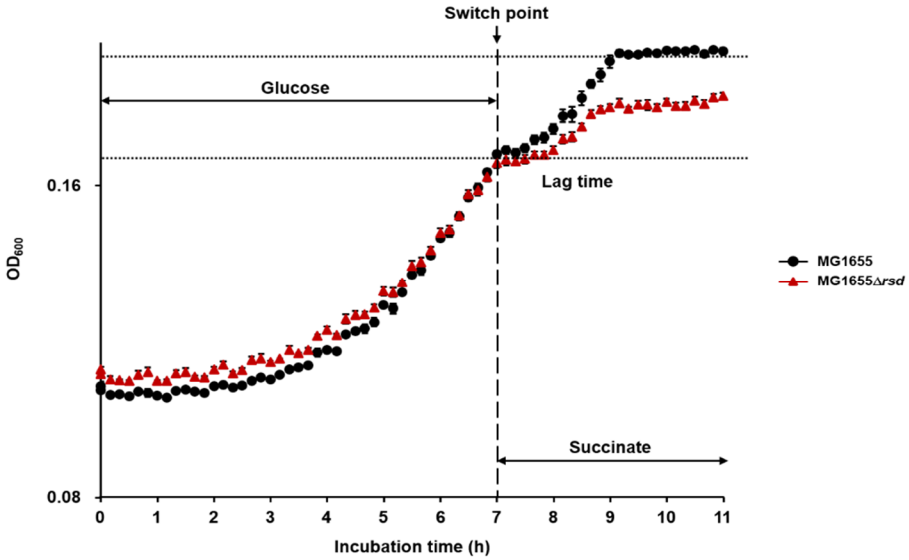

Figure II-23. Rsd is involved in the response to a carbon source downshift.

E. coli strains grown overnight in LB medium were harvested, washed, and then suspended in MOPS minimal medium containing 0.04% glucose and 0.08% succinate. After inoculation, 100-µl aliquots of each strain were transferred into a 96-well plate and growth was monitored at 600 nm using a multimode microplate reader (TECAN). The mean and standard deviation (SD) of three measurements are shown.

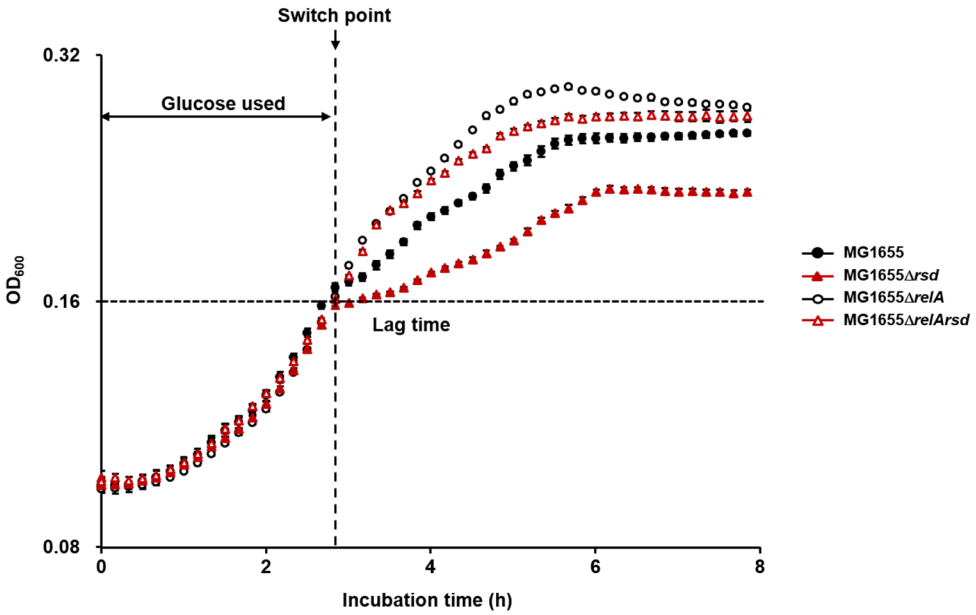

Figure II-24. Rsd is required to counterbalance RelA-mediated (p)ppGpp accumulation during a carbon source downshift.

E. coli strains grown overnight in LB medium were harvested, washed, and then suspended in MOPS minimal medium containing 0.1% casamino acids and 0.02% glucose. After inoculation, 100-µl aliquots of each strain were transferred into a 96-well plate and growth was monitored at 600 nm using a multimode microplate reader (TECAN). The mean and standard deviation (SD) of three measurements are shown.

5. Discussion

The activities of RelA and SpoT are regulated by different stress signals. While RelA possessing only (p)ppGpp synthetic activity responds primarily to amino acid starvation, SpoT having both (p)ppGpp synthetic and hydrolytic activities functions as a hub protein that integrates various stress signals including fatty acid, phosphate, iron and carbon source starvation (Hauryliuk et al., 2015). Because the hydrolytic activity of SpoT is crucial for balancing cellular (p)ppGpp concentrations, disruption of the *spoT* gene is lethal in *relA*-proficient *E. coli* strains due to the accumulation of too much (p)ppGpp (Baba et al., 2006; Xiao et al., 1991). It was recently revealed that the enzymatic activity of RelA is also activated by ppGpp itself (Shyp et al., 2012). This positive allosteric feedback regulation mechanism also supports the importance of the SpoT-mediated (p)ppGpp hydrolysis in relaxing the stringent response.

There have been a few studies on the regulation of the SpoT activity through protein-protein interactions. ObgE was previously shown to interact with SpoT to maintain the low level of (p)ppGpp under normal growth conditions (Raskin et al., 2007). However, a more recent study has shown that the effect of ObgE overexpression on the intracellular level of (p)ppGpp is negligible (Verstraeten et al., 2015). Likewise, the *obgE* deletion mutant did not show an increase in the (p)ppGpp level as opposed to previous findings, suggesting that ObgE is not responsible for the regulation of SpoT activity *in vitro* and *in vivo* (Persky et al., 2009). Acyl carrier protein (ACP) has also been shown to interact with SpoT to stimulate the (p)ppGpp synthetase activity of SpoT in response to fatty acid starvation (Battesti and Bouveret, 2006). A direct interaction of SpoT with enzyme IIA^{Ntr} of the nitrogen-related PEP-dependent phosphotransferase system has been reported in R. eutropha (Karstens et al., 2014) and *C. crescentus* (Ronneau et al., 2016), but these interactions appeared to inhibit SpoT (p)ppGpp hydrolase activity.

However, despite the physiological importance, little is known about the molecular mechanism stimulating the (p)ppGpp hydrolase activity of SpoT in *E. coli*. In this study, we demonstrate that Rsd directly interacts with SpoT to stimulate its (p)ppGpp hydrolase activity both *in vitro* and *in vivo*. As expected from the fact that Rsd can form a tight complex only with the dephosphorylated form of HPr (Park et al., 2013; Park et al., 2015) and that the phosphorylation state of HPr can be changed by the type of sugar available in the medium (Choe et al., 2017; Park et al., 2013), the stimulatory effect of Rsd on SpoT (p)ppGpp hydrolase activity was influenced by the sugar source supplemented (Figures II-19 and II-20). Thus, this study provides the first example of a regulator stimulating SpoT (p)ppGpp hydrolase activity and the first example of a direct link between the sugar PTS and the stringent response. The TGS domain of SpoT functions as the site for Rsd binding as well as for acyl-ACP binding (Battesti and Bouveret, 2006). Recently, the TGS domain of RelA has been shown to be the site for recognition of charged or uncharged CCA ends of cognate tRNA (Brown et al., 2016; Loveland et al., 2016). Given these pivotal roles of the TGS domain, this domain appears to be a regulatory link between carbon, lipid, and amino acid metabolism and the stringent response.

Although Rsd was identified as an antagonist of σ^{70} in *E. coli* (Jishage and Ishihama, 1998), no obvious phenotype has been observed in rsd deletion or overexpression strains to date. However, we showed that the overproduction of Rsd significantly decreased the intracellular (p)ppGpp levels (Figure II-10). Moreover, the *relA* mutant strains expressing Rsd exhibits severe growth defects under SHX-induced stress condition similar to that of the *relA spoT* double mutant ((p)ppGpp0) strain (Figure II-9). Furthermore, the rsd mutant showed a longer diauxic lag and less efficient growth during the carbon source downshift from glucose to casamino acids or succinate

(Figures 21 and 23) than the wild-type strain. We confirmed that these growth characteristics of both the Rsd-overexpressing and *rsd*-deficient strains were not associated with the anti-σ^{70} activity of Rsd but with its stimulation of the SpoT (p)ppGpp hydrolase activity (Figures II-13 and II-21). Therefore, this study provides clear genotype-phenotype correlations in both Rsd overexpression and deletion strains.

Considering its critical role in the stringent response, the (p)ppGpp hydrolase activity of SpoT must be tightly regulated to ensure that it is stimulated only when necessary. Under good carbon conditions, the intracellular (p)ppGpp concentrations are maintained at a low level (Dai et al., 2016). Thus, stimulation of the SpoT (p)ppGpp hydrolase activity is unnecessary. When cells are growing on glucose, HPr is dephosphorylated and sequesters Rsd so that the (p)ppGpp hydrolase activity of SpoT will be maintained at a basal level. However, when glucose is exhausted, the (p)ppGpp level abruptly increases in a RelA-dependent manner to efficiently coordinate gene expression necessary to resume growth on poor carbon sources (Lazzarini et al., 1971). However, uncontrolled accumulation of (p)ppGpp can cause severe growth inhibition (Sun et al., 2010) or cell death (Aizenman et al., 1996). Therefore, sophisticated control of SpoT-mediated (p)ppGpp hydrolysis is necessary to balance the intracellular (p)ppGpp concentrations. This can be achieved by phosphorylation of HPr. When cells are transited to poor carbon conditions such as casamino acids or succinate, HPr is predominantly phosphorylated and thus Rsd can interact with and stimulate the SpoT-catalyzed (p)ppGpp hydrolysis to counterbalance the RelA-catalyzed synthesis (Figures II-21, II-23 and II-24). In this way, the intracellular level of (p)ppGpp can be adjusted to allow *E. coli* to adapt to carbon source fluctuations. Therefore, Rsd functions as a direct link between the PTS-dependent diauxic shift and the SpoT-mediated stringent response.

6. References

Aizenman, E., H. Engelberg-Kulka, and G. Glaser. 1996. An *Escherichia coli* chromosomal "addiction module" regulated by guanosine [corrected] 3',5'-bispyrophosphate: a model for programmed bacterial cell death. *Proc Natl Acad Sci U S A*. 93:6059-6063.

An, G., J. Justesen, R.J. Watson, and J.D. Friesen. 1979. Cloning the *spoT* gene of *Escherichia coli:* identification of the *spoT* gene product. *J Bacteriol*. 137:1100-1110.

Atkinson, G.C., T. Tenson, and V. Hauryliuk. 2011. The RelA/SpoT homolog (RSH) superfamily: distribution and functional evolution of ppGpp synthetases and hydrolases across the tree of life. *PLoS One*. 6:e23479.

Baba, T., T. Ara, M. Hasegawa, Y. Takai, Y. Okumura, M. Baba, K.A. Datsenko, M. Tomita, B.L. Wanner, and H. Mori. 2006. Construction of *Escherichia coli* K-12 in-frame, single-gene knockout mutants: the Keio collection. *Mol Syst Biol*. 2:2006 0008.

Barabote, R.D., and M.H. Saier, Jr. 2005. Comparative genomic analyses of the bacterial phosphotransferase system. *Microbiol Mol Biol Rev*. 69:608-634.

Battesti, A., and E. Bouveret. 2006. Acyl carrier protein/SpoT interaction, the switch linking SpoT-dependent stress response to fatty acid metabolism. *Mol Microbiol*. 62:1048-1063.

Bougdour, A., and S. Gottesman. 2007. ppGpp regulation of RpoS degradation via anti-adaptor protein IraP. *Proc Natl Acad Sci U S A*. 104:12896-12901.

Braedt, G., and J. Gallant. 1977. Role of the *rel* gene product in the control of cyclic adenosine 3',5'-monophosphate accumulation. *J Bacteriol*. 129:564-566.

Brown, A., I.S. Fernandez, Y. Gordiyenko, and V. Ramakrishnan. 2016.

Ribosome-dependent activation of stringent control. *Nature*. 534:277-280.

Cashel, M., and J. Gallant. 1969. Two compounds implicated in the function of the RC gene of *Escherichia coli*. *Nature*. 221:838-841.

Choe, M., Y.H. Park, C.R. Lee, Y.R. Kim, and Y.J. Seok. 2017. The general PTS component HPr determines the preference for glucose over mannitol. *Sci Rep*. 7:43431.

Corrigan, R.M., L.E. Bellows, A. Wood, and A. Grundling. 2016. ppGpp negatively impacts ribosome assembly affecting growth and antimicrobial tolerance in Gram-positive bacteria. *Proc Natl Acad Sci U S A*. 113:E1710-1719.

Dai, X., M. Zhu, M. Warren, R. Balakrishnan, V. Patsalo, H. Okano, J.R. Williamson, K. Fredrick, Y.P. Wang, and T. Hwa. 2016. Reduction of translating ribosomes enables *Escherichia coli* to maintain elongation rates during slow growth. *Nat Microbiol*. 2:16231.

Dalebroux, Z.D., and M.S. Swanson. 2012. ppGpp: magic beyond RNA polymerase. *Nat Rev Microbiol*. 10:203-212.

Datsenko, K.A., and B.L. Wanner. 2000. One-step inactivation of chromosomal genes in *Escherichia coli* K-12 using PCR products. *Proc Natl Acad Sci U S A*. 97:6640-6645.

Deutscher, J., F.M. Ake, M. Derkaoui, A.C. Zebre, T.N. Cao, H. Bouraoui, T. Kentache, A. Mokhtari, E. Milohanic, and P. Joyet. 2014. The bacterial phosphoenolpyruvate:carbohydrate phosphotransferase system: regulation by protein phosphorylation and phosphorylation-dependent protein-protein interactions. *Microbiol Mol Biol Rev*. 78:231-256.

Deutscher, J., C. Francke, and P.W. Postma. 2006. How phosphotransferase system-related protein phosphorylation regulates carbohydrate metabolism in bacteria. *Microbiol Mol Biol Rev*. 70:939-1031.

Gentry, D.R., and M. Cashel. 1996. Mutational analysis of the *Escherichia coli spoT* gene identifies distinct but overlapping regions involved in ppGpp synthesis and degradation. *Mol Microbiol*. 19:1373-1384.

Harshman, R.B., and H. Yamazaki. 1971. Formation of ppGpp in a relaxed and stringent strain of *Escherichia coli* during diauxie lag. *Biochemistry*. 10:3980-3982.

Haseltine, W.A., and R. Block. 1973. Synthesis of guanosine tetra- and pentaphosphate requires the presence of a codon-specific, uncharged transfer ribonucleic acid in the acceptor site of ribosomes. *Proc Natl Acad Sci U S A*. 70:1564-1568.

Haugen, S.P., W. Ross, and R.L. Gourse. 2008. Advances in bacterial promoter recognition and its control by factors that do not bind DNA. *Nat Rev Microbiol*. 6:507-519.

Hauryliuk, V., G.C. Atkinson, K.S. Murakami, T. Tenson, and K. Gerdes. 2015. Recent functional insights into the role of (p)ppGpp in bacterial physiology. *Nat Rev Microbiol*. 13:298-309.

Hernandez, V.J., and H. Bremer. 1991. *Escherichia coli* ppGpp synthetase II activity requires *spoT*. *J Biol Chem*. 266:5991-5999.

Jishage, M., and A. Ishihama. 1998. A stationary phase protein in *Escherichia coli* with binding activity to the major s subunit of RNA polymerase. *Proc Natl Acad Sci U S A*. 95:4953-4958.

Karimova, G., J. Pidoux, A. Ullmann, and D. Ladant. 1998. A bacterial two-hybrid system based on a reconstituted signal transduction pathway. *Proc Natl Acad Sci U S A*. 95:5752-5756.

Karstens, K., C.P. Zschiedrich, B. Bowien, J. Stulke, and B. Gorke. 2014. Phosphotransferase protein $EIIA^{Ntr}$ interacts with SpoT, a key enzyme of the stringent response, in *Ralstonia eutropha* H16. *Microbiology*. 160:711-722.

Kim, H.M., Y.H. Park, C.K. Yoon, and Y.J. Seok. 2015. Histidine

phosphocarrier protein regulates pyruvate kinase A activity in response to glucose in *Vibrio vulnificus*. *Mol Microbiol*. 96:293-305.

Kriel, A., A.N. Bittner, S.H. Kim, K. Liu, A.K. Tehranchi, W.Y. Zou, S. Rendon, R. Chen, B.P. Tu, and J.D. Wang. 2012. Direct regulation of GTP homeostasis by (p)ppGpp: a critical component of viability and stress resistance. *Mol Cell*. 48:231-241.

Kuroda, A., H. Murphy, M. Cashel, and A. Kornberg. 1997. Guanosine tetra- and pentaphosphate promote accumulation of inorganic polyphosphate in *Escherichia coli*. *J Biol Chem*. 272:21240-21243.

Lazzarini, R.A., M. Cashel, and J. Gallant. 1971. On the regulation of guanosine tetraphosphate levels in stringent and relaxed strains of *Escherichia coli*. *J Biol Chem*. 246:4381-4385.

Lee, C.R., S.H. Cho, M.J. Yoon, A. Peterkofsky, and Y.J. Seok. 2007. *Escherichia coli* enzyme IIA^{Ntr} regulates the K^+ transporter TrkA. *Proc Natl Acad Sci U S A*. 104:4124-4129.

Lee, C.R., M. Kim, Y.H. Park, Y.R. Kim, and Y.J. Seok. 2014. RppH-dependent pyrophosphohydrolysis of mRNAs is regulated by direct interaction with DapF in *Escherichia coli*. *Nucleic Acids Res*. 42:12746-12757.

Loveland, A.B., E. Bah, R. Madireddy, Y. Zhang, A.F. Brilot, N. Grigorieff, and A.A. Korostelev. 2016. Ribosome*RelA structures reveal the mechanism of stringent response activation. *Elife*. 5.

Mechold, U., H. Murphy, L. Brown, and M. Cashel. 2002. Intramolecular regulation of the opposing (p)ppGpp catalytic activities of Rel_{Seq}, the Rel/Spo enzyme from *Streptococcus equisimilis*. *J Bacteriol*. 184:2878-2888.

Mechold, U., K. Potrykus, H. Murphy, K.S. Murakami, and M. Cashel. 2013. Differential regulation by ppGpp versus pppGpp in *Escherichia coli*. *Nucleic Acids Res*. 41:6175-6189.

Miller, J.H. 1972. Experiments in molecular genetics. Cold Spring Harbor Laboratory, Cold Spring Harbor, N.Y. xvi, 466 p. pp.

Mitchell, J.E., T. Oshima, S.E. Piper, C.L. Webster, L.F. Westblade, G. Karimova, D. Ladant, A. Kolb, J.L. Hobman, S.J. Busby, and D.J. Lee. 2007. The *Escherichia coli* regulator of sigma 70 protein, Rsd, can up-regulate some stress-dependent promoters by sequestering sigma 70. *J Bacteriol*. 189:3489-3495.

Murray, K.D., and H. Bremer. 1996. Control of *spoT*-dependent ppGpp synthesis and degradation in *Escherichia coli*. *J Mol Biol*. 259:41-57.

Neira, J.L., F. Hornos, C. Cozza, A. Camara-Artigas, O. Abian, and A. Velazquez-Campoy. 2018. The histidine phosphocarrier protein, HPr, binds to the highly thermostable regulator of sigma D protein, Rsd, and its isolated helical fragments. *Arch Biochem Biophys*. 639:26-37.

Park, S., Y.H. Park, C.R. Lee, Y.R. Kim, and Y.J. Seok. 2016. Glucose induces delocalization of a flagellar biosynthesis protein from the flagellated pole. *Mol Microbiol*. 101:795-808.

Park, Y.H., C.R. Lee, M. Choe, and Y.J. Seok. 2013. HPr antagonizes the anti-s^{70} activity of Rsd in *Escherichia coli*. *Proc Natl Acad Sci U S A*. 110:21142-21147.

Park, Y.H., S.H. Um, S. Song, Y.J. Seok, and N.C. Ha. 2015. Structural basis for the sequestration of the anti-s^{70} factor Rsd from s^{70} by the histidine-containing phosphocarrier protein HPr. *Acta Crystallogr D Biol Crystallogr*. 71:1998-2008.

Paul, B.J., M.B. Berkmen, and R.L. Gourse. 2005. DksA potentiates direct activation of amino acid promoters by ppGpp. *Proc Natl Acad Sci U S A*. 102:7823-7828.

Persky, N.S., D.J. Ferullo, D.L. Cooper, H.R. Moore, and S.T. Lovett. 2009. The ObgE/CgtA GTPase influences the stringent response to amino acid starvation in *Escherichia coli*. *Mol Microbiol*. 73:253-266.

Piper, S.E., J.E. Mitchell, D.J. Lee, and S.J. Busby. 2009. A global view of *Escherichia coli* Rsd protein and its interactions. *Mol Biosyst*. 5:1943-1947.

Postma, P.W., J.W. Lengeler, and G.R. Jacobson. 1993. Phosphoenolpyruvate:carbohydrate phosphotransferase systems of bacteria. *Microbiol Rev*. 57:543-594.

Potrykus, K., and M. Cashel. 2008. (p)ppGpp: still magical? *Annu Rev Microbiol*. 62:35-51.

Raskin, D.M., N. Judson, and J.J. Mekalanos. 2007. Regulation of the stringent response is the essential function of the conserved bacterial G protein CgtA in *Vibrio cholerae*. *Proc Natl Acad Sci U S A*. 104:4636-4641.

Ronneau, S., K. Petit, X. De Bolle, and R. Hallez. 2016. Phosphotransferase-dependent accumulation of (p)ppGpp in response to glutamine deprivation in *Caulobacter crescentus*. *Nat Commun*. 7:11423.

Sankaranarayanan, R., A.C. Dock-Bregeon, P. Romby, J. Caillet, M. Springer, B. Rees, C. Ehresmann, B. Ehresmann, and D. Moras. 1999. The structure of threonyl-tRNA synthetase-tRNA^{Thr} complex enlightens its repressor activity and reveals an essential zinc ion in the active site. *Cell*. 97:371-381.

Schmidt, A., K. Kochanowski, S. Vedelaar, E. Ahrne, B. Volkmer, L. Callipo, K. Knoops, M. Bauer, R. Aebersold, and M. Heinemann. 2016. The quantitative and condition-dependent *Escherichia coli* proteome. *Nat Biotechnol*. 34:104-110.

Seyfzadeh, M., J. Keener, and M. Nomura. 1993. *spoT*-dependent accumulation of guanosine tetraphosphate in response to fatty acid starvation in *Escherichia coli*. *Proc Natl Acad Sci U S A*. 90:11004-11008.

Shyp, V., S. Tankov, A. Ermakov, P. Kudrin, B.P. English, M. Ehrenberg, T. Tenson, J. Elf, and V. Hauryliuk. 2012. Positive allosteric feedback regulation of the stringent response enzyme RelA by its product. *EMBO Rep*. 13:835-839.

Sun, D., G. Lee, J.H. Lee, H.Y. Kim, H.W. Rhee, S.Y. Park, K.J. Kim, Y. Kim, B.Y. Kim, J.I. Hong, C. Park, H.E. Choy, J.H. Kim, Y.H. Jeon, and J. Chung. 2010. A metazoan ortholog of SpoT hydrolyzes ppGpp and functions in starvation responses. *Nat Struct Mol Biol*. 17:1188-1194.

Traxler, M.F., D.E. Chang, and T. Conway. 2006. Guanosine 3',5'-bispyrophosphate coordinates global gene expression during glucose-lactose diauxie in *Escherichia coli*. *Proc Natl Acad Sci U S A*. 103:2374-2379.

Verstraeten, N., W.J. Knapen, C.I. Kint, V. Liebens, B. Van den Bergh, L. Dewachter, J.E. Michiels, Q. Fu, C.C. David, A.C. Fierro, K. Marchal, J. Beirlant, W. Versees, J. Hofkens, M. Jansen, M. Fauvart, and J. Michiels. 2015. Obg and Membrane Depolarization Are Part of a Microbial Bet-Hedging Strategy that Leads to Antibiotic Tolerance. *Mol Cell*. 59:9-21.

Vinella, D., C. Albrecht, M. Cashel, and R. D'Ari. 2005. Iron limitation induces SpoT-dependent accumulation of ppGpp in *Escherichia coli*. *Mol Microbiol*. 56:958-970.

Wolf, Y.I., L. Aravind, N.V. Grishin, and E.V. Koonin. 1999. Evolution of aminoacyl-tRNA synthetases--analysis of unique domain architectures and phylogenetic trees reveals a complex history of horizontal gene transfer events. *Genome Res*. 9:689-710.

Xiao, H., M. Kalman, K. Ikehara, S. Zemel, G. Glaser, and M. Cashel. 1991. Residual guanosine 3',5'-bispyrophosphate synthetic activity of *relA* null mutants can be eliminated by *spoT* null mutations. *J Biol Chem*.

266:5980-5990.

Blattner, F.R., G. Plunkett, 3rd, C.A. Bloch, N.T. Perna, V. Burland, M. Riley, J. Collado-Vides, J.D. Glasner, C.K. Rode, G.F. Mayhew, J. Gregor, N.W. Davis, H.A. Kirkpatrick, M.A. Goeden, D.J. Rose, B. Mau, and Y. Shao. 1997. The complete genome sequence of *Escherichia coli* K-12. *Science*. 277:1453-1462.

Chang, A.C., and S.N. Cohen. 1978. Construction and characterization of amplifiable multicopy DNA cloning vehicles derived from the P15A cryptic miniplasmid. *J Bacteriol*. 134:1141-1156.

Choe, M., Y.H. Park, C.R. Lee, Y.R. Kim, and Y.J. Seok. 2017. The general PTS component HPr determines the preference for glucose over mannitol. *Sci Rep*. 7:43431.

Datsenko, K.A., and B.L. Wanner. 2000. One-step inactivation of chromosomal genes in *Escherichia coli* K-12 using PCR products. *Proc Natl Acad Sci U S A*. 97:6640-6645.

Karimova, G., N. Dautin, and D. Ladant. 2005. Interaction network among *Escherichia coli* membrane proteins involved in cell division as revealed by bacterial two-hybrid analysis. *J Bacteriol*. 187:2233-2243.

Karimova, G., J. Pidoux, A. Ullmann, and D. Ladant. 1998. A bacterial two-hybrid system based on a reconstituted signal transduction pathway. *Proc Natl Acad Sci U S A*. 95:5752-5756.

Karimova, G., A. Ullmann, and D. Ladant. 2000. A bacterial two-hybrid system that exploits a cAMP signaling cascade in *Escherichia coli*. *Methods Enzymol*. 328:59-73.

Karimova, G., A. Ullmann, and D. Ladant. 2001. Protein-protein interaction between *Bacillus stearothermophilus* tyrosyl-tRNA synthetase

subdomains revealed by a bacterial two-hybrid system. *J Mol Microbiol Biotechnol*. 3:73-82.

LaVallie, E.R., E.A. DiBlasio, S. Kovacic, K.L. Grant, P.F. Schendel, and J.M. McCoy. 1993. A thioredoxin gene fusion expression system that circumvents inclusion body formation in the *E. coli* cytoplasm. *Biotechnology (N Y)*. 11:187-193.

Lee, C.R., B.M. Koo, S.H. Cho, Y.J. Kim, M.J. Yoon, A. Peterkofsky, and Y.J. Seok. 2005. Requirement of the dephospho-form of enzyme IIA^{Ntr} for derepression of *Escherichia coli* K-12 *ilvBN* expression. *Mol Microbiol*. 58:334-344.

Park, S., Y.H. Park, C.R. Lee, Y.R. Kim, and Y.J. Seok. 2016. Glucose induces delocalization of a flagellar biosynthesis protein from the flagellated pole. *Mol Microbiol*. 101:795-808.

Park, Y.H., C.R. Lee, M. Choe, and Y.J. Seok. 2013. HPr antagonizes the anti-σ^{70} activity of Rsd in *Escherichia coli*. *Proc Natl Acad Sci U S A*. 110:21142-21147.

Reddy, P., A. Peterkofsky, and K. McKenney. 1989. Hyperexpression and purification of *Escherichia coli* adenylate cyclase using a vector designed for expression of lethal gene products. *Nucleic Acids Res*. 17:10473-10488.

Chapter III.

A pGpG-specific phosphodiesterase in *Vibrio cholerae*

1. Abstract

The bacterial second messenger cyclic diguanylate monophosphate (c-di-GMP) controls various cellular processes in bacteria. C-di-GMP is enzymatically synthesized by GGDEF domain-containing diguanylate cyclases and degraded by HD-GYP domain-containing phosphodiesterases (PDEs) to 2GMP or by EAL domain-containing PDE-As to 5'-phosphoguanylyl-(3',5')-guanosine (pGpG). Since excess pGpG feedback inhibits PDE-A activity and thereby can lead to uncontrolled accumulation of c-di-GMP, a PDE(s) degrading pGpG to 2GMP (PDE-B) has been assumed to exist. Recently, it has been shown that the oligoribonuclease Orn harbors PDE-B activity in *Pseudomonas aeruginosa*, although it exhibits a broad substrate specificity toward di- to pentaribonucleotides (nanoRNAs) in addition to pGpG. Here, we identified a pGpG-specific PDE-B that we named PggH in *Vibrio cholerae*. While PggH possesses a DHH/DHHA1 domain which is usually responsible for the exonuclease activity toward various substrates, it could not degrade pApA and other nanoRNAs. High-resolution structure of PggH reveals the basis for its narrow substrate specificity. The unique dimeric assembly of the enzyme appears to reduce the structural flexibility of the active site, and thereby allow the access of only pGpG. The substrate specificity and the lower K_m of PggH than that of Orn for pGpG indicate that PggH could be the major PDE-B enzyme in *V. cholerae*. Increased expression of PggH during stationary phase and higher sensitivity of the *pggH* mutant to oxidative stress suggest that the PggH activity might be implicated in completion of the c-di-GMP signaling pathway under stress conditions in *V. cholerae*.

2. Introduction

Cyclic bis-(3′-5′)-diguanylic acid (c-di-GMP) is a widely conserved bacterial second messenger found in all major bacterial phyla (Romling et al., 2013). It was first discovered in 1987 as an activator of the cellulose synthase from *Komagataeibacter xylinus* (formerly known as *Gluconacetobacter xylinus*) by Moshe Benziman (Ross et al., 1987). C-di-GMP has shown to be associated with diverse cellular processes such as bacterial growth, motility, virulence, biofilm formation and cell cycle progression (Jenal et al., 2017). Low levels of cellular c-di-GMP up-regulate motility by inducing flagellar expression, assembly, or motor function (Hengge, 2009), and are also required for the expression of acute virulence genes (Tamayo et al., 2007), whereas high c-di-GMP levels stimulate the biosynthesis of fimbriae, adhesins, various matrix exopolysaccharides and biofilm formation (Hengge, 2009; Jenal and Malone, 2006; Romling and Amikam, 2006). Moreover, the c-di-GMP-dependent spatiotemporal control of protein degradation is a key step in cell cycle progression in *Caulobacter crescentus* (Duerig et al., 2009).

C-di-GMP is synthesized from two GTP molecules by diguanylate cyclases (DGCs) harboring the GGDEF domain, which is named after its conserved motif glycine-glycine-aspartate-glutamate-phenylalanine (Jenal et al., 2017). C-di-GMP is degraded by phosphodiesterases (PDEs), such as HD-GYP domain-containing enzymes and EAL domain-containing enzymes (Schirmer and Jenal, 2009). HD-GYP-domain-containing PDEs hydrolyze c-di-GMP to yield two molecules of GMP in a one-step reaction (Bellini et al., 2014). However, EAL domain-containing PDEs (PDE-As) degrade c-di-GMP into the linear product 5′-phosphoguanylyl-(3′,5′)-guanosine (pGpG), which is the intermediate product (Schmidt et al., 2005; Tamayo et al., 2005). Thus, the c-di-GMP degradation by EAL-domain enzymes requires a second PDE enzyme (PDE-B), which hydrolyze pGpG into two GMP

molecules, to increase the hydrolysis rate of c-di-GMP and complete the signaling process (Cohen et al., 2015). The EAL domain proteins are more abundant than HD-GYP domain proteins, indicating that the hydrolysis process by EAL domain proteins is likely the major route for degradation of c-di-GMP.

The high level of pGpG is known to block the turn-over of c-di-GMP by inhibiting c-di-GMP-specific PDE-As. The PDE activity of *Escherichia coli* YfgF, an EAL-containing PDE-A, is inhibited by high concentrations of pGpG (Lacey et al., 2010) and that of the EAL-containing response regulator RocR from *Pseudomonas aeruginosa* is also inhibited by excess amounts of pGpG in the competitive inhibition mode with c-di-GMP (Orr et al., 2015). These findings suggest that controlling the cellular pGpG concentration is crucial for sustaining the c-di-GMP signaling pathway in bacteria. Oligoribonuclease (Orn) mainly consists of the RNase-T domain and is a 3'-to-5' exoribonuclease specific for very short RNA chains (nanoRNAs) (Niyogi and Datta, 1975; Zhang et al., 1998). Recently, it has been uncovered that Orn can degrade pGpG into GMP for complete hydrolysis of c-di-GMP (Cohen et al., 2015; Conner et al., 2017; Orr et al., 2015). However, its broad substrate specificity indicate that Orn is involved in global gene expression change rather than in the c-di-GMP signaling pathway. Depletion of Orn caused the accumulation of nanoRNAs (di- to pentaribonucleotides), which serve as primers for transcription initiation (Goldman et al., 2011). Consistently, a global alteration in gene expression (approximately 20% of all known transcripts in *P. aeruginosa*) was observed in Orn-depleted cells presumably by the priming effects of the nanoRNAs (Goldman et al., 2011). Furthermore, in *Vibrio cholerae*, *Escherichia coli*, and several other bacteria, the oligoribonuclease is essential, while none of c-di-GMP-metabolizing enzymes are indispensable (Vercruysse et al., 2014), supporting that the major function of Orn is in nanoRNA degradation rather

than in the c-di-GMP metabolism.

Here, we report that *V. cholerae* VCA0593 is a pGpG-specific PDE-B (hereafter we name it PggH for phosphoguanylyl guanylate hydrolase), which is highly conserved within the genus *Vibrio*. We discuss the structural basis for the narrow substrate specificity of PggH and its role as a modulator of cellular c-di-GMP concentrations under stress conditions in *V. cholerae*.

3. Materials and Methods

3.1. Bacterial strains, plasmids, and culture conditions.

The bacterial strains, plasmids and oligonucleotides used in this study are listed in Tables III-1 and III-2. Bacterial cells were grown at 37°C in LB medium. All plasmids were constructed using standard polymerase chain reaction (PCR)-based cloning procedures and verified by sequencing.

The up- and down-stream regions of the *pggH* gene were amplified by PCR using primer pairs of PB421-PB422 and PB423-PB424, respectively. After digestion of the two PCR products, the XmaI-SphI and SphI-XbaI fragments, respectively, were cloned into the corresponding sites of the suicide vector pDM4 to generate the plasmid pDM4-PggH. To construct an *pggH* deletion mutant of the *V. cholerae* N16961 strain, the *E. coli* SM10 λ*pir* strain carrying pDM4-PggH was conjugated with *V. cholerae* N16961, and the transconjugants were selected. Integration was confirmed by PCR, and the exoconjugants were selected in LB containing 10% sucrose. Deletion of *pggH* in the selected colonies was confirmed by PCR.

To construct pJK1113-P_{pggH}::*lacZ*, the linearized product of pJK1113 and the *pggH* promoter region was amplified by PCR using primer pairs of PB425-PB426 and PB427-PB428, respectively. And then, these PCR products were combined using the EZ-Fusion™ Cloning kit (Enzynomics). Then, the *lacZ* ORF amplified by PCR from *E. coli* chromosome using the primers PB429 and PB430 (Table III-2) was digested with NcoI and SalI and inserted into the corresponding site of pJK1113.

To construct pJK1113-VieA, the linearized product of pJK1113 and the ORF region of *VieA* gene (VC1652) region was amplified by PCR using primer pairs of PB437-PB438 and PB439-PB440, respectively. And then, these PCR products were combined using the EZ-Fusion™ Cloning kit (Enzynomics).

3.2. Purification of overexpressed proteins.

His-tagged proteins (His-PggH and His-Orn) were purified using TALON metal affinity resin according to the manufacturer's instructions (Takara Bio). The protein was eluted with the binding buffer (20 mM HEPES-NaOH, pH 7.6, 100 mM NaCl, 5 mM β-mercaptoethanol, and 5% glycerol) containing 150 mM imidazole. The fractions containing His-tagged proteins were concentrated using Amicon Ultracel-3K centrifugal filters (Merck Millipore). To obtain homogeneous His-tagged protein (>98% pure) and to remove imidazole, the concentrated pool was dialyzed against a large volume of imidazole-free binding buffer. The purified protein was stored at -80°C until use.

3.3. Size exclusion chromatography (SEC).

The eluted proteins were further purified by size exclusion chromatography (HiLoad Superdex 200 26/600; GE Healthcare). The column was calibrated using calibration kit containing several standard preparations (GE Healthcare). The column was pre-equilibrated with buffer containing 150 mM NaCl, 20 mM Tris-HCl (pH 8.0), and 2 mM β-mercaptoethanol. The purify of protein was estimated by SDS-PAGE. The proteins sample were stored frozen at -80°C.

3.4. *In vitro* assay for pGpG hydrolyzing activity.

The *in vitro* pGpG hydrolyzing activity of was assayed in a 100 μl reaction mixture containing 50 mM Tris-HCl (pH 8.0), 10 mM $MnCl_2$, 250 mM NaCl, 5 mM β-mercaptoethanol, and pGpG and indicated concentrations of proteins. After incubation at 37°C for the indicated time, the reaction was terminated by the addition of 20 mM EDTA, and then trifluoroacetic acid was added to a final concentration of 10%. The reaction product generated

from pGpG was then analyzed by high performance liquid chromatography (HPLC) using a Varian dual pump system connected to an ultraviolet-visible detector. A 20-μl reaction mixture was applied to a Supelcosil LC-18-T reverse phase chromatography column (Sigma Aldrich) equilibrated with 100 mM KH_2PO_4 and 8 mM tetrabutyl ammonium hydrogen sulfate (pH 2.6) in water and then chromatographed using a linear gradient of 0–30% methanol containing 100 mM KH_2PO_4 and 8 mM tetrabutyl ammonium hydrogen sulfate (pH 2.6) at a flow rate of 1 ml/min for 30 min. The eluted nucleotides were detected at 254 nm.

3.5. Assay for pGpG hydrolyzing activity in cell lysates

V. cholerae cells grown in 10 ml LB medium were harvested at an OD_{600} of ~0.7 by centrifugation at 9,000 × g for 10 min at 4°C. The supernatant was discarded, and pellets were resuspended in 600 μl PDE assay buffer, which contained 50 mM Tris-HCl (pH 8.0), 10 mM $MgCl_2$, 250 mM NaCl, 5 mM β-mercaptoethanol, 1 mM PMSF. Then, cells were disrupted by two passages through a French pressure cell at 10,000 psi. pGpG was added to the lysates at a concentration of ～20 μM, and cell lysates were divided into 100-μl aliquots. After aliquots of these lysates were incubated at 37°C for the indicated time, the reaction was terminated by the addition of 20 mM EDTA, and then trifluoroacetic acid was added to a final concentration of 10%. The reaction product generated from pGpG was then analyzed by high performance liquid chromatography (HPLC).

3.6. Crystallization of the protein for structural determination.

The crystals of the native protein were obtained as described previously (Yongdae et al., 2017). To obtain Mn^{2+} bound crystals, the concentrated protein (10 mg/ml) was crystallized using the hanging-drop diffusion

method under a reservoir solution containing 0.2 M manganese chloride, Tris-HCl (pH 8.5), 12% (v/v) PEG 4000, 2 mM Tris(2-carboxyethyl) phosphine (TCEP) at 14°C.

3.7. Structural determination and refinement.

The crystals were transferred to 2-μl of cryo-protection buffer containing the reservoir solution and additional 30% (wt/vol) (±)-2-methyl-2,4-pentanediol (MPD) for 1 min, and then were flash-cooled in liquid nitrogen for data collection under cryogenic conditions. To solve the phasing problem, 10 mM zinc chloride was added in cryo-protection buffer of several crystals. The datasets of Zn soaked crystal were collected on a direct X-ray detector Pilatus 6M (Dectris, Switzerland), equipped in beamline 5C of Pohang Accelerator Laboratory, Republic of Korea, at a wavelength of 1.2822 Å and Mg^{2+} bound crystals at 0.9795Å The crystal of PggH belonged to the space group $P2_12_12$, with unit cell dimensions of a =68.4 Å, b = 148.3 Å, and c = 58.8 Å. The program HKL-2000 was employed to process, merge, and scale the diffraction datasets (Otwinowski and Minor, 1997). Data collection statistics are provided in Table III-3. Anomalous signals from four Zn sites were found in each subunit, and the resulting electron density map was sufficiently clear to build an initial model using the programs PHENIX and COOT (Adams et al., 2010; Emsley and Cowtan, 2004). The Mn^{2+}-bound structure was determined by direct refinement using the Zn^{2+}-soaked structure.

3.8. RNA isolation and qRT-PCR.

V. cholerae cells were grown in LB medium containing appropriate antibiotics and 0.02% arabinose. Cells were harvested at exponential phase (OD_{600} ~0.6) or stationary phase (OD_{600} ~1.2) and total RNA was prepared using MiniBEST Universal RNA Extraction Kit (Takara Bio). Genomic

DNA was removed using RNase-free DNase I (Promega). The same amount of RNA (2000 ng) from each culture was converted into cDNA using cDNA EcoDry^{TM} Premix (Takara Bio). cDNAs were diluted 30-fold and subjected to qRT-PCR analyses using gene-specific primers and SYBR Premix Ex Taq II (Takara Bio). Amplification and detection of specific products were performed using the CFX96 Real-Time System (Bio-Rad). For normalization of the transcript level, the *rrsG* gene was used as a reference. The relative expression level was calculated as the difference between the threshold cycle (Ct) of the target gene and the Ct of the reference gene for each template.

Table III-1. Bacterial strains and plasmids used in this study

Strain or plasmid	Genotype or phenotype	Source
Strains		
V. cholerae		
N16961	Wild type, O1 serogroup, El Tor biotype	Lab stock
N16961Δ*pggH*	N16961 with Δ*pggH*	This study
N16961Δ*lacZ*	N16961 with Δ*lacZ*	Lab stock
E. coli		
ER2566	F⁻ λ⁻ f*huA2* [*lon*] *ompT lacZ*::*T7* gene 1 *gal sulA*11 Δ(*mcrC-mrr*)114::IS10 R(*mcr*-73::miniTn10-TetS)2 R(*zgb*-210::Tn10)(TetS) *endA1* [*dcm*]	New England Biolabs
SM10 λ*pir*	*thi-1 thr leu tonA lacY supE recA*::RP4-2-Tc::Mu λ *pir*, OriT of RP4, Km^r; conjugational donor	(Miller and Mekalanos, 1988)
Plasmids		
pETDuet-1	Cloning vector; Amp^R	Novagen
pET-HisPggH	pETDuet-1–derived expression vector for His-PggH	This study
pET-HisOrn	pETDuet-1–derived expression vector for His-Orn	This study
pET-HisPggH(H282A)	pETDuet-1–derived expression vector for His-PggH (His 282 to Ala)	This study
pET-HisPggH(D13N)	pETDuet-1–derived expression vector for His-PggH (Asp 13 to Asn)	This study
pET-HisPggH(D13A)	pETDuet-1–derived expression vector for His-PggH (Asp 13 to Ala)	This study
pET-HisPggH(D67N)	pETDuet-1–derived expression vector for His-PggH (Asp 67 to Asn)	This study
pET-HisPggH(D67A)	pETDuet-1–derived expression vector for His-PggH (Asp 67 to Ala)	This study
pDM4	Suicide vector for homologous recombination into *V. cholerae* chromosome, OriR6K, Cm^r	(Milton et al., 1996)
pDM4-PggH	pDM4-based suicide vector for deletion of PggH, Cm^r	This study
pJK1113	pBAD24 with *oriT* of RP4 and *nptI*, P_{BAD}; Km^R, Amp^R	(Lee et al., 2018)
pJK1113-P_{pggH}::*lacZ*	pJK1113-derived vector for *pggH* promoter *lacZ* reporter fusion, Km^R, Amp^R	This study
pJK1113-PggH	pJK1113-derived expression vector for PggH, Km^R, Amp^R	This study
pJK1113-Orn	pJK1113-derived expression vector for Orn, Km^R, Amp^R	This study
pJK1113-PggH(D13N)	pJK1113-derived expression vector for PggH (Asp 13 to Asn), Km^R, Amp^R	This study
pJK1113-VieA	pJK1113-derived expression vector for VieA, Km^R, Amp^R	This study
pJK1113-VieA(E170A)	pJK1113-derived expression vector for VieA (Glu 170 to Ala), Km^R, Amp^R	This study

Table III-2. Oligonucleotides used in this study

Name	Oligonucleotide sequence (5'-3')	Use(s)
PB407	GAAGAGGGGATCCCATGTCATCACTCAAGTATCG (BamHI)	Construction of
PB408	GATAAATGTCGACCTATTTGCGCTGAATCA (SalI)	pET-HisPggH
PB409	ACCATTGGATCCCATGTCTTTCAGCGACCAGAATC (BamHI)	Construction of
PB410	CCGATAGTCGACTTAGATCTTGAATACCGCCTTAC (SalI)	pET-HisOrn
PB411	ATGGTGGGGGTGGAGCCGCTGCCGCAGGTACCTGC	Construction of
PB412	GCAGGTACCTGCGGCAGCGGCTCCACCCCCACCAT	pET-HisPggH(H282A)
PB413	ATTAGTGACACGCAGTAATTTTGATGGTTTGGTGT	Construction of
PB414	ACACCAAACCATCAAAATTACTGCGTGTCACTAAT	pET-HisPggH(D13N)
PB415	ATTAGTGACA CGCAGTGCTT TTGATGGTTTGGTGT	Construction of
PB416	ACACCAAACCATCAAAAGCACTGCGTGTCACTAAT	pET-HisPggH(D13A)
PB417	CGCGCATT TGGTATTTAATCATCACCACTCAGAAA	Construction of
PB418	TTTCTGAGTGGTGATGATTAAATACCAAATGCGCG	pET-HisPggH(D67N)
PB419	CGCGCATT TGGTATTTGCTCATCACCACTCAGAAA	Construction of
PB420	TTTCTGAGTGGTGATGAGCAAATACCAAATGCGCG	pET-HisPggH(D67A)
PB421	TCATCTCCCGGGGCCGTATCCTCACCAAAACCCGC (XmaI)	
PB422	GTTCTTGCATGCTCAAAGCTTTGAGATCCCTGCCC (SphI)	Construction of
PB423	ATTTGAGCATGCGCAAATAGACCCTGATTTATCAG (SphI)	pDM4-PggH
PB424	TAAAGTTCTAGATGTGCCCAACTCACCGAAGGTC (XbaI)	
PB425	CCATGGTACCCGGGGATCCTCTAGAGTCGACCTGC	
PB426	TTGGTAACGAATCAGACAATTGACGGCTTGACGG	
PB427	TGTCTGATTCGTTACCAAGTTACGGGTTGCATATCAGTATTCTAC	Construction of
PB428	GATCCCCGGGTACCATGGGTTCTTCCCTCTTCAAAGCTTTGAG ATCCCTGCCC	pJK1113-P_{pggH}::*lacZ*
PB429	AAAAAACCATGGCCACCATGATTACGGATTCACTGGC (NcoI)	
PB430	TTTTTTGTCGACTTATTTTTGACACCAGACCAACTGG (SalI)	
PB431	AAGAACGAATTCATGTCATCACTCAAGTATCGAT (EcoRI)	Construction of
PB432	TCAAATGTCGACTTAACCATCCGCATTGATCTGGG (SalI)	pJK1113-PggH
PB433	ACCATTGAATTCATGTCTTTCAGCGACCAGAATC (EcoRI)	Construction of
PB434	CCGATAGTCGACTTAGATCTTGAATACCGCCTTAC (SalI)	pJK1113-Orn
PB435	ATTAGTGACACGCAGTAATTTTGATGGTTTGGTGT	Construction of
PB436	ACACCAAACCATCAAAATTACTGCGTGTCACTAAT	pJK1113-PggH(D13N)
PB437	AAGCTTGGCTGTTTTGGCGGATGAGAG	
PB438	GGTGAATTCCTCCTGCTAGCCCAAAAAAACGGGTATG	Construction of
PB439	GCTAGCAGGAGGAATTCACCATGAAAATAATGATAGTAG	pJK1113-VieA
PB440	CCGCCAAAACAGCCAAGCTTCTATTTTAATGTTACAAAACGCAC C	
PB441	GTGGGGCGATGGTCGGCGTTGCAGCGCTAGTACGTTACGAGC	Construction of
PB442	GCTCGTAACGTACTAGCGC TGC AACGCCGACCATCGCCCCAC	pJK1113-VieA(E170A)
RpoS-F	CTTACGTGGTGATGAAGCCG	qRT-PCR
RpoS-R	CCGCGTTCTGGATCGAATTT	

Table III-3. X-ray diffraction and refinement statistics

	Native PggH	PggH Mn^{2+} binding form
Data collection		
Beam line	PAL 5C	PAL 5C
Wavelength (Å)	1.2822	0.9795
Space group	$P2_12_12$	$P2_12_12$
Cell dimensions		
a, b, c (Å)	70.9, 148.6, 58.0	68.4, 148.3, 58.8
α, β, γ (°)	90, 90, 90	90, 90, 90
Resolution (Å)	50.00-2.30 (2.34-2.30)	38.25-1.90 (1.97-1.90)
R_{pim}	0.073 (0.013)	0.038 (0.206)
$I/\sigma I$	6.9 (4.9)	6.9 (4.9)
Completeness (%)	87.9 (82.2)	87.9 (82.2)
Redundancy	8.7 (5.8)	8.7 (5.8)
Refinement		
Resolution (Å)		1.90
No. of reflections		43967
R_{work}/R_{free}		0.2058/0.2517
No. of total atoms		4840
Wilson B-factor (Å)		20.50
R.M.S deviations		
Bond lengths (Å)		0.007
Bond angles (°)		0.86
Ramachandran plot		
Favored (%)		97.43
Allowed (%)		2.57
Outliers (%)		0
PDB ID		

* Values in parentheses are for the highest resolution shell.

** $R_{pim.} = \Sigma_{hkl}(1/(n-1))^{1/2}\Sigma_i|I_i(hkl) - [I(hkl)]|/\Sigma_{hkl}\Sigma_i I_i(hkl)$.

4. Results

4.1. Characterization of VCA0593 in *Vibrio cholerae*.

4.1.1. Oligoribonuclease activity of *Vibrio cholera* Orn.

pGpG hydrolysis is critical for the completion of the c-di-GMP signaling pathway (Cohen et al., 2015; Orr et al., 2015). In a previous study, pGpG binding proteins were identified using high-throughput DRaCALA-based screen on *V. cholerae* El Tor N16961 complete genome ORF library (Orr et al., 2015). Among the proteins found in this screen were EAL domain and HD-GYP domain proteins, ribonucleases (RNases), previously unidentified pGpG-binding proteins, and one hypothetical protein. Of these, VC0341, an ortholog of the *E. coli* oligoribonuclease Orn, mainly consists of the RNase-T domain (Figure III-1). Orn was previously shown to specifically cleave short oligoribonucleotides in *E. coli* (Niyogi and Datta, 1975; Zhang et al., 1998), and has recently been reported as the primary pGpG-degrading enzyme in *P. aeruginosa* that is required for c-di-GMP turnover (Orr et al., 2015). However, in *V. cholerae,* VC0341 was shown to be an essential exonuclease (Vercruysse et al., 2014) like *E. coli* Orn, which is an essential component of the mRNA-decay pathway (Ghosh and Deutscher, 1999). Therefore, we wondered whether VC0341 (hereafter Orn) is required for completing the degradation of mRNA to mononucleotides or for c-di-GMP turnover in *V. cholerae*.

We first determined the exonuclease activity of purified recombinant *V. cholerae* Orn using several nanoRNAs including pGpG as substrate by reverse phase RP-HPLC (Figure III-2 and III-3). Like its *P. aeruginosa* ortholog, *V. cholerae* Orn could hydrolyze pGpG as expected. It could also utilize pApA, pGpGpApApA and pApApApApA as substrate as well. These results led us to speculate that Orn has broad substrate specificity and there might be other pGpG binding protein(s) might be responsible for specific degradation of pGpG in *V. cholerae*.

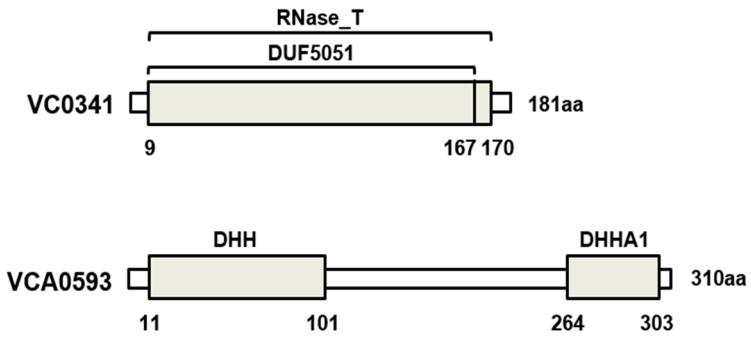

Figure III-1. Comparison of domain structure of VC0341 and VCA0593. VCA0593 possesses DHH and DHHA1 domains present in DHH/DHHA1 family proteins, which have the conserved Asp-His-His motif in the active site at N-terminus and subdomain DHHA1 at C-terminus, as represented by the single-stranded DNA exonuclease RecJ and 3'-phosphoadenosine 5'-phosphate (pAp) phosphatase. VC0341 possesses RNase_T domain present in a variety of exonuclease proteins, such as ribonuclease T and the epsilon subunit of DNA polymerase III. The numbers indicated under domains are amino acid positions in the full-length proteins.

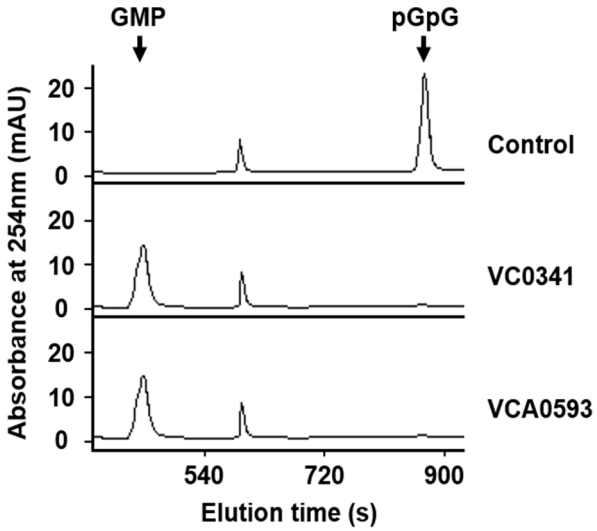

Figure III-2. pGpG hydrolyzing activity of VC0341 and VCA0593.

Degradation of pGpG and production of GMP by 2.2 μg VC0341 or VCA0593 was assessed by HPLC after 10 min incubation at 37°C.

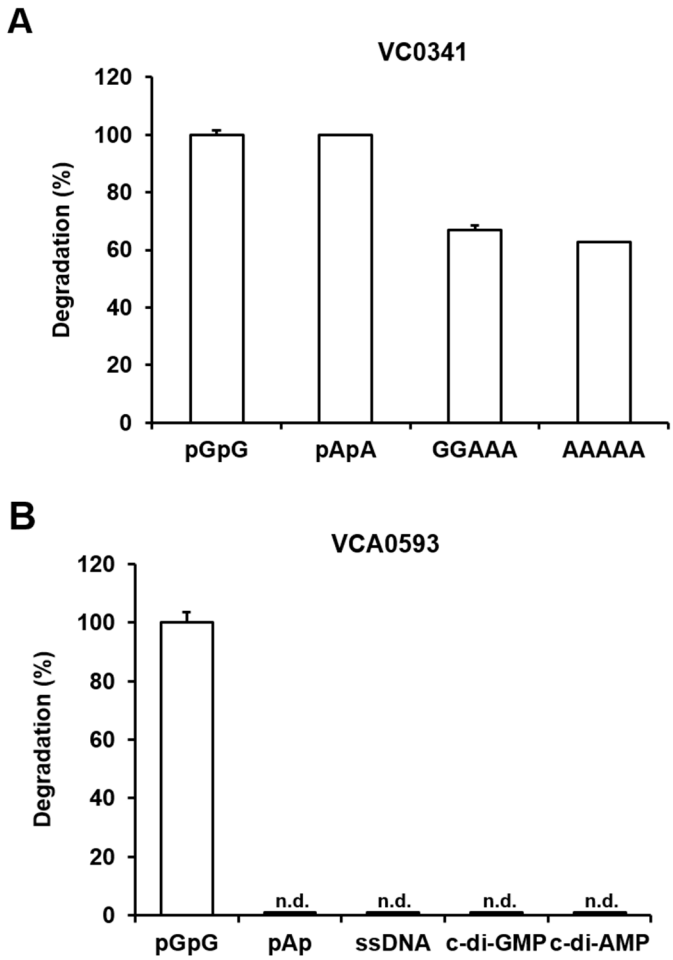

Figure III-3. VCA0593 is a pGpG-specific phosphodiesterase.

Degradation of nanoRNAs including pGpG, 3'-phosphoadenosine 5'-phosphate (pAp), single-stranded DNA (ssDNA), and cyclic dinucleotides (c-di-GMP and c-di-AMP) by indicated proteins were assessed by HPLC after 20 min incubation at 37°C. Values represent the means and SDs of three technical replicates. n.d = not detected.

4.1.2. Characterization and purification of VCA0593 in *V. cholerae*.

VCA0593, a chromosome II-encoded hypothetical protein, was also predicted to be a pGpG binding protein in *V. cholerae* El Tor N16961 (Orr et al., 2015) . It possesses DHH (residues 11-101) and DHHA1 (residues 264-303) domains (Figure III-1) and belongs to DHH/DHHA1 family proteins, which have the conserved Asp-His-His motifs, one in the active site at the N-terminus and another in the subdomain DHHA1 at the C-terminus, as represented by the cyclic di-nucleotide phosphodiesterase YybT and 3'-phosphoadenosine 5'-phosphate (pAp) phosphatase (Rao et al., 2010). Since several DHH/DHHA1 domain proteins are known to hydrolyze cyclic di-nucleotides and pAp, we measured the phosphodiesterase activity of VCA0593 toward these nucleotides and pGpG by HPLC. Surprisingly, while VCA0593 exhibited the phosphodiesterase activity toward pGpG, it could not hydrolyze ssDNA, pAp, c-di-GMP, or c-di-AMP (Figure III-2 and III-3). Therefore, we named it PggH (for phosphoguanylyl guanylate hydrolase).

4.1.3. PggH is highly conserve within *Vibrio* species.

PggH is highly conserved among major *Vibrio* species (Figure III-4). A protein BLAST search (Fisher et al., 2016) against the nonredundant protein sequences database at NCBI showed that the amino acid sequence of PggH is well conserved in the genus *Vibrio* (>77% amino acid identity) as well as within the *V. cholerae* species (>98% amino acid identity), suggesting that PggH may function as a pGpG-specific phosphodiesterase B in most species belonging to the genus *Vibrio*.

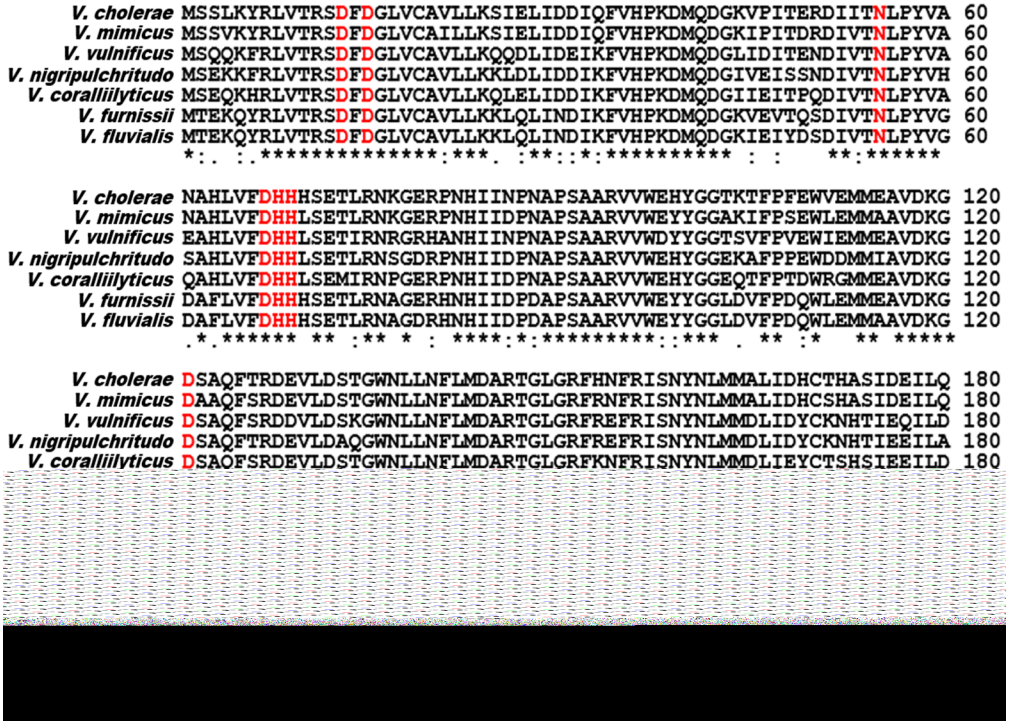

Figure III-4. PggH is highly conserved within *Vibrio* species.

The alignment of amino acid sequences of PggH homologues from *Vibrio* species using ClustalW software. The metal-coordinating residues and substrate-binding residue of PggH homologues are marked in red and blue, respectively.

4.2. pGpG-specific phosphodiesterase activity of PggH.

4.2.1. Characterization of pGpG hydrolytic activity of PggH.

The N-terminally hexahistidine-tagged form of PggH exhibited an apparent molecular mass of ~36 kDa (Figure III-5A). As most DHH/DHHA1 domain proteins function as a homodimer with an exception of the monomeric DNase RecJ (Srivastav et al., 2014), gel filtration analysis revealed that PggH is a homodimer (Figure III-5B). PggH showed the highest PDE-E activity toward pGpG in the presence of Mn^{2+}, whereas the lowest activity in the presence of Ca^{2+}, among divalent metal ions tested in this study as a cofactor (Figure III-6), similar to *E. coli* Orn (Niyogi and Datta, 1975). The Km and k_{cat} value of PggH for pGpG was determined by analyzing the initial rate of pGpG hydrolysis at different concentrations of substrate. Double-reciprocal plots of pGpG hydrolyzing activity at various substrate concentration showed the K_m and k_{cat} value of 12.11 μM and 0.14 s^{-1}, respectively (Figure III-7). Since it was previously shown that increasing concentrations of pGpG over a range of 2-20 μM increased inhibition of the c-di-GMP degradation by PDEs (Cohen et al., 2015), the catalytic activity of PggH appears to be enough to accelerate the decay of the c-di-GMP signal *in vivo*.

4.2.2. Orn degrades various two to five nucleotides (nanoRNAs) including pGpG with its broad substrate specificity.

Orn possesses RNase_T domain (Figure III-1) present in a variety of exonuclease proteins, such as ribonuclease T and the epsilon subunit of DNA polymerase III (Koonin and Deutscher, 1993). Orn is a 3'-to-5' exoribonuclease specific for short oligoribonucleotides (Zhang et al., 1998) and has a crucial role in completing the mRNA decay pathway (Ghosh and Deutscher, 1999). *V. cholerae* Orn has a high sequence

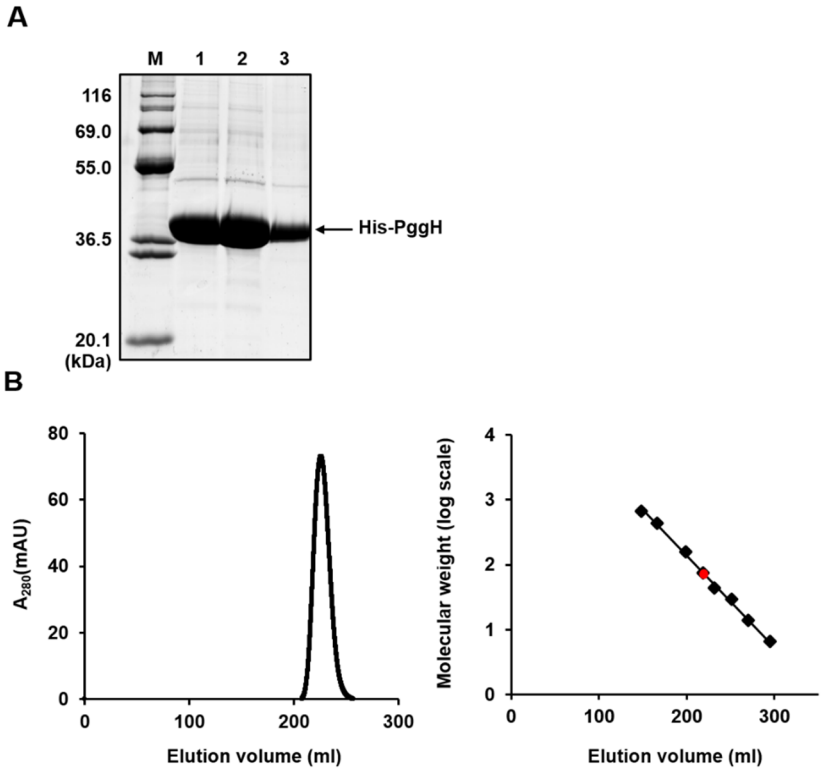

Figure III-5. Characterization and purification of PggH.

(A) His-tagged PggH was expressed and purified from *E. coli*, and then was analyzed by SDS-PAGE stained with Coomassie brilliant blue R. Lane M, molecular mass markers (KOMA Biotech); lane1, first eluted fraction; lane 2, second eluted fraction; lane 3, third eluted fraction. (B) Size exclusion chromatography elution profile for measuring the molecular size of PggH (left). Standard curve of size exclusion chromatography (right); 148.5 ml: (669 kDa) 166.21 ml: Ferritin (440 kDa) 199.1 ml: Aldolase (158 kDa) 218.23 ml: Conalbumin (75 kDa) 231.27 ml: Ovalbumin (44 kDa) 250.82 ml: carbonic anhydrase (29 kDa) 269.66 ml: Ribonuclease A (13.7 kDa) 294.97 ml: Aprotinin (6.5 kDa). The red spot at ~72 kDa indicates the molecular weight of the protein which corresponds to a homodimer (monomer size, ~36 kDa).

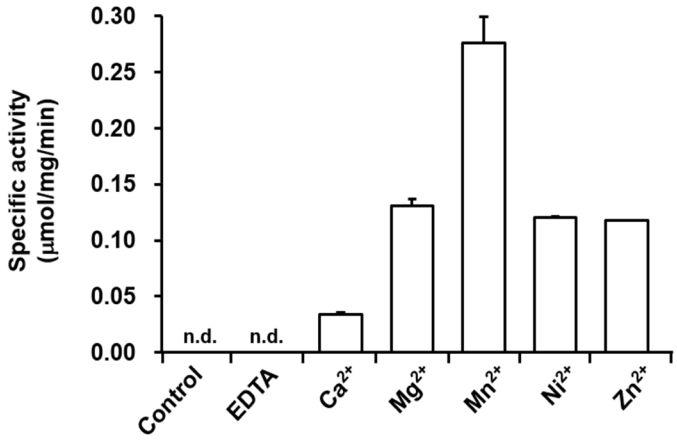

Figure III-6. Characterization of pGpG hydrolyzing activity of PggH.

Cleavage of pGpG by purified 1.06 μg PggH in the presence of indicated metal cations. Specific activity is expressed as the micromoles of GMP produced per minute per milligram of PggH. Values represent the means and SDs of three technical replicates. n.d = not detected.

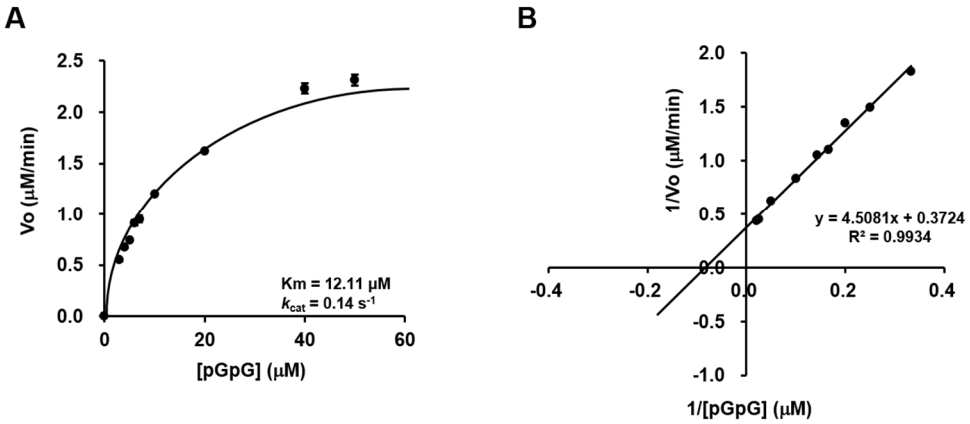

Figure III-7. Kinetics of PggH in cleavage of pGpG.

(A-B) Kinetics of PggH in cleavage of pGpG. The rate of pGpG hydrolysis (μM of GMP produced/min) measured at different pGpG concentrations was plotted as a function of μM pGpG. Data were fitted with the Michaelis-Menten kinetics (A) and a Lineweaver-Burk plot (B) to extrapolate the Km value of 12.11 μM and k_{cat} value of 0.14 s^{-1} for PggH. Values represent the means and SDs of three technical replicates.

identity (68%) to the *E. coli* Orn, and was essential for cell viability (Vercruysse et al., 2014) like *E. coli* (Ghosh and Deutscher, 1999). As shown in Table III-4, Orn efficiently hydrolyzed RNA homo- and heteropentamer (5'-AAAAA-3', 5'-GGAAA-3') and also, it rapidly degraded pApA and pGpG nanoRNAs. pApA and pGpG are produced from cleavage of bacterial signaling molecules, bis-(3′,5′)-cyclic diadenylic acid (c-di-AMP) and c-di-GMP, respectively (Uemura et al., 2013). pApA also inhibited the corresponding c-di-AMP PDE GdpP in *Staphylococcus aureus* (Bowman et al., 2016).

4.2.3 PggH specifically degrade pGpG with its narrow substrate specificity.

To compare substrate specificity between *V. cholerae* Orn and PggH, we examined the activity of PggH toward cleavage of nanoRNAs, such as RNA homo- and heteropentamer (5'-AAAAA-3', 5'-GGAAA-3') and pApA, pGpG (Table III-4). PggH specifically hydrolyzed pGpG whereas RNA homo- and heteropentamer, and pApA were not degraded. As shown in Figure III-3, no activity was detected with ssDNA and pAp. PggH did not degrade cyclic dinucleotide (c-di-GMP, c-di-AMP), either. Taken together, these findings suggest that PggH is a linear dinucleotide pGpG-specific phosphodiesterase.

	Specific activity (μmol/mg/min)	
Substrate	PggH	Orn
AAAAA	0	0.25 ± 0.03
GGAAA	0	0.26 ± 0.05
pApA	0	0.34 ± 0.01
pGpG	0.20 ± 0.01	0.35 ± 0.01

Table III-4. Specific degradation of pGpG by PggH.

Degradation of two to five nucleotides (nanoRNAs) by 1.12 μg PggH or 1.15 μg Orn *in vitro* as assessed by HPLC after 15 min incubation at 37°C. Specific activity is expressed as the micromoles of final product per minute per milligram of enzyme protein. Values represent the means and SDs of three technical replicates.

4.3. Structural basis for the pGpG specificity of PggH.

4.3.1. Structural determination of PggH.

To investigate the structural basis for the substrate specificity of PggH, we determined crystal structure of the protein in the presence of Mn^{2+} at 1.9 Å resolution (Figure III-8). The asymmetric unit contained two proteins that closely interact each other, which is consistent with the result from the size exclusion chromatography. The two DHHA1 domains in the dimer form a tight interaction while no direct interaction between the DHH domains is found in the dimeric unit (Figure III-8A).

4.3.2. Identification of metal binding sites in DHH domain and GGGH motif in the DHHA1 domain.

Each protomer contains a putative active site between the DHH domain and DHHA1 domain. A Mn^{2+} ion is coordinated by Asp15, Asn55, His68, His69, and Asp121 in the DHH domain of each active site (Figure III-8B). All the residues were strictly conserved among PggH homologues in *Vibrio* species (Figure III-4). Of these, His68 and His69 are from the conserved DHH motif. Interestingly, two sulfate ions were found near the Mn^{2+} binding region only in one protomer in the asymmetric unit (Figure III-8B). The sulfate ions could mimic the phosphate moieties of the substrate pGpG.

The DHHA1 domain of PggH contains the highly conserved GGGH motif but does not contain the partially conserved RxRxR motif. The GGGH motif was previously characterized to bind the phosphate moiety using the histidine residue (Uemura et al., 2013). Mutation at the histidine residue (His282 in PggH) abolished the hydrolysis activities of PggH, confirming the role of the motif in binding of the nucleotide (Figure III-9). The residues were strictly conserved among PggH homologues in *Vibrio* species (Figure III-4).

4.3.3. Structural comparison with the canonical NrnA protein.

By structural comparison to other DHH/DHHA1 domain containing proteins, several structural features of PggH were found. Strikingly, the PggH structure showed a novel dimeric arrangement suggesting a conformational rigidity between the domains. The DHH and DHHA1 domain is intervened by the DHHA1 domain of the other subunit unlike the other dimeric DHH/DHHA1 domain containing proteins (Figure III-8C). This interaction reduced the space of the two domains, which appears to limit the mobility of the domains. The structural rigidity was further found within the protomer. The DHH domain and DHHA1 domain are connected via a long α-helix unlike the canonic DHH/DHHA1 domain containing proteins. NrnA from *Bacteriodes fragilis* seemed to be mobile since the two domains are connected by a flexible linker in the crystal structure (Uemura et al., 2013) (Figure III-8D). Thus, our findings suggest that the more rigid and small active site of PggH is the molecular nature of the pGpG-specific activity. The small or tight active site cavity of PggH would enable the distinguish the pGpG from pApA by preventing the binding of pApA to the site.

4.3.4. Searching for the active site of PggH.

We found that Asp13 and Asp67 are indirectly related to the binding of Mn^{2+} in the crystal structure (Figure III-8B inset). Asp13 and Asp67 make hydrogen bonds with Asn55, and His69, respectively, both of which coordinate the Mn^{2+}. Mutations of these residues abolished the enzymatic activity, confirming the importance of the residues maybe in stabilizing the positions of the Mn^{2+} coordinating residues (Figure III-8). The residues were strictly conserved among PggH homologues in *Vibrio* species (Figure III-4).

Figure III-8. Crystal Structure of PggH.

(A) Overall structure of PggH homodimer. Ribbon representations of the dimer structure of PggH. The two molecules are presented in different colors as follows: Protomer A (DHH domain; light cyan, DHHA1 domain; cyan, α11 helix; grey), and protomer B (DHH domain; pink, DHHA1 domain; magenta, α11 helix; grey). Two sulfates are colored yellow. Mn^{2+} ion is presented as purple sphere. (B) The active site and the metal binding site. The active site is presented in a red rectangle and the metal binding site is presented in a blue rectangle (left). Two sulfates are colored yellow. Mn^{2+} ion is presented as purple sphere. Detailed view of the active site and metal binding site is presented right. The metal binding site is presented in the blue box and the metal coordinating residues color green. Overall view of the active site is presented in the red box. (C) Comparison of dimeric structure between NrnA and PggH. Surface representations of homodimeric structures of PggH, and NrnA. The DHH domains are colored light cyan and pink. The DHHA1 domains are colored cyan and magenta. The active site between DHH domain and DHHA1 domain is presented as broken black circle. (D) Comparison of monomeric structure between NrnA and PggH. Ribbon representations of monomeric structures of PggH, and NrnA. The DHH domains are colored light cyan and the DHHA1 domains are colored cyan. The linker helix of PggH is colored gray. Metal ions are represented as purple spheres. The linker helix of PggH and the linker loop of Rv2837c are highlighted as broken black rectangles.

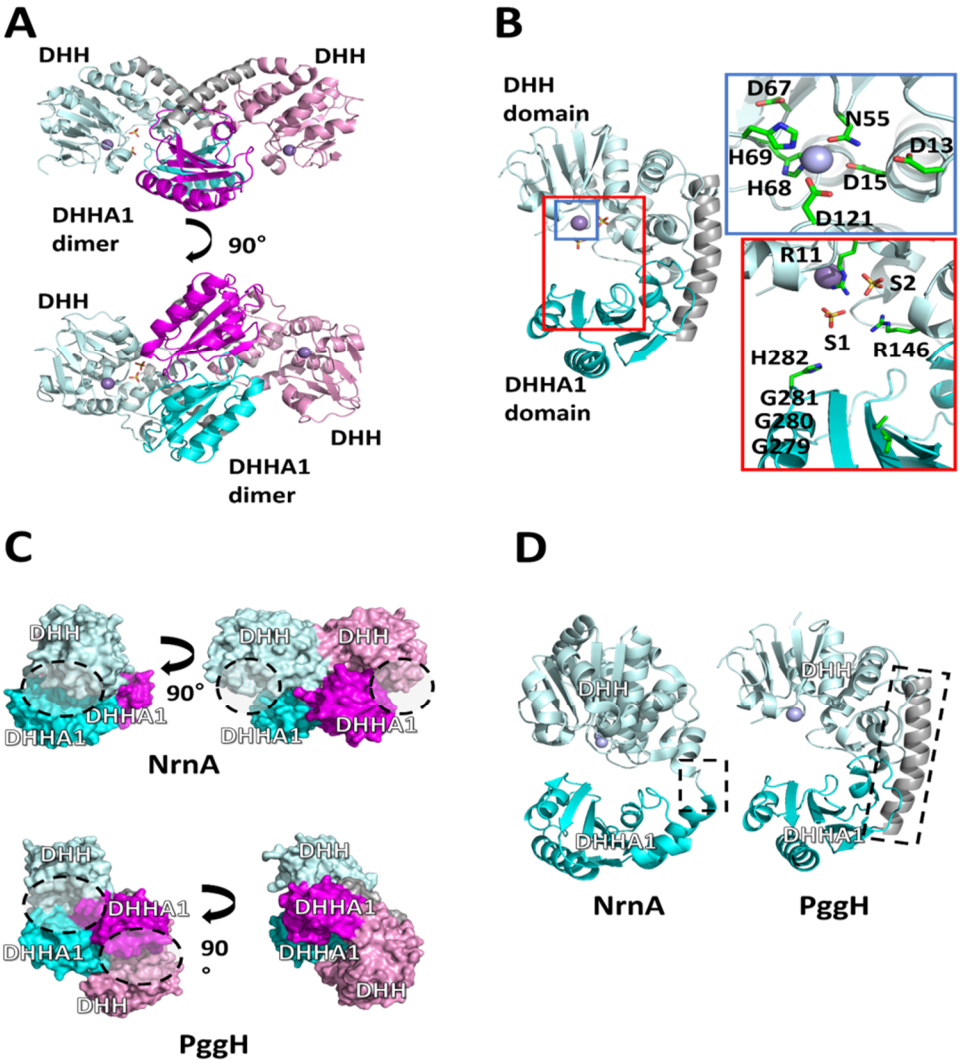
A
DHH
DHH
DHHA1
dimer
90°
DHH
DHH
DHHA1
dimer
B
DHH
domain
DHHA1
domain
D67
N55
D13
H69
D15
H68
D121
R11
S2
S1
R146
H282
G281
G280
G279
C
DHH
DHH
DHH
90°
DHHA1
DHHA1
DHHA1
NrnA
DHH
DHHA1
DHHA1
90
°
DHH
DHH
DHHA1
DHHA1
DHH
PggH
D
DHH
DHHA1
DHH
DHHA1
NrnA
PggH

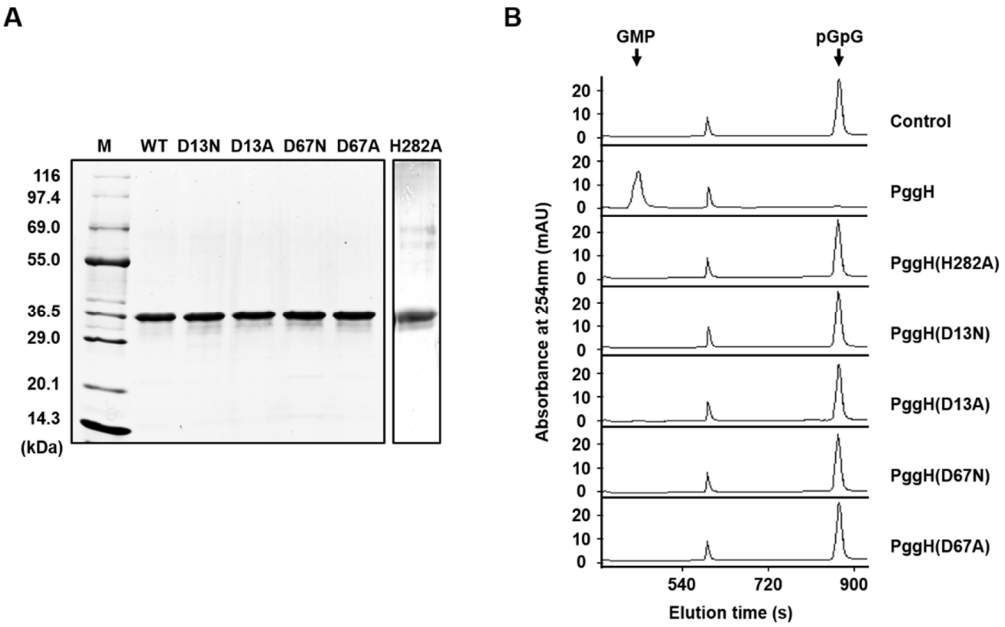

Figure III-9. Searching for the active site of PggH.

(A) Purification of PggH (WT) and several active site mutant forms of PggH (D13N, D13A, D67N, D67A, H282A). Approximately 3 μg of each indicated protein was loaded. Lane M, molecular mass markers (KOMA Biotech). (B) Degradation of pGpG and production of GMP by 2.2 μg PggH (WT) or mutant forms of PggH (H282A, D13N, D13A, D67N, D67A) was assessed by HPLC after 10 min incubation at 37°C.

4.4. *V. cholerae* PDE-B enzyme, PggH, is required to respond to oxidative stress.

4.4.1. An *pggH*-deficient mutant is defective in hydrolyzing pGpG.

Because our results indicate that PggH is a pGpG-specific phosphodiesterase with its intrinsic structural nature, we first compared pGpG hydrolysis by cell lysates from wild-type and *pggH* mutant strains (Figure III-10). Lysates of the *pggH* mutant still convert pGpG into GMP, suggesting that there are additional proteins with pGpG hydrolase activity including Orn. However, PggH apparently accounts for more than 50% of the total pGpG-hydrolyzing activity in cell lysates, indicating that PggH is a physiologically relevant enzyme responsible for pGpG turnover in *V. cholerae*.

4.4.2. The expression level of *pggH* increases in the stationary phase of growth.

We next investigated the role of PggH in the stationary phase of growth. During the stationary phase of growth, the amounts of nanoRNAs are more abundant compared to the exponential phase. Consistently, ectopic production of Orn in *E. coli* decreased the cellular nanoRNA concentrations only in a stationary phase of growth (Vvedenskaya et al., 2012). Thus, we speculated that PggH can efficiently degrade pGpG in the stationary phase. To examine the physiological role of PggH in stationary phase of growth in comparison with Orn, we measured the transcriptional level of *pggH* using the *lacZ* reporter gene. We first fused *pggH* promoter region with *lacZ* reporter gene to measure the expression level of *pggH* during growth of *V. cholerae*. As shown in Figure III-11, the expression level of *pggH* increased as cells entered into stationary phase of growth, which was contrasted to that of Orn of *E. coli* (Vvedenskaya et al., 2012).

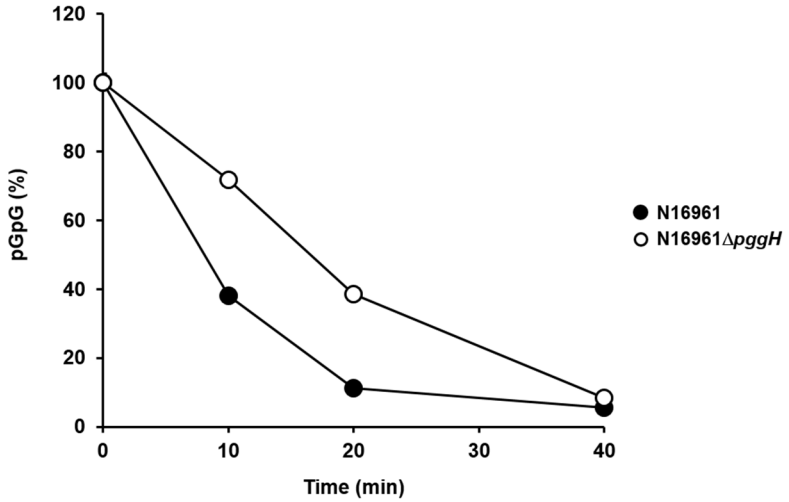

Figure III-10. An *pggH*-deficient mutant is defective in hydrolyzing pGpG.

Degradation of 20 μM pGpG by whole cell lysates of *V. cholerae* N16961 or N16961Δ*pggH* strains was assessed by HPLC at indicated time points after incubation at 37°C. Values represent the means and SDs of three technical replicates. Representative data from two independent experiments are presented.

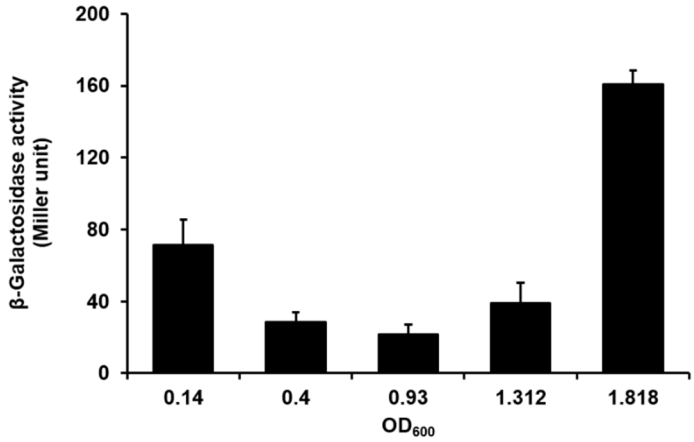

Figure III-11. The expression level of *pggH* increases in the stationary phase of growth.

Expression level of *pggH* during growth of *V. cholerae* was measured by measuring the β-galactosidase activities of promoter-*lacZ* fusion constructs introduced into *lacZ* deletion mutant. Values represent the means and SDs of three technical replicates.

4.4.3. PggH regulate the expression level of *rpoS* through modulating cellular c-di-GMP concentrations.

We next examined the role of PggH in regulation of the level of c-di-GMP. To probe the cellular concentration of c-di-GMP, we measured the expression level of *rpoS* that is repressed at higher c-di-GMP concentrations (Wang et al., 2014; Wang et al., 2011) (Figure III-12). The *V. cholerae pggH* mutant carrying the PggH-expressing plasmid exhibited a higher expression level of *rpoS* than that carrying control empty plasmid in a stationary phase of growth, whereas the *pggH* mutant carrying Orn-expressing plasmid did not. These data indicate that PggH can more efficiently hydrolyze pGpG than Orn to relieve the inhibition of c-di-GMP degradation in the stationary phase.

4.4.4. pGpG-specific activity of PggH is required for *V. cholerae* to respond to oxidative stress.

Since PggH regulates the expression level of *rpoS* in a stationary phase of growth through regulating cellular c-di-GMP levels, we tested whether PggH is required to environmental stress responses, like the other DHH/DHHA1 domain-containing phosphodiesterase (Rao et al., 2010). Cells with different expression levels of PggH did not exhibit any significant difference in response to osmotic stress (Figure III-13). However, as shown in Figure III-14, an *pggH* mutant carrying control plasmid was more sensitive to oxidative stress compared to the wild-type strain. While an *pggH* mutant carrying wild-type PggH-expressing plasmid was significantly resistant, that carrying an inactive form of PggH(D13N)-expressing plasmid did not.

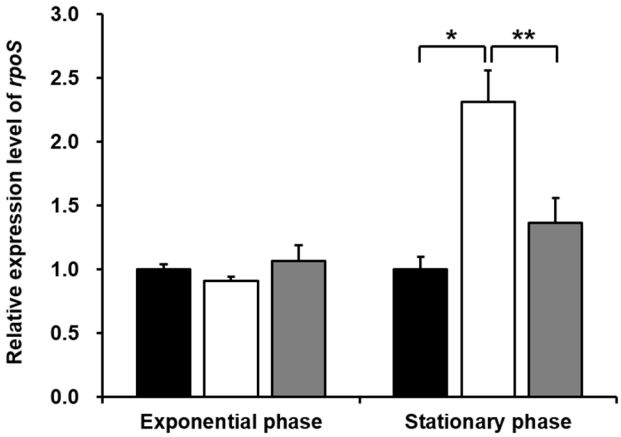

Figure III-12. The effect of PggH on the expression level of *rpoS* in the stationary phase of growth.

Total RNA was isolated from *pggH* deletion mutant harboring the control vector pJK1113 (black bar), the PggH expression vector pJK1113-PggH (white bar), or the Orn expression vector pJK1113-Orn (gray bar) grown to exponential phase or stationary phase in LB medium containing 0.02% arabinose. Then, the relative transcript level of *rpoS* was determined by quantitative reverse transcriptase PCR (qRT-PCR), as described in Materials and Methods. The mean and standard deviation (SD) of three independent measurements are shown. Statistically significant differences by Student's t-test are indicated as *$P < 0.05$ and **$P < 0.005$.

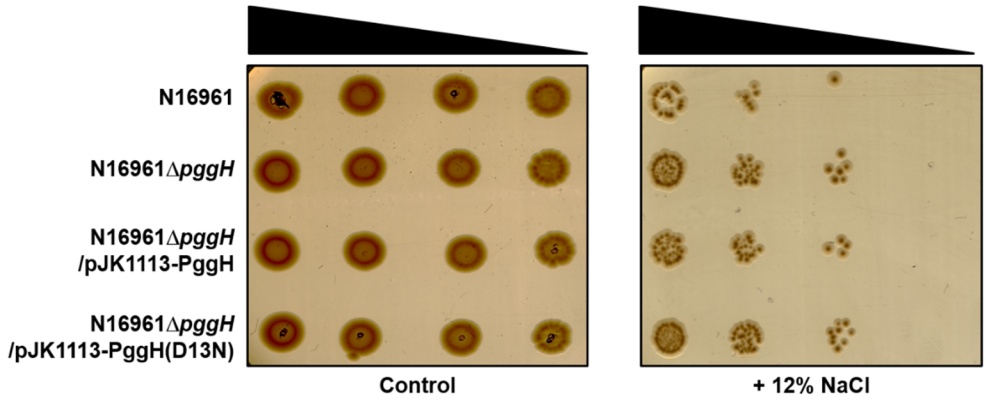

Figure III-13. PggH is not required for osmotic stress response.

Stationary phase cells of the indicated strains grown in LB medium were incubated with or without 12% NaCl for 120 min at 37°C and serially diluted 10-fold from ~10^9 to ~10^6 cells/ml. A 2-μl aliquots were spotted onto LB agar plates before incubation at 37°C for 16-18 h.

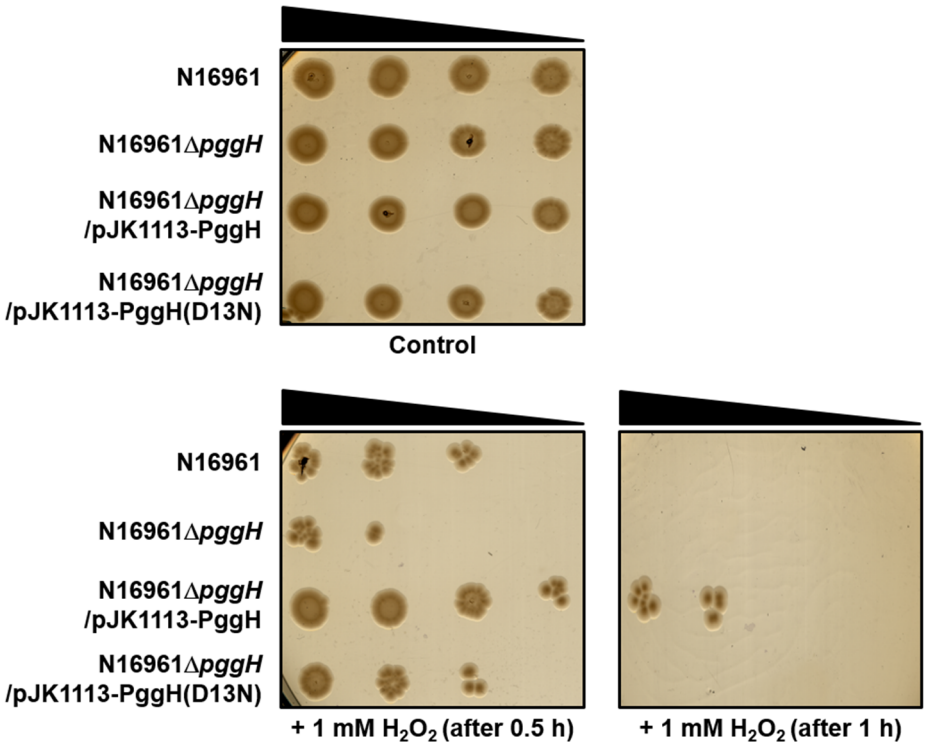

Figure III-14. Requirement of pGpG hydrolyzing activity of PggH in response to oxidative stress.

Stationary phase cells of the indicated strains grown in LB medium were incubated with or without 1 mM H_2O_2 for 30 min or 60 min at 37°C and serially diluted 10-fold from ~10^9 to ~10^6 cells/ml. A 2-μl aliquots were spotted onto LB agar plates before incubation at 37°C for 16-18 h.

4.4.5. PggH regulates cellular c-di-GMP levels as a PDE-B enzyme under oxidative stress condition.

To verify the sensitivity of *pggH* mutant is due to the increased concentration of c-di-GMP, we constructed an *pggH* mutant expressing c-di-GMP phosphodiesterase VieA (Tamayo et al., 2005) and tested the oxidative stress response (Figure III-15). Compared to an *pggH* mutant carrying control plasmid, that carrying VieA-expressing plasmid apparently reversed the sensitivity to oxidative stress similar to that carrying PggH-expressing plasmid. However, an *pggH* mutant harboring an inactive form of VieA(E170A)-expressing plasmid (Tamayo et al., 2005) did not, indicating that the *pggH* mutant accumulates cellular c-di-GMP levels, thus leading to more susceptible to oxidative stress.

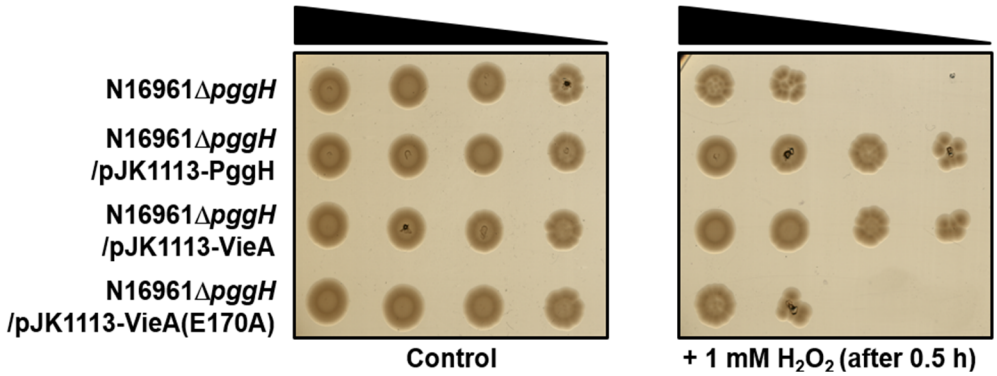

Figure III-15. Requirement of PggH as a PDE-B enzyme in response to oxidative stress.

Stationary phase cells of the indicated strains grown in LB medium were incubated with or without 1 mM H_2O_2 for 30 min at 37°C and serially diluted 10-fold from ~10^9 to ~10^6 cells/ml. A 2-μl aliquots were spotted onto LB agar plates before incubation at 37°C for 16-18 h.

5. Discussion

In this study, we investigated two proteins which were identified as pGpG binding proteins from *V. cholerae* genome using the DRaCALA based methods (Orr et al., 2015). Sequence and functional analyses strongly suggested that *V. cholerae* Orn is the orthologue of *E. coli* Orn that is responsible for break-down of nanoRNAs in the mRNA degradation pathways. Although Orn was bound to pGpG, it was unlikely that Orn is solely responsible for the pGpG degradation because Orn can degrade various lengths of nanoRNAs and its activity is interfered by diverse nanoRNAs (Figure III-16A). We noted PggH as the pGpG-specific PDE-B in the c-di-GMP degradation pathway. The purified PggH specifically hydrolyzed pGpG, but not the other nanoRNAs. Furthermore, PggH was not interfered by the other nanoRNAs (Figure III-16B), which is distinguished from Orn. We determined the crystal structure of PggH at the high resolution to gain the structural reasons of the function of PggH. The DHH and DHHA1 domain of one subunit in the dimer is intervened by the DHHA1 domain of the other subunit. The small and rigid active sites could account for the narrow substrate specificity to pGpG and the non-inhibition by the other nanoRNAs. Taken together, we concluded that PggH is the pGpG-specific PDE-B in the c-di-GMP degradation pathway (Figure III-17). The biochemical properties of PggH also agree well with the proposed function of PggH. PggH exhibited a lower Km value by about 3-fold than Orn, indicating that PggH is more efficient in lower concentration of pGpG than Orn even though Orn might be display higher activity at high concentration of pGpG with higher k_{cat} values (Figure III-18). This prediction is well consistent with the previous report that cellular pGpG concentrations was apparently lower in the stationary phase compared to exponential phase of growth (Orr et al., 2015). Furthermore, PggH would increase the importance in degradation of pGpG because

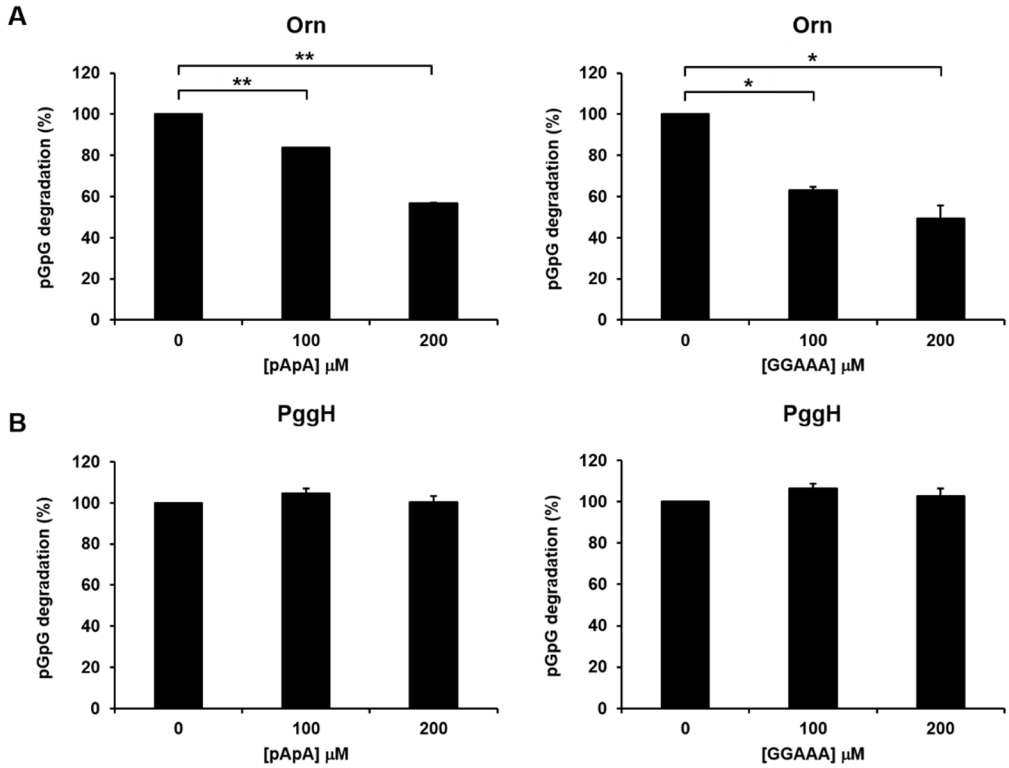

Figure III-16. The effect of nanoRNAs on the pGpG hydrolyzing activity of Orn and PggH.

(A) Degradation of pGpG by 0.1 μg Orn in the presence of various concentrations of nanoRNAs pApA or GGAAA as assessed *in vitro* by HPLC after 9 min incubation at 37°C. Values represent the means and SDs of three technical replicates. Statistically significant differences by Student's t-test are indicated as *P < 0.05 and **P < 0.005. (B) Degradation of pGpG by 0.5 μg PggH in the presence of various concentrations of nanoRNAs pApA GGAAA as assessed *in vitro* by HPLC after 40 min incubation at 37°C. Values represent the means and SDs of three technical replicates.

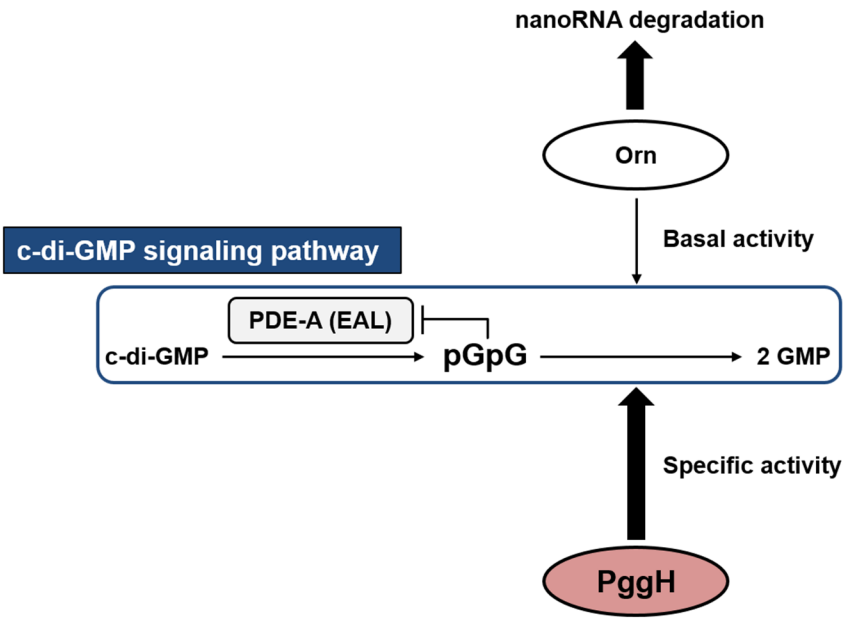

Figure III-17. Model for the physiological role of PggH in c-di-GMP signaling pathway.

Excess amounts of pGpG inhibits PDE-A activity to elevate c-di-GMP concentrations, thus cells require a second phosphodiesterase (PDE-B) to degrade pGpG and complete c-di-GMP signaling pathway. In *V. cholerae*, the Orn regulates the abundance of pGpG. However, Orn has a broad substrate specificity and excess nanoRNAs inhibit its pGpG hydrolyzing activity, suggesting the requirement of pGpG-specific phosphodiesterase. This is achieved by the pGpG-specific phosphodiesterase, PggH. It specifically degrades only pGpG and this activity is required for modulating cellular c-di-GMP levels, thus allowing *V. cholerae* cells to respond to oxidative stress conditions.

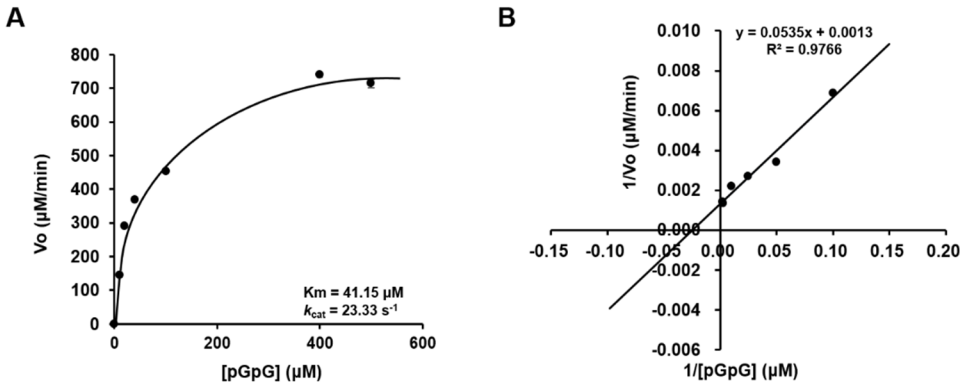

Figure III-18. Kinetics of Orn in cleavage of pGpG.

(A-B) Kinetics of Orn in cleavage of pGpG. The rate of pGpG hydrolysis (µM of GMP produced/min) measured at different pGpG concentrations was plotted as a function of µM pGpG. Data were fitted with the Michaelis-Menten kinetics (A) and a Lineweaver-Burk plot (B) to extrapolate the Km value of 41.15 µM and k_{cat} value of 23.33 s^{-1} for Orn. Values represent the means and SDs of three technical replicates.

the activity of PggH is not affected by cellular nanoRNAs unlike Orn. Since the working concentration of c-di-GMP is as low as nanomolar concentrations in *V. cholerae* and PDE-A to cleave c-di-GMP becomes inhibited by ~20 μM of pGpG (Cohen et al., 2015), the complete decomposition of cellular pGpG would be important to terminate c-di-GMP pathways. Thus, the enzymes with lower Km value would be more important that the one with higher k_{cat} value.

During the stationary phase of growth, Orn preferentially degrades various accumulated nanoRNAs (Vvedenskaya et al., 2012), thus Orn cannot efficiently hydrolyze pGpG. Consistent with this, pGpG-hydrolyzing activity of Orn was apparently decreased by various nanoRNAs. Our results confirmed the highlighted role of PggH during the stationary phase of growth compared to Orn. We further investigated the functional role of PggH in response to the oxidative stress. Since increased cellular c-di-GMP levels decrease the expression of *rpoS* to render *V. cholerae* more susceptible to the environmental stresses (Wang et al., 2014; Wang et al., 2011), the lowering of cellular c-di-GMP level is important in coping with the stresses. Our results also suggested that deletion of PggH is more susceptible to the oxidative stresses. Taken together, these data indicate that PggH as a PDE-B enzyme is required to complete c-di-GMP signaling pathway under oxidative stress conditions in *V. cholerae*.

PggH was annotated as exopolyphosphatase and belongs to NrnA superfamily (in a NCBI protein blast search). *Bacillus subtilis* NrnA, which has catalytic N-terminal DHH domain and the substrate binding C-terminal DHHA1 domain (Schmier et al., 2017), is a bifunctional enzyme with the nanoRNase and 3'-phosphoadenosine 5'-phosphate (pAp)-phosphatase activity and is preferably found in genomes that lack Orn or CysQ homologs (Postic et al., 2012). Because *V. cholerae* encodes both Orn (VC0341) and CysQ (VC2722), *V. cholerae* has no homologs of

NrnA (in a NCBI protein blast search).

Although PggH has higher binding affinity for pGpG than Orn (compare Figures III-7 and III-18), we cannot rule out the possibility that other macromolecular partner(s) are involved in regulating PggH PDE activity, as previously demonstrated for other c-di-GMP-metabolizing enzymes (Romling et al., 2013). In *Xanthomonas campestris*, HD-GYP domain PDE, RpfG, physically interacts with two diguanylate cyclase (GGDEF) domains to control a subset of RpfG-mediated virulence functions (Ryan et al., 2010). The periplasmic protein YfiR from *P. aeruginosa* interacts with and represses the activity of membrane bound diguanylate cyclase YfiN (Malone et al., 2012). The *heme*-nitric oxide/oxygen-binding (H-NOX) domain, as a selective NO sensor, regulates c-di-GMP metabolism by its direct interaction with diguanylate cyclase (Liu et al., 2012; Plate and Marletta, 2012). Additionally, the diguanylate cyclase SadC interacts with and recruits c-di-GMP-binding protein WarA to the inner membrane and this interaction contributes *P. aeruginosa* to escape from host immune system (McCarthy et al., 2017). Therefore, further studies on the regulation of PggH PDE activity may help to understand how pGpG-specific PDE coordinates c-di-GMP homeostasis.

6. References

Adams, P.D., P.V. Afonine, G. Bunkoczi, V.B. Chen, I.W. Davis, N. Echols, J.J. Headd, L.W. Hung, G.J. Kapral, R.W. Grosse-Kunstleve, A.J. McCoy, N.W. Moriarty, R. Oeffner, R.J. Read, D.C. Richardson, J.S. Richardson, T.C. Terwilliger, and P.H. Zwart. 2010. PHENIX: a comprehensive Python-based system for macromolecular structure solution. *Acta Crystallogr D Biol Crystallogr*. 66:213-221.

Bellini, D., D.L. Caly, Y. McCarthy, M. Bumann, S.Q. An, J.M. Dow, R.P. Ryan, and M.A. Walsh. 2014. Crystal structure of an HD-GYP domain cyclic-di-GMP phosphodiesterase reveals an enzyme with a novel trinuclear catalytic iron centre. *Mol Microbiol*. 91:26-38.

Bowman, L., M.S. Zeden, C.F. Schuster, V. Kaever, and A. Grundling. 2016. New Insights into the Cyclic Di-adenosine Monophosphate (c-di-AMP) Degradation Pathway and the Requirement of the Cyclic Dinucleotide for Acid Stress Resistance in *Staphylococcus aureus*. *J Biol Chem*. 291:26970-26986.

Cohen, D., U. Mechold, H. Nevenzal, Y. Yarmiyhu, T.E. Randall, D.C. Bay, J.D. Rich, M.R. Parsek, V. Kaever, J.J. Harrison, and E. Banin. 2015. Oligoribonuclease is a central feature of cyclic diguanylate signaling in *Pseudomonas aeruginosa*. *Proc Natl Acad Sci U S A*. 112:11359-11364.

Conner, J.G., D. Zamorano-Sanchez, J.H. Park, H. Sondermann, and F.H. Yildiz. 2017. The ins and outs of cyclic di-GMP signaling in *Vibrio cholerae*. *Curr Opin Microbiol*. 36:20-29.

Duerig, A., S. Abel, M. Folcher, M. Nicollier, T. Schwede, N. Amiot, B. Giese, and U. Jenal. 2009. Second messenger-mediated spatiotemporal control of protein degradation regulates bacterial cell cycle progression. *Genes Dev*. 23:93-104.

Emsley, P., and K. Cowtan. 2004. Coot: model-building tools for molecular

graphics. *Acta Crystallogr D Biol Crystallogr*. 60:2126-2132.

Fisher, C.R., E.E. Wyckoff, E.D. Peng, and S.M. Payne. 2016. Identification and Characterization of a Putative Manganese Export Protein in *Vibrio cholerae*. *J Bacteriol*. 198:2810-2817.

Ghosh, S., and M.P. Deutscher. 1999. Oligoribonuclease is an essential component of the mRNA decay pathway. *Proc Natl Acad Sci U S A*. 96:4372-4377.

Goldman, S.R., J.S. Sharp, I.O. Vvedenskaya, J. Livny, S.L. Dove, and B.E. Nickels. 2011. NanoRNAs prime transcription initiation in vivo. *Mol Cell*. 42:817-825.

Hengge, R. 2009. Principles of c-di-GMP signalling in bacteria. *Nat Rev Microbiol*. 7:263-273.

Jenal, U., and J. Malone. 2006. Mechanisms of cyclic-di-GMP signaling in bacteria. *Annu Rev Genet*. 40:385-407.

Jenal, U., A. Reinders, and C. Lori. 2017. Cyclic di-GMP: second messenger extraordinaire. *Nat Rev Microbiol*. 15:271-284.

Koonin, E.V., and M.P. Deutscher. 1993. RNase T shares conserved sequence motifs with DNA proofreading exonucleases. *Nucleic Acids Res*. 21:2521-2522.

Lacey, M.M., J.D. Partridge, and J. Green. 2010. *Escherichia coli* K-12 YfgF is an anaerobic cyclic di-GMP phosphodiesterase with roles in cell surface remodelling and the oxidative stress response. *Microbiology*. 156:2873-2886.

Liu, N., Y. Xu, S. Hossain, N. Huang, D. Coursolle, J.A. Gralnick, and E.M. Boon. 2012. Nitric oxide regulation of cyclic di-GMP synthesis and hydrolysis in *Shewanella woodyi*. *Biochemistry*. 51:2087-2099.

Malone, J.G., T. Jaeger, P. Manfredi, A. Dotsch, A. Blanka, R. Bos, G.R. Cornelis, S. Haussler, and U. Jenal. 2012. The YfiBNR signal transduction mechanism reveals novel targets for the evolution of

persistent *Pseudomonas aeruginosa* in cystic fibrosis airways. *PLoS Pathog*. 8:e1002760.

McCarthy, R.R., M.J. Mazon-Moya, J.A. Moscoso, Y. Hao, J.S. Lam, C. Bordi, S. Mostowy, and A. Filloux. 2017. Cyclic-di-GMP regulates lipopolysaccharide modification and contributes to *Pseudomonas aeruginosa* immune evasion. *Nat Microbiol*. 2:17027.

Niyogi, S.K., and A.K. Datta. 1975. A novel oligoribonuclease of *Escherichia coli*. I. Isolation and properties. *J Biol Chem*. 250:7307-7312.

Orr, M.W., G.P. Donaldson, G.B. Severin, J. Wang, H.O. Sintim, C.M. Waters, and V.T. Lee. 2015. Oligoribonuclease is the primary degradative enzyme for pGpG in *Pseudomonas aeruginosa* that is required for cyclic-di-GMP turnover. *Proc Natl Acad Sci U S A*. 112:E5048-5057.

Otwinowski, Z., and W. Minor. 1997. Processing of X-ray diffraction data collected in oscillation mode. *Methods Enzymol*. 276:307-326.

Plate, L., and M.A. Marletta. 2012. Nitric oxide modulates bacterial biofilm formation through a multicomponent cyclic-di-GMP signaling network. *Mol Cell*. 46:449-460.

Postic, G., A. Danchin, and U. Mechold. 2012. Characterization of NrnA homologs from *Mycobacterium tuberculosis* and *Mycoplasma pneumoniae*. *RNA*. 18:155-165.

Rao, F., R.Y. See, D. Zhang, D.C. Toh, Q. Ji, and Z.X. Liang. 2010. YybT is a signaling protein that contains a cyclic dinucleotide phosphodiesterase domain and a GGDEF domain with ATPase activity. *J Biol Chem*. 285:473-482.

Romling, U., and D. Amikam. 2006. Cyclic di-GMP as a second messenger. *Curr Opin Microbiol*. 9:218-228.

Romling, U., M.Y. Galperin, and M. Gomelsky. 2013. Cyclic di-GMP: the

first 25 years of a universal bacterial second messenger. *Microbiol Mol Biol Rev*. 77:1-52.

Ross, P., H. Weinhouse, Y. Aloni, D. Michaeli, P. Weinberger-Ohana, R. Mayer, S. Braun, E. de Vroom, G.A. van der Marel, J.H. van Boom, and M. Benziman. 1987. Regulation of cellulose synthesis in *Acetobacter xylinum* by cyclic diguanylic acid. *Nature*. 325:279-281.

Ryan, R.P., Y. McCarthy, M. Andrade, C.S. Farah, J.P. Armitage, and J.M. Dow. 2010. Cell-cell signal-dependent dynamic interactions between HD-GYP and GGDEF domain proteins mediate virulence in *Xanthomonas campestris*. *Proc Natl Acad Sci U S A*. 107:5989-5994.

Schirmer, T., and U. Jenal. 2009. Structural and mechanistic determinants of c-di-GMP signalling. *Nat Rev Microbiol*. 7:724-735.

Schmidt, A.J., D.A. Ryjenkov, and M. Gomelsky. 2005. The ubiquitous protein domain EAL is a cyclic diguanylate-specific phosphodiesterase: enzymatically active and inactive EAL domains. *J Bacteriol*. 187:4774-4781.

Schmier, B.J., C.M. Nelersa, and A. Malhotra. 2017. Structural Basis for the Bidirectional Activity of *Bacillus* nanoRNase NrnA. *Sci Rep*. 7:11085.

Srivastav, R., D. Kumar, A. Grover, A. Singh, B.A. Manjasetty, R. Sharma, and B. Taneja. 2014. Unique subunit packing in *mycobacterial* nanoRNase leads to alternate substrate recognitions in DHH phosphodiesterases. *Nucleic Acids Res*. 42:7894-7910.

Tamayo, R., J.T. Pratt, and A. Camilli. 2007. Roles of cyclic diguanylate in the regulation of bacterial pathogenesis. *Annu Rev Microbiol*. 61:131-148.

Tamayo, R., A.D. Tischler, and A. Camilli. 2005. The EAL domain protein VieA is a cyclic diguanylate phosphodiesterase. *J Biol Chem*. 280:33324-33330.

Uemura, Y., N. Nakagawa, T. Wakamatsu, K. Kim, G.T. Montelione, J.F. Hunt, S. Kuramitsu, and R. Masui. 2013. Crystal structure of the ligand-binding form of nanoRNase from *Bacteroides fragilis*, a member of the DHH/DHHA1 phosphoesterase family of proteins. *FEBS Lett*. 587:2669-2674.

Vercruysse, M., C. Kohrer, B.W. Davies, M.F. Arnold, J.J. Mekalanos, U.L. RajBhandary, and G.C. Walker. 2014. The highly conserved bacterial RNase YbeY is essential in *Vibrio cholerae*, playing a critical role in virulence, stress regulation, and RNA processing. *PLoS Pathog*. 10:e1004175.

Vvedenskaya, I.O., J.S. Sharp, S.R. Goldman, P.N. Kanabar, J. Livny, S.L. Dove, and B.E. Nickels. 2012. Growth phase-dependent control of transcription start site selection and gene expression by nanoRNAs. *Genes Dev*. 26:1498-1507.

Wang, H., J.C. Ayala, J.A. Benitez, and A.J. Silva. 2014. The LuxR-type regulator VpsT negatively controls the transcription of *rpoS*, encoding the general stress response regulator, in *Vibrio cholerae* biofilms. *J Bacteriol*. 196:1020-1030.

Wang, H., J.H. Wu, J.C. Ayala, J.A. Benitez, and A.J. Silva. 2011. Interplay among cyclic diguanylate, HapR, and the general stress response regulator (RpoS) in the regulation of *Vibrio cholerae* hemagglutinin/protease. *J Bacteriol*. 193:6529-6538.

Yongdae, J., P. Young-Ha, L. Jae-Woo, J. Inseong, P. Chaewoon, S. Yeong-Jae, and H. Nam-Chul. 2017. Purification, crystallization and preliminary X-ray crystallographic analysis of VCA0593 with a c-di-GMP binding activity in *Vibrio cholerae*. *Biodesign*. 5:70-73.

Zhang, X., L. Zhu, and M.P. Deutscher. 1998. Oligoribonuclease is encoded by a highly conserved gene in the 3'-5' exonuclease superfamily. *J Bacteriol*. 180:2779-2781.

Lee, J.W., Y.H. Park, and Y.J. Seok. 2018. Rsd balances (p)ppGpp level by stimulating the hydrolase activity of SpoT during carbon source downshift in *Escherichia coli*. *Proc Natl Acad Sci U S A*. 115:E6845-E6854.

Miller, V.L., and J.J. Mekalanos. 1988. A novel suicide vector and its use in construction of insertion mutations: osmoregulation of outer membrane proteins and virulence determinants in *Vibrio cholerae* requires *toxR*. *J Bacteriol*. 170:2575-2583.

Milton, D.L., R. O'Toole, P. Horstedt, and H. Wolf-Watz. 1996. Flagellin A is essential for the virulence of *Vibrio anguillarum*. *J Bacteriol*. 178:1310-1319.

국문 초록

박테리아 뉴클레오타이드 이차신호전달 물질은 세포내 또는 세포외 환경 신호를 전달한다. 이러한 신호 전달 시스템은 박테리아 생리에 광범위한 영향을 미치기 때문에 박테리아는 이차신호전달 물질의 대사와 신호 전달을 조절하는 다양한 효소를 지니고 있다. 이 효소를 이용하여, 박테리아는 다양한 주위환경 신호에 반응하여 이차신호전달 물질의 세포 내 농도를 정교하게 조절 하며, 만약 이 물질의 양이 제대로 조절되지 않으면 세포의 성장 억제 및 세포사망, 불균형 표현형을 야기하기 때문에 이 신호물질의 정교한 생체 제어는 세포 생리학에 매우 중요하다. 현재까지 cAMP의 대사와 신호 메커니즘에 관한 연구는 비교적 잘 알려져 있지만, 박테리아 내 다른 뉴클레오타이드 이차신호전달 물질들의 조절 기작은 거의 알려져 있지 않다.

대장균에서 (p)ppGpp 신호 전달은 두 가지 효소, (p)ppGpp를 합성하는 RelA 단백질과 (p)ppGpp를 합성 또는 분해하는 SpoT 단백질에 의해 매개된다. 다양한 영양 스트레스에 대응하여, 이 두 단백질들은 세포 내 (p)ppGpp 농도를 정교하게 조절하여 박테리아 세포가 스트레스 조건에 적응할 수 있게 한다. 특히, SpoT 단백질은 대장균내 (p)ppGpp를 가수분해 할 수 있는 유일한 효소이며, 세포 내 (p)ppGpp가 과량 축적되면 심각한 세포 성장 억제 및 세포사를 야기하기 때문에 SpoT 단백질의 활성은 매우 정밀하게 조절되어야 한다. 하지만, 현재까지 SpoT 단백질의 활성이 어떻게 조절 되는지는 거의 알려져 있지 않다. 조절 기작을 찾기 위해 ligand fishing 실험을 수행 하였고, 이를 통해 대장균의 Rsd 단백질이 SpoT 단백질과 직접 상호작용하여 SpoT 단백질의 (p)ppGpp

를 부수는 활성을 증가 시킨다는 것을 확인 하였다. 또한, 이러한 조절은 PEP 의존 당 수송 시스템의 일반적인 구성요소인 HPr 단백질의 인산화 상태에 의해 제어된다는 사실을 밝혔다. 본 연구에서는 이러한 실험 결과를 통해, Rsd 단백질은 주변 탄소원에 따라 대장균의 긴축 반응을 조절하는 새로운 조절자임을 밝혔다.

c-di-GMP 신호 전달에서, phosphodiesterases A (PDE-As) 효소는 c-di-GMP를 pGpG로 분해한다. 하지만, 세포 내 pGpG가 축적되면 PDE-A 효소의 활성을 저하 시키기 때문에 세포는 이 신호 전달 시스템 내의 세포 내 pGpG 농도를 낮추기 위한 추가적인 phosphodiesterases B (PDE-Bs) 효소를 필요로 한다. 녹농균에서 Orn 단백질이 pGpG를 분해 함으로써 PDE-B 활성을 가진다고 보고되었다. 하지만 Orn 단백질은 pGpG 뿐만 아니라 다양한 2~5개의 뉴클레오타이드 (nanoRNAs)를 부수는 광범위한 기질특이성을 가지고 있다. 본 연구에서는 생화학적 실험 방법 및 구조 분석을 통해 pGpG만을 특이적으로 부수는 PggH 단백질의 존재를 비브리오 콜레라균에서 새로이 확인 하였다. 이러한 실험 결과를 통해 이 단백질이 c-di-GMP 신호 전달을 완료하기 위해 필요한 새로운 PDE-B 효소로서 기능을 가진다는 사실을 밝혔다.

주요어:
박테리아 뉴클레오타이드 이차신호전달 물질, (p)ppGpp, 당 신호 전달, 단백질-단백질 상호작용, c-di-GMP, pGpG, 포스포디에스터 가수분해효소

학번: 2013-22451